12-2007

THE ROLE OF COMPUTER AIDED ENGINEERING IN DEVELOPING A COMBINED TRASH AND RECYCLING TRUCK : A CASE STUDY

Peter Johnston
Clemson University, jud.johnston@gmail.com

THE ROLE OF COMPUTER AIDED ENGINEERING IN DEVELOPING A COMBINED TRASH & RECYCLING TRUCK: A CASE STUDY

A Thesis
Presented to
the Graduate School
of Clemson University

In Partial Fulfillment
of the Requirements for the Degree
Master of Science
Mechanical Engineering

---

by
Peter Judson Johnston
December 2007

Accepted by:
Dr. Joshua Summers, Advisor
Dr. Gregory Mocko
Dr. Harry Law

ABSTRACT

This work will illustrate how Environmental America Inc., EAI, and the Clemson University design team utilized lean manufacturing principles to revolutionize the curbside waste collection process. Through the application of lean manufacturing principles the number of non-value added steps was significantly reduced and the information gathered from the lean process tree acted as a framework to develop initial constraints and criteria for the vehicle's development. The design team was asked to construct the fifth iteration of the prototype collection vehicle in an effort to minimize vehicle cost, size and weight. An extensive case study will be presented which illustrates how the design team utilized CAE to optimize the proposed prototype baling system. The investigation is conducted through the use of an "observer as participant" form of case study (1). The EAI combined collection vehicle was selected as the focus of the study due to the complexity and size of the system, as it has a significantly larger scope than those presented in classic academic engineering design projects. Since previous prototypes have been developed without the use of CAE software or additional engineering tool support, a benchmark for comparison exists which will directly demonstrate the benefits and limitations of the chosen software. Currently, CAE and FEA software is often used for product validation, system optimization, and parametric studies, however, this paper will demonstrate how CAE and FEA can be utilized to verify physical experimentation. The results of this case study will show that although the use of CAE significantly reduces lead time and cost associated with product development, the software can be extremely hazardous when used inappropriately.

ACKNOWLEDGEMENTS

I would like to thank Dr. Joshua Summers for helping me conduct this research as well as for helping me widen my base of engineering knowledge throughout the course of my graduate studies. Dr. Gregory Mocko and Dr. Harry Law, I thank you for the opportunity to collaborate with you throughout the development of this work. Finally, I would like to thank Environmental America Inc. for giving me the opportunity to work on this revolutionary project.

DEDICATION

This thesis is dedicated to Peter and Kristi Johnston, my loving and supporting parents.

TABLE OF CONTENTS

Page

Page

Page

LIST OF TABLES

LIST OF FIGURES

Figure Page

List of Figures (Continued)

Figure Page

List of Figures (Continued)

Figure Page

List of Figures (Continued)

Figure Page

LIST OF ABBREVIATIONS

MSW- Municipal Solid Waste

MRF- Material Reclamation Facility

EAI- Environmental America, Inc.

CAE- Computer Aided Engineering

FEA- Finite Element Analysis

CAD- Computer Aided Design

CAM- Computer Aided Manufacturing

VP- Virtual Prototyping

PLC- Programmable Logic Controller

PAYT- Pay-as-you-throw

CAYR- Credit-as-you-recycle

NIMBY- Not In My Back Yard

CHAPTER 1

INTRODUCTION

In recent years, through the use of lean manufacturing principles, companies around the world have been able to significantly impact the efficiency of production flow. Similarly, green design has become an important topic for discussion in the past decade; researchers are attempting to minimize system waste, therefore resulting in some form of positive environmental impact. An analysis of the curbside collection process for both municipal solid waste (MSW) and recyclables from a lean manufacturing standpoint exposes an abundance of non-value added activities. By eliminating or reducing these steps, the efficiency of the process can be drastically improved (2; 3). Environmental America Inc. (EAI) has proposed a "lean" collection process which will improve material flow through the implementation of a specialized vehicle which collects and processes both MSW and recycled goods. This vehicle, coupled with localized, low-impact material offloading facilities has the potential to revolutionize the curbside collection process. Not only will this system increase process efficiency, but the owner will be able to generate revenue directly by selling the processed goods to a purchaser. In the past, recycled goods were simply sold to material reclamation facilities (MRF) who acted as a third party between the collector and the buyer (4), therefore minimizing the profit for the collecting agency. By processing the goods onboard the vehicle, the collectors completely eliminate the need for the MRF, thus maximizing revenue. The design team's research supports EAI's vision by optimizing the vehicle layout as well as streamlining process operations. Through the use of computer aided engineering software, CAE, and engineering knowledge it is believed that a superior prototype vehicle can be developed

in a fraction of the time required for previous prototypes. Design superiority will be determined using the following characteristics:

- Cost
- Weight
- Strength
- Maintainability
- Manufacturability

Review of Lean Manufacturing

Manufacturing companies worldwide are beginning to transition from the conventional mass production system to a more efficient system of production called Lean Manufacturing. Lean manufacturing focuses entirely on improving production flow by attempting to eliminate all associated wastes (3). By implementing lean manufacturing principles companies are minimizing residual waste and streamlining production flow. Moreover, many companies are recycling scrap material generated during production, therefore further eliminating waste from the system. Unfortunately, many of the recycling agencies which service these companies have failed to eliminate the waste associated with the collection and processing of the recycled goods.

Lean manufacturing is defined as the "systematic approach to identifying and eliminating waste through continuous improvement of production flow (5)". Every step of activity that does not directly add market form or function to the product is classified as a non-value added step (2). Conversely, value added steps are those which transform the product into something that the customer is indeed willing to pay for. The main objective of lean manufacturing is to seek out and eliminate the non-value added steps

from a process, while streamlining the value added aspects; thus, yielding a far more efficient process.

Companies employing lean manufacturing principles focus entirely on improving production flow through the elimination of waste, which encompasses all steps which hinder smooth flow. A 2003 study conducted by the US Environmental Protection Agency (USEPA) investigated the relationship between lean manufacturing and the environment. During the investigation, they uncovered a very interesting piece of information. The study showed that lean manufacturing produces an operational and cultural environment that is extremely conducive to waste and pollution prevention, through the minimization of material and scrap (6).

Since the application of lean manufacturing principles appears to have significant benefits regarding waste and pollution prevention, then why does this technique have trouble gaining traction with the companies that collect and recycle the waste? It is possible that the collection programs and companies are simply resisting change. It is also possible that a method for the implementation of lean principles has not been developed. In 2004, at the Illinois Manufacturing Extension Center's Conference titled "Manufacturing Matters", information regarding the benefits of a lean system was presented (7). It was determined that companies that embraced lean manufacturing have a median return on invested capital of approximately seventeen percent, while companies that have failed to utilize lean principles only have a ROIC of ten percent.

The Toyota Production System, analyzed by Ohno, is considered to be the revolutionary system that has developed into lean manufacturing (8). In his system, Ohno separates waste into seven individual categories: overproduction, inventory,

defects, processing, transportation, waiting, and motion. However, most of the manufacturing community has recently adopted an eighth waste, people, to the system. The "people" category most often refers to the underutilization of people. Each of these "wastes" adds cost to the process without adding any market form or function and therefore must be eliminated or reduced in order to streamline the production process. By indentifying the different "wastes" associated with a given process, the manufacturer/company is then able to develop an accurate plan for eliminating or minimizing the effects. This approach was adopted by EAI in an attempt to increase the efficiency of the collection process for both municipal solid waste and recyclables.

Computer Aided Engineering

Computer Aided Engineering software has been rapidly advancing over the past two decades to a point where most major companies rely on these tools for product development. However, some people remain skeptical of the advantages of such systems. CAE is defined as the use of computer systems in all engineering activities spanning from concept generation to product fabrication. Lately, the definition seems to have expanded due to the introduction of more powerful CAE software which incorporates high level FEA tools and allows users to streamline the production flow throughout the facility. Many definitions propose that CAE tools are only systems which specifically help the engineer in analytical design, for instance FEA. Similarly, it has been suggested that computer aided design (CAD) and computer aided manufacturing (CAM) also be considered CAE tools. For simplicity, this paper will utilize the term CAE as a set of tools which encompasses all computer based systems from conceptual design through the end of the product life cycle.

The first major large scale implementation of CAE and CAD software as well as virtual prototyping (VP) techniques was the creation of the Boeing 777 (13). Boeing engineers believed that the amount of rework, caused by part interference, could be significantly improved by creating a full scale model and assembling it virtually. In the mid-80's, the Boeing Company made its first investment in 3-D computer aided design software, but conducted limited development with the systems. In 1990, Boeing adopted a new CAE multidisciplinary approach, in which designers, engineers, suppliers, etc., worked concurrently to create a new airplane design. The use of advanced computer systems allowed 238 individual design teams to share their information in real-time.

Boeing utilized the CAD package CATIA[1], created by Dassault Systemes, for all 3-D modeling of the design. The software allowed engineers and designers to not only model the components, but also provided the ability to conduct full scale assembly/disassembly, tolerance studies and FEA simulations. As a result of the limited history of CAE software, Boeing was hesitant to rely solely on the results of the computer model, thus creating an initial physical mock-up of the nose section of the aircraft in an attempt to validate the results (13). The virtual model yielded such accurate results, all plans for future mock-ups were immediately cancelled.

When production finally began on the 777, Boeing determined that they had exceeded their goal of reducing error and rework by 50 percent. All newly designed components were assembled with such accuracy that the first 777 to roll off of the production line was 0.023 inches away from perfect alignment, while most other commercial aircraft are typically a half of an inch out of alignment (13). Due to the

[1] http://www.3ds.com/corporate/about-us/brands/catia/

success of this project, many major companies followed in the footsteps of Boeing by transitioning from physical development and testing into a virtual environment. The design team believes that the implementation of a similar system will allow for the optimization of the combined collection truck developed by EAI, thus resulting in a significant decrease in weight, size, sound and cost, while increasing the functionality and market appeal of the vehicle.

Research Objective

The objective of this research was to illustrate how EAI utilized lean manufacturing principles to revolutionize the curbside waste collection process as well as to investigate the benefits and limitations of CAE systems in the full scale development of a combined collection vehicle and its sub-systems. This investigation is conducted through an "observer as participant" case study (1). The project was carried out over a period of two years by four Clemson Mechanical Engineering Graduate Students with relative expertise in: machine design, testing, fabrication, analysis and modeling. The combined collection vehicle is chosen as a subject of study because of its complexity, as it is a larger scope than typical academic engineering design projects. Furthermore, this project was a re-engineering project, thus providing a benchmark for comparison between the role of CAE and engineering knowledge, and the initial approach without engineering tool support.

The research first demonstrates how EAI and the design team utilized lean manufacturing principles to streamline the current curbside collection process. Through the development of a new "leaner" collection process, the design team was able to generate a number of constraints and criteria to assist the creation of a prototype vehicle.

Next, the current prototype vehicle will be unveiled and the limitations of the system will be discussed. An extensive case study will be presented which demonstrates how the design team utilized CAE to optimize the proposed prototype baling system. The goal of the case study is to reveal the effect that both CAE and engineering knowledge have on large scale vehicle design. An additional case will be presented to demonstrate a technique for validating results from physical experimentation with simulated results. By using the existing vehicle as a benchmark, the results of the redesigned system will illustrate the benefits and the limitations of using CAE based development.

Chapter 2 details how EAI utilized lean manufacturing principles to develop a "leaner" collection process and also presents the current prototype collection vehicle. In Chapter 3, the design team presents a number of improvements to the collection vehicle after identifying possible design flaws in the current prototype. A brief overview of the current baling system is found in Chapter 4, while Chapters 5 through 7 illustrate the case study of the redesign of the mobile baling system. Chapter 8 provides conclusions as well as future work which needs to be investigated.

CHAPTER 2

APPLICATION OF LEAN MANUFACTURING PRINCIPLES TO IMPROVE THE CURBSIDE COLLECTION PROCESS AND COLLECTION VEHICLE

Analysis of Current Municipal Solid Waste & Recycling Collection Process

The current standard for the residential waste collection process consists of the curbside pickup of municipal solid waste (MSW) and recyclable material in two steps with two individual vehicles, one for the collection of MSW and one for recyclables. Generally, there are multiple operators for each truck, with a maximum of three per vehicle. A simplified model of the curbside collection process was examined from a value added versus non-value added lean manufacturing standpoint (2), as seen in Figure 2.1 and Figure 2.2. It is also important to note that the collection process often varies from state to state and even from county to county, and is based on the programs and facilities in place.

Analysis of Wastes in the Recycling Collection Process

Generally, the curbside recycling process consists of a collection vehicle with one or two operators. The number of vehicles in service as well as the number of operators required is dictated by the population of the city or municipality and the number of households on a daily route. Figure 2.1 below is a simplified representation of the curbside recycling collection process.

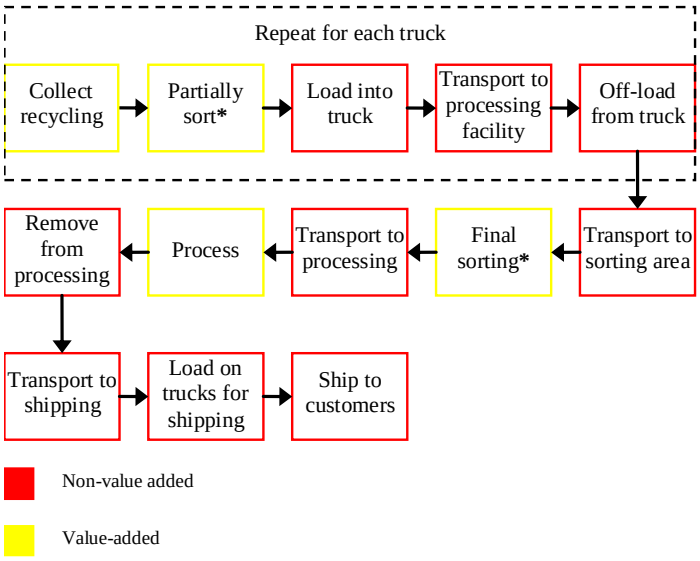

Figure 2.1: Typical Recycling Collection Process (5)

As illustrated in the figure above, value added steps are shown in yellow and non-value added steps in red. Any activity or process which does not add to the market form or function of the product (specific things which the customer is willing to pay for) is considered a non-value added process or activity; these are the wastes which lean attempts to eliminate. In contrast, value added activities are those which transform the product into something that the customer is willing to pay for (2). When considering the manufacturing of a product, value added activities are often physical transformations of the product to conform the end result towards customer desires or expectations (5). The first five steps shown in Figure 2.1 are conducted every day by all trucks in service, while the first three steps of collecting, partially sorting, and loading are repeated at every household on a vehicles daily route. The remaining eight steps take place at the MRF and occur as often as necessary. By eliminating or minimizing the number of non-value added steps in the process, the efficiency of the curbside collection of recyclables can be positively affected. For instance, by processing the goods in the vehicle, the recyclables

only have to be transported to their final destination, minimizing the movement of the product and therefore increasing efficiency. Unfortunately, motion and transportation wastes (8) such as transporting and loading goods cannot be eliminated, but they can be minimized.

Analysis of Wastes in the MSW Collection Process

The curbside collection of MSW generally consists of a standard refuse collection vehicle with either a two or three man crew. Similar to the collection of recyclables, the number of vehicles in service is dictated by the population of the city or municipality; multiple vehicles are operated in order to service all of the households on a weekly or biweekly basis. The conventional daily curbside collection process for MSW is demonstrated below in Figure 2.2. The collection of MSW is a value added activity because the homeowner or customer pays for the collection service. Similarly, off-loading the MSW into a landfill is also considered a value added activity. Although the collection companies are charged large fees to deposit waste in the landfill, the process is still considered value added because the customers are actually the residents whose taxes pay for the MSW to be deposited into the landfill.

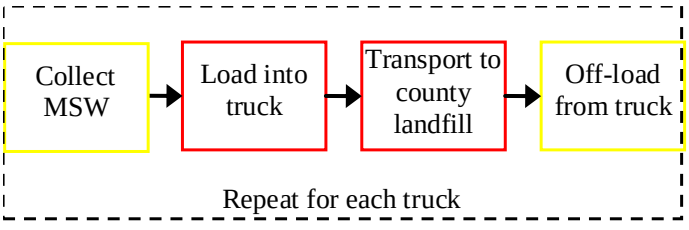

Figure 2.2: Typical MSW Collection Process (5)

Unfortunately, loading the waste into the collection vehicle and transporting it to the county landfill are non-value added steps, and are considered motion and transportation wastes respectively (8). The curbside collection of MSW is a relatively "lean" process with only 50% of its operations considered to be non-value added. Much like the transportation of recyclables, it is not feasible to eliminate these two non-value added steps; however, an attempt should be made to minimize the effort spent on these steps. In the current process, each refuse truck in service travels to the landfill and back at the end of each day's route. Therefore, the amount of time and labor associated with this waste is substantial. Moreover, the large number of trips to the landfill increases gasoline consumption, vehicle wear and required maintenance. Thus, reducing the number of refuse trucks which travel to the landfill each day would not only minimize the time associated with this non-value added step, but it would create a significant cost advantage and potentially extend the service life of the refuse vehicles. EAI hopes to realize the savings fully by proving that three of their combined collection vehicles can replace four standard trucks (2 MSW and 2 recyclables) (5).

Proposed Municipal Solid Waste & Recycling Collection Process

By analyzing the curbside MSW and recyclable collection process from a lean manufacturing standpoint, a significant number of non-value added activities were identified and can either be eliminated or reduced, making the overall process more efficient. Environmental America Inc. (EAI) has proposed a collection process which will improve the overall material flow through the use of a "collection vehicle specializing in the combined collection of raw waste and recyclable waste" (14). Their

"hybrid" collection vehicle, when combined with localized, low-impact material off-loading facilities has the potential to revolutionize the industry.

Current Prototype Vehicle

EAI has proposed using a single "hybrid" collection vehicle which is designed to collect and process both MSW and recyclable materials. Through the implementation of this vehicle, the non-value added activities or "wastes" of the collection process will be either reduced or minimized, thus effectively streamlining the process. The process wastes are removed through the clever design of the collection vehicle. By sorting and processing all recyclable goods onboard, the use of a material reclamation facility (MRF) is no longer necessary, which would eliminate the wastes associated with it. Furthermore, the tasks once accomplished by two unique vehicles, one for MSW and one for recyclables, can now be performed by a single vehicle, consequently reducing labor costs, vehicle maintenance, and energy consumption.

The original EAI prototype vehicle, illustrated in Figure 2.3 below, was designed to be operated by a three man crew.

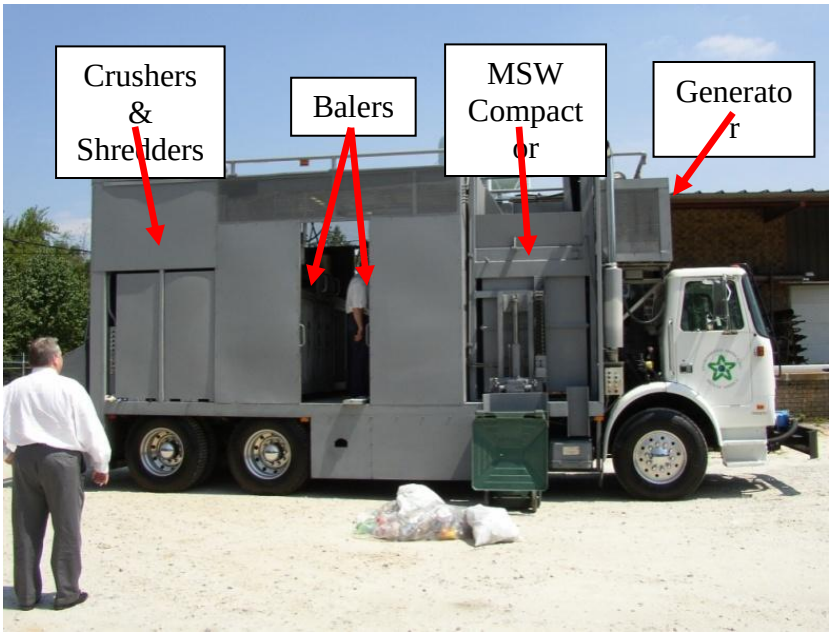

Figure 2.3: EAI Collection Vehicle

The truck utilizes a sorting table, located at the rear of the vehicle, where one operator collects and completely sorts the recyclables by loading them into specific hoppers, as seen in Figure 2.4. Once the hopper is full, through the use of a Programmable Logic Controller (PLC), the materials are lifted above the truck, deposited in the proper location and then processed. Multiple processing systems are used onboard to process the recyclables; plastics are shredded, while a variety of glasses, aluminum, and steel are crushed. The processed goods are collected in one of four large containers located in the rear of the vehicle. When the bin is completely filled, the container is simply removed with a forklift and replaced.

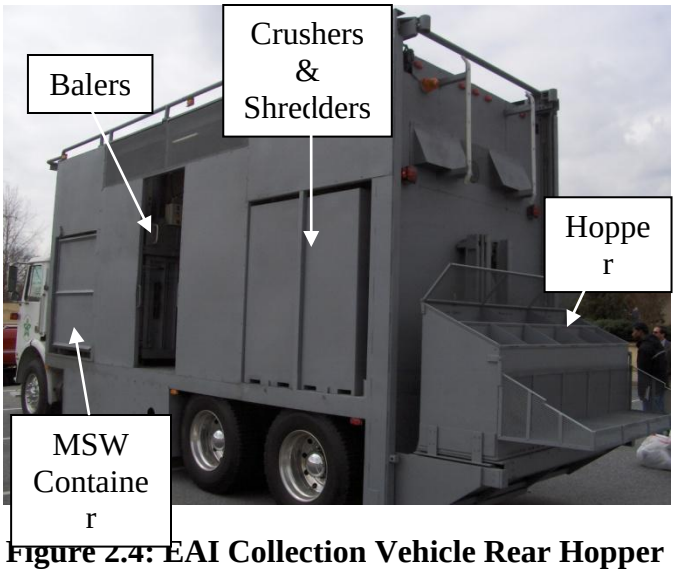

Figure 2.4: EAI Collection Vehicle Rear Hopper

Additionally, the prototype vehicle uses a baling system which is located in the open center of the vehicle, shown below in Figure 2.5. The baling system is managed by a second operator who sorts paper, cardboard, and chipboard into one of six individual bins. Once a densified bale is achieved, the operator positions one of two hydraulic rams directly over the desired bale and compacts the materials to store them more efficiently.

Figure 2.5: Baling System of Current EAI Prototype Vehicle

When the material is off-loaded, the baler doors are opened and the material is removed through the aisle. The final operator, the driver, is responsible for attaching the trash can to the automated side loader, seen in Figure 2.3 above, which empties the MSW into the truck where it is compacted. Similar to the shredded and crushed materials, a full MSW container can be off-loaded on the driver's side of the vehicle through the use of a high capacity fork lift.

Revised Curbside Collection

The revised curbside collection process proposed by EAI is shown in Figure 2.6, in which the first few phases of the recycling and MSW collection processes are conducted on the same vehicle. Due to the combined nature of this vehicle, the MSW collection is conducted concurrently with recyclable collection, sorting and processing, thus reducing the lead time once associated with all of these steps. The two disconnected sorting steps of the current process are replaced by one step conducted by two operators at the curbside, therefore streamlining the process further. It is important to note that since the material is only sorted once in the proposed process, it is imperative to train and motivate operators in an attempt to avoid or minimize possible contamination because unfavorable levels of impurities significantly reduce the value of the bale.

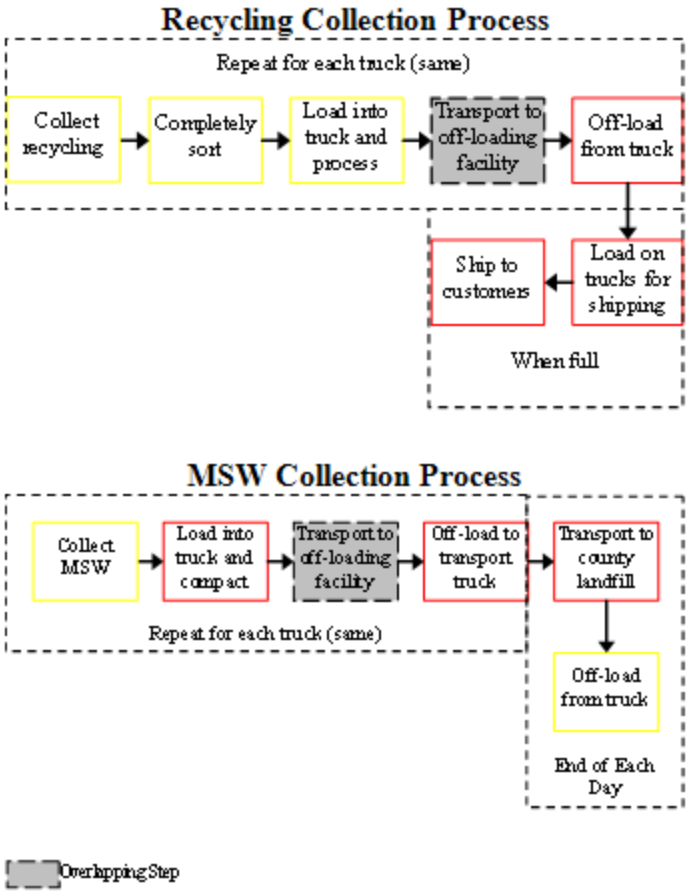

Figure 2.6: Proposed MSW & Recycling Collection Process (5)

By sorting and processing the recyclables onboard, an abundance of the motion and transportation wastes (8) identified can be eliminated or reduced. The processing of recyclables onboard makes landing the material onto the truck a value added process because it directly results in transforming the material into something which the recycling company is willing to purchase. Similarly, due to the onboard processing of recyclables, the processed materials no longer have to be transported to a MRF for additional sorting and processing because it is offloaded from the truck in its final state. The material is either offloaded directly onto a transport truck where it will await final shipping to a

customer or will be stored at a local, low impact facility until final transportation is required. This process is repeated for the entire fleet of vehicles until the transport trucks are full, upon which they are shipped to the final customer.

In order for this process to be realized in its entirety, EAI proposes the implementation of multiple local, low impact off-loading facilities. This is a unique solution because currently, most municipalities or cities utilize a central county facility. Essentially, EAI proposes that each city or municipality would build and maintain their own off-loading location. Each of these facilities would require less than an acre of land and would consist of a small building and a loading dock. To make this proposal more appealing to neighbors, the only material stored inside of the building will be the processed recyclables, which are not malodorous, and would only be stored for a very limited amount of time, until a full truck-load is achieved. The only required equipment at these off-load facilities are forklifts, thus, not only will these facilities have minimal effect on the environment, but they will also be extremely affordable.

The benefit of the low impact off-loading facilities is that their relative location to the service route is significantly reduced when compared to the current system. The close location of the facilities will drastically reduce the transportation waste associated with the current recycling collection process. By minimizing the distance between the service route and the off-load facility, labor, energy consumption, vehicle service life and maintenance are reduced. One significant benefit of the local, low impact facilities is that each city or municipality is able to generate their own revenue from the sale of recyclables.

EAI's proposed MSW collection process states that the material is to be off-loaded from the vehicles at the same local low impact facility as the recyclables. In the vehicle, the compacted MSW is housed in a closed container; this container will be off-loaded at the end of each trucks route and moved onto a large transfer truck. At the end of the day, the entire truck load of MSW will be transported to the landfill and dumped, thus reducing the frequency of which raw waste is transported. Similarly, instead of having each collection vehicle travel to the landfill, only one or two transfer trucks will be required to make the trip, depending on the number of households being served. This is a very important change because currently every refuse vehicle makes this trip on a daily basis. Due to the location of the landfills, which are usually on the perimeter of the county, this is an extremely wasteful practice. Not only is the proposed process beneficial from an environmental standpoint, but it also has inherent financial benefits due to the cost of fuel and maintenance. Unfortunately, in order to implement this system, two non-value added steps have to be added to the process, which conflicts with the goal of leaning the process.

The two non-value added steps which would be added to the proposed process consist of transporting the MSW to the off-loading facility and off-loading the MSW to the transport truck. Although these steps do not add value to the process, they are indeed necessary in order to fully realize the reduction in transportation to the landfill. The negative impact of these non-value added steps is eased by the fact that all of the vehicles are already required to travel to the off-loading facility to deliver the processed recyclables. As a result of the combined collection process of the vehicle, the step denoted as "transporting to the off-loading facility" overlaps between the collection of

MSW and recyclables, as demonstrated in Figure 2.6. So, this non-value added step is already accounted for in the collection and processing of recyclables. Therefore, the only additional step required is the transfer of the MSW from the collection vehicle onto the transport truck. This process can be easily achieved through the use of a forklift and can be carried out concurrently with the offloading of the recyclables. As a result, the negative impact of the non-value added steps is negated by the highly positive impact of reducing the number of collection vehicles which travel to the landfill. Unfortunately, due to current policies in place with regards to the creation and use of transfer stations, a second MSW off-loading design was investigated. The second off-loading scenario is much simpler, but does not fully realize the benefits of the "lean" collection process. In this scenario, all collection vehicles travel to the landfill to off-load the collected MSW. Although the system does fully realize the "lean" collection process, it can be implemented immediately because it conforms to all current governmental policies.

While the proposed MSW and recycling curbside collection process, along with EAI's collection vehicle, significantly reduces the number of non-value added activities as well as streamlines the value added aspects, it also reduces vehicle fleet and personnel for a given municipality. The collection vehicle proposed by EAI is designed to collect and process waste from 350 households as opposed to the current standard 500 households typically serviced by refuse and recycling trucks. Unfortunately, this does not result in a direct replacement of two vehicles with one, but it is necessary in order to maintain vehicle maneuverability. However, three of EAI's combined collection vehicles can replace two refuse and two recycling trucks. An example of a fleet which could service approximately 4,000 houses per day is shown below in Figure 2.7.

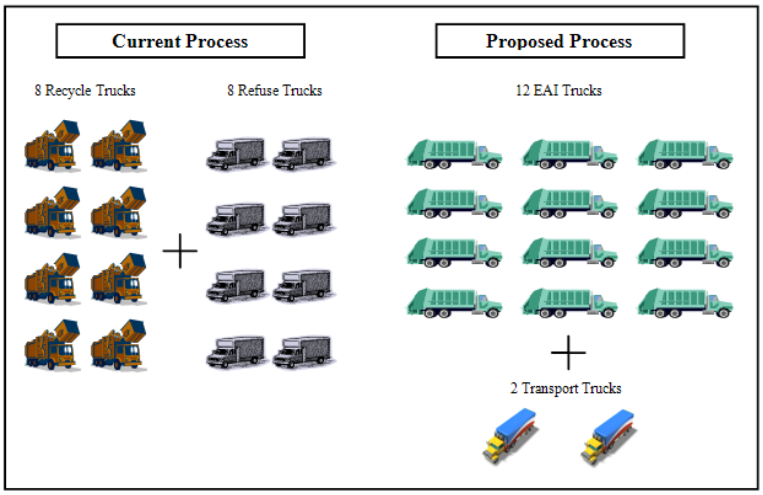

Figure 2.7: Vehicle Fleet: Current vs. Proposed Curbside Collection Process (5)

In the example above, the proposed process replaces 16 collection vehicles with 12 combined collection vehicles and 2 transport trucks. Thus, resulting in direct savings in capital investment as well as a significant reduction of personnel required. Furthermore, fewer vehicles results in a reduction in energy consumption and required maintenance. In the current process a three man crew is required to operate refuse vehicles and two for the recycling trucks, resulting in 40 workers in the example above. In the proposed process, only 2 men are required to operate the combined collection vehicles and one for the transport trucks. If the transport truck drivers also operate the collection vehicles, only 24 workers are required to service the same number of households, resulting in a 40% reduction in labor.

MSW & Recycling in the City of Clemson

In 2005, the Sanitation Department in Clemson, South Carolina collected approximately 5,556,000 pounds of MSW and 1,002,000 pounds of recyclables (15). The collected materials were then shipped individually over a distance of 20,200 miles to

deliver the waste to landfills and reclamation facilities. The Sanitation Department which services this area owns 12 vehicles that are dedicated to waste management, but only half of those vehicles are assigned specifically to the collection of MSW and recyclables. The other vehicles that are in service provide specialized collection needs, like lawn waste collection (16).

Residential collection of MSW and recyclables is a process which occurs weekly for each route. Each city resident is provided with a wheeled container for MSW and a smaller bin used to handle recyclables. The resident is asked to haul all of the waste to the curbside for disposal. At this time, the city puts all of the responsibility of recycling on the residents; if they are unwilling to sort the recyclables from their trash, there is no immediate consequence. Currently all MSW is collected by a truck which is manned by a two person crew and services about 500 houses a day. At the end of each day the crew members drive to the landfill to deposit the collected MSW regardless of whether or not the truck is full. The recycling collection is carried out on the same day as the MSW collection. A truck dedicated to recycling, follows behind the garbage truck and collects the unsorted goods. The vehicle is operated by one man who acts as the driver as well as the loader. At the end of the day the operator takes the vehicle to the Pickens County Material Reclamation Facility where the goods are sorted further. At the present time, the city of Clemson generates no revenue from their recycling program.

In 2006 the city of Clemson charged each household a monthly sanitation services fee of $6 (16). This service fee covers collection of all curbside waste for the month. Unfortunately, the overall expense to collect the waste and transport it to its final location is approximately $21.40 per household per month, nearly three and a half times the

amount that is being paid by the customer. This rather large difference is offset by revenues found in the city's General Fund, which is primarily made up of property tax monies (15). Due to the fact that the city has to dip into its General fund to help cover the cost of waste collection, they are looking for ways to minimize the difference between the monthly service fee and the actual cost of collection. Similarly, the city is trying to increase the recycling rates to meet national standards.

Presently, the city of Clemson transports all of the collected recyclables to the Pickens County recycling center where they are processed, stored and ultimately sold. Unfortunately, the city of Clemson sees no monetary return on the recyclables. Pickens County keeps all of the revenues generated from the sale of these recyclables, approximately $400,000 annually, but they are investigating the possibility of incentive programs to return some of the revenue back to the municipalities. Currently, due to operating costs and lack of revenue generated from the collection of recyclables, the city of Clemson is operating at an annual budget deficit of $46,000 in order to run their trash collection program.

Troy suggests that the city could swing their annual budget deficit to a $31,000 budget surplus through the implementation of the prototype combined MSW and recyclable collection vehicle (15). Table 2.1 shows the current operating cost for trash collection in Clemson along with the revised operating cost after implementing the combined collection vehicle and associated collection process.

Table 2.1: Recommended Sanitation Dept. Revenues & Expenses (Fiscal Year 2005-2006) (16)

Total Operating Revenues	$135,350.00
Total Operating Expenses	$181,577.00
Operating Income	($46,227.00)
Projected Recycling Revenue	$77,720.46
Revised Operating Income	$31,493.46

Table 2.1, shown above, demonstrates the budget surplus that could be realized through the implementation of the combined MSW and recycling vehicle. The revenue that can be generated through the sale of the processed recycling is approximately $78,000. Although the recyclables generate a significant amount of income for the city, the table above does not consider budget savings from the "leaned" collection process. Further research should be conducted to determine the influence of the combined collection vehicle on the city's total operating expense. It is believed that the combined collection vehicle will have significant influence on the total operating expense for the city, therefore yielding an annual budget surplus which is greater than depicted in the table above. As discussed in the previous section, some simple examples of the benefits that the combined collection truck has on the annual operating costs are reduced amount of collection vehicles, manpower and energy. In regards to the number of collection vehicles, it was shown previously that four collection vehicles can be replaced by three of the combined collection vehicles. By reducing the number of vehicles in service as well as the number of crew members required to operate them, the budget necessary to sustain the program is minimized. Similarly, through the implementation of low impact off loading facilities, the trucks are no longer required to travel to the landfill or the MRF on

a daily basis, saving on wages and on energy costs (gas, etc.) required to travel to these locations. Many of the benefits of the combined collection vehicle still remain unknown and will stay that way until the truck is implemented on a large scale.

Pay-as-you-throw & Credit-as-you-recycle

For many years municipalities have used programs like "pay-as-you-throw" (PAYT) as a way to regulate MSW disposal. The principle is that the more the throw away the more you pay, therefore the volume of MSW waste will be minimized. Troy suggests a similar program in order to drive the recycling rates to a maximum (15). This program is called "credit-as-you-recycle" (CAYR) and acts as a way to help residents offset or even eliminate the monthly sanitation service fee. Troy believes that by implementing a "positive" incentive program, the recycling rate can be driven to an all time high. He suggests using the proposed combined collection vehicle as a testbed to determine the legitimacy of this hypothesis.

Unfortunately, the hypothesis can only be validated through the development and implementation of the combined collection vehicle. Currently there is no vehicle on the market that can process both MSW and individual recyclable materials. The proposed vehicle has the means to prove the hypothesis and help to further develop PAYT and CAYR programs. Some future work needs to be conducted to determine how to accurately credit CAYR customers. Some research questions have been posed to facilitate this process. Are the customers credited as an individual or a group? Are the recyclables weighed as PET, HDPE, aluminum, etc. or are they weighed as a whole? If so, how is the value determined for this "bulk" recycled material? These are just a few questions that need to be answered in order to properly implement a CAYR program.

Once the questions are answered, the proper equipment can be added to the vehicle to ensure that the proper data is being collected. This work is a long way off and will be applied on future EAI combined collection vehicles.

Conclusion

With the current local governmental policies in place, the truck design which offloads MSW at the landfill can be implemented immediately. While this does not realize the full potential of leaning the curbside collection process, it is a significant improvement to the process in place. As the idea of transfer stations becomes more widely accepted, the ability to offload MSW containers onto a transport truck will be realized. Unfortunately, until the current policies are changed and transfer stations become more prevalent the full potential of applying lean manufacturing principles to the curbside collection process cannot be achieved.

While this may not be the ultimate solution to eliminating "waste" from the curbside collection process, it is certainly a viable solution and a step in the right direction. EAI is currently working with Clemson University to refine the collection vehicle and process with hopes of entering the market place in 2008. The company plans to apply this same onboard processing method to the future design of commercial waste collection vehicles for stadium events and high rise apartments.

To date, investors associated with EAI have spent on the order of three million dollars over the past decade developing the current prototype system. The design team at Clemson University has been asked to develop the fifth iteration of the prototype vehicle in an effort to minimize vehicle cost, size and weight. Currently, the prototype vehicle exceeds the Department of Motor Vehicles width and double axle weight requirements as

well as OSHA sound standards. The design team believes that the combination of engineering knowledge and Computer Aided Engineering software, CAE, will facilitate the creation of a vehicle which will conform to all required standards, while optimizing the amount of effort and capital required to successfully complete the project.

CHAPTER 3

PROPOSED VEHICLE DESIGN

Using the current prototype as a benchmark, the team redesigned the vehicle. Early in the redesign it was apparent that there were a number of areas for improvement: the vehicle chassis, MSW processing/off-loading, and recyclable material processing/offloading systems. Design for Standardizations and Design for Assembly guidelines were considered in an attempt to reduce the complexity of the system (17). The proposed vehicle consists of a low entry chassis, side loading/offloading trash compactor, and a baling system for recycled goods. Also, the vehicles superstructure is made entirely of recycled aluminum, making it more appealing to the market. Similarly, the vehicle is able to run off of a bio-diesel mixture, which makes the truck more environmentally friendly.

Chassis design

The first area for improvement for vehicle is the platform for the system. The current prototype requires a three man crew, utilizing a standard cab to house two of the operators and a rear jump seat for the third. This increases the cycle time of the vehicle because all of the tasks must be completed by crew members who are located in the raised cab of the vehicle. The use of a low entry chassis can effectively minimize the process cycle time and many commercial truck manufacturers provide a low entry option (18; 19). These vehicles often come standard with left hand drive driver's seat, standing right hand drive driver's seat and single step low entry access points (maximum step-up of 18 inches) (18). The use of the standing right hand drive eliminates the need for the driver to climb down from left side of the cab and walk to the curb, effectively reducing

cycle time. Additionally, the low entry chassis reduces the number of required operators from three to two, thus eliminating the need for a jump seat. In this case the driver drives on the right hand side of the vehicle and acts as the loader. Most low entry options are priced slightly higher than with standard entry vehicles, but the personnel savings, elimination of the jump seat and the reduction in cycle time should make up for the increase in capital cost (18).

Since the suggested vehicle design combines the benefit of a recycling truck and a MSW collection truck into one, the task of collecting these goods can be accomplished through the use of fewer vehicles. The personnel required to operate these vehicles is reduced by approximately 35%-40% depending on the trash compactor design, as discussed in the following section.

MSW Processing

The second major area for improvement was the system used to load, process, and off-load all collected municipal solid waste. The design team determined that there are two distinct scenarios to investigate when developing this system. The initial design utilizes a closed container which can be off-loaded from the collection vehicle onto a transport truck. Unfortunately, there are a few implications that must be considered. Offloading the closed container of MSW requires the use of a local transfer station, which many cities and municipalities will simply not allow due to a not in my back yard (NIMBY) mentality. By completely enclosing the containers, the cleanliness of the local transfer stations can be significantly increased, thus making it possible to negotiate an agreement with municipalities. While there is a considerable amount of red tape associated with the implementation of this off-loading scenario, there is a substantial

return on investment which is not realized with the alternative solution. As previously discussed, the use of this system will reduce the number of vehicles travelling to the landfill on a daily basis, consequently decreasing vehicle fuel consumption, vehicle emissions, and personnel cost, while improving the service life of the vehicles. Unfortunately, the political red tape isn't the only negative aspect of this system. In order to empty the closed MSW containers, an extremely expensive forklift will be required at every landfill.

The second scenario for off-loading is far simpler, but does not fully realize the advantages of the proposed "lean" collection process. In this scenario, the vehicles travel individually to the landfill to off-load the collected MSW. The obvious benefit of this system is that it eliminates the need to reverse current local and state government policies regarding transfer stations and it can be implemented immediately. However, the implementation of this system will increase vehicle wear, emissions and personnel costs. Similarly, since the delivery of the MSW to the landfill is a non-value added step, the process is no longer as lean as possible. Therefore, from a lean manufacturing standpoint, the first scenario is superior, but due to policies in place nationwide, it is very unlikely that it can be implemented on a large scale at this time. Thus, the first generation of the "hybrid" collection vehicle will need to be designed with a MSW processing system that can off-load the compacted MSW at any location.

Recyclable Processing

Another large area for improvement is the system(s) used to process the recyclables. Currently, the processing systems for the recyclables are numerous and unique, which is not advantageous for the production, operation, and maintenance of the

vehicle. EAI's current prototype vehicle utilizes both hydraulic and electric motors to power the shredding, crushing and baling units. In order to accommodate the high power consumption of all of these individual systems, a large externally mounted generator was required. Unfortunately, although the generator is required for the current vehicle, it is a large source of uncontained sound, making the vehicle unable to conform to current DMV and OSHA sound standards (20). This transition can be made through use of a single unique recyclable processing method which only utilizes hydraulic power. By eliminating the electrical system, the vehicles sound output will be greatly reduced, allowing it to comply with DMV and OSHA sound requirements.

The design team also investigated the benefits of two of the current recyclable processing systems; baling and shredding. It is important to note that the redesign of the EAI prototype vehicle focused significantly on the techniques used to process plastics because they are often considered the most complicated material to process. Conversations with various contacts within the field of recycling indicated that the market is more willing to accept PET and HDPE plastics, in either baled or shredded form. In order to evaluate the viability of the two processing techniques, we must first define baling and shredding. Recycle.net (21) defines baled PET and HDPE plastic as follows:

> ***"Assorted PET bottles or containers compacted into secure bundles with a minimum weight density of 10 lb./ft3. May contain Post Consumer PET Soda Bottles of mixed colors"***

And,

> ***"HDPE Mixed Postconsumer Scrap (baled) shall consist of assorted High Density Polyethylene (HDPE) bottle and container scrap compacted into secure bundles with a minimum weight density of 10 lb./ft3."***

The standard process for creating bales utilizes at least one hydraulic ram which is used to compress the sorted recyclables. Once densified, the material is strapped with multiple steel bands, which run laterally and longitudinally. It is standard practice for these bales to be moved using forklifts to an area where they are stored until a full truck load, more than 40,000 pounds, is achieved. It is necessary to accumulate a full truck load before selling the processed material because a bulk load returns the highest market value.

The typical definition for shredded plastics is not as simple and straight forward as one might imagine. Recycle.net (21) offers definitions regarding the spot market prices of shredded plastics:

> **"Colored PET Regrind shall consist of reground sorted colored PET bottles or containers. HDPE Mixed Postconsumer Scrap (loose) shall consist of reground flake of assorted High Density Polyethylene (HDPE) bottle and container scrap."**

The problem with shredded recyclables lies in the fact that there is no set standard regarding the size of shredded flakes that are defined as regrind. For example, a representative from Canusa Hershman Recycling Company stated that they accept plastic regrind flakes that are 3/8 inch in diameter (22). While, a representative from Polychem USA considered regrind to be 1/8 inch or smaller in size (23). Also, there does not appear to be a standard method or technique for generating said flake quality. This information varies from one recycling company to another due to the fact that regrind is

usually produced at the recycling facilities. The recycling companies seem to prefer bales to shredded plastic due to the ease of transportation of the bales compared to loose regrind. Similarly, there is minimal information regarding the standard for producing and cleaning the processed flakes as well as an established efficient method for transporting them to the recycling facilities.

A mobile shredding system on the vehicle would operate in a similar fashion as the units on the current prototype vehicle. The sorted recyclables are fed manually or automatically into a chute and quickly engaged by a shredding device; the processed material passes through the shredder and is deposited into a container. EAI has demonstrated interest in utilizing an industrial vacuum to remove the processed goods. Although this solution appears to make off-loading processed material much simpler, it introduces a number of complexities to the system. First, the vehicle will need to be outfitted with a robust plumbing system, which will sustain a large negative pressure scenario. Also, this solution introduces a new system required at the local, low impact off-loading facilities. The once simple, low cost structures will require a large power supply as well as the very expensive vacuum system. Furthermore, in order to pass the processed recyclables through the vacuum system, the material must be sufficiently dry before off-loading, thus requiring the addition of a drier to the vehicle, which increases cost and weight. Finally, once off-loaded at the local facility, the processed recyclables must be re processed and thoroughly cleaned in order to meet customer specifications for regrind size and contamination. In order to realize full market value, the material would have to be stored until more than 40,000 pounds could be sold at one time. Therefore, a

packaging method would have to be developed to make the shredded plastic easier to handle.

The design team was offered a number of recommendations from the representative at Polychem USA who works mainly in the sales of plastics. He suggested that shredding or grinding of a material should not be considered by a pre-recycling firm unless "they know what they are doing" (23). He also mentioned that although some plastics enter the recycling facility in shredded form, the recycling company is most likely going to reprocess the material again. However, while handling the processed shredded plastics with a vacuum would indeed be innovative, if the city wants a recycling firm to pick up the plastics, it is expected that it be in the form of bales.

Baling Recyclables On-truck

The feasibility of a mobile baling unit for recyclables was assessed using EAI's most current prototype vehicle. Data gathered from a 125 house "blue box" test, which was conducted by EAI, was utilized to quantify the volume reduction achieved by shredding plastic. Also, standard volume-to-weight conversions were used to estimate the volume reduction for the baling of plastic. In order to be widely accepted by recycling firms, a bale of plastic must have a minimum density of 10 pounds per cubic foot. The estimated values for the volume reduction from shredding and baling plastic are shown for the expected collection of 350 households in Figure 3.1.

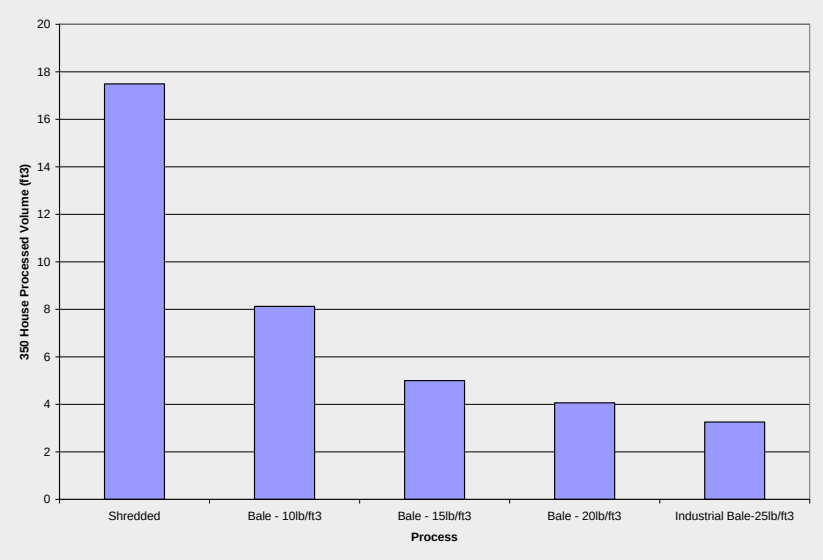

Figure 3.1: Volume Reduction of Shredding vs. Baling Plastics (5)

Figure 3.1, pictured above, demonstrates that the volume reduction achieved by baling is significantly larger than that of shredding. Therefore, an experiment was performed to determine the feasibility of baling plastic onboard the vehicle because the balers were previously only used to process cardboard, chipboard, and other paper products.

An experiment was conducted using a single overhead hydraulic cylinder baler which is located on the current EAI prototype vehicle. The test would determine if the minimum density required by the recycling firms could be achieved using this elementary system. It was necessary to complete this test because all available commercial balers can easily achieve this density; however, those units are significantly larger and often use multiple horizontal stroke cylinders. PET plastic was processed during this test because it is often regarded as the material with greatest "spring back" or material rebound after

compression. Thus, the results of the test demonstrate the absolute worst case scenario for plastics and higher densities should be able to be achieved with HDPE plastic.

The procedure for this test was quite simple; first the baler was filled to the top with loose PET bottles and containers of various sizes, from 20 oz. bottles to 3 liter bottles. Then the material was compacted with the hydraulic ram, the ram was returned to the starting position, and more bottles were added. This sequence was repeated until a densified bale was achieved, as seen below in Figure 3.2.

Figure 3.2: PET Plastic Bale

The densified bale had a final weight of 208 pounds with outer dimensions of 24 x 28 x30 inches, yielding a density of approximately 17 pounds per cubic foot. As a result, the mobile baling system greatly exceeded the minimum required density of 10 pounds per cubic foot and will therefore be widely accepted by recycling companies. It is important to note that all bottles and containers had the caps removed before baling to ensure the maximum density of the bale. It is imperative to remove the caps due to the fact that the hydraulic ram does not generate enough force to burst the containers.

Therefore, a device will be designed for the vehicle which will automatically remove the caps from all containers regardless of size.

The experiment demonstrated that the recycled plastics can be baled onboard the truck through the use of a baling system similar to that of the current prototype vehicle. Due to the abnormally small size of the bales when compared to industrial bales, a number of recycling companies were contacted to ensure that the bales would be acceptable. In both cases, the representatives stated that the bales would be accepted and one company determined that they could offer a higher price for the bales due to their low level of contamination from the removal of all bottle caps. Therefore, the optimal processing method for all recyclables, except glass, is baling.

Recyclable Offloading

The proposed design solution will utilize a low impact, low complexity offloading facility. This facility will have a small footprint and generate very little noise pollution. The vehicles will offload their bales onsite, via a forklift, to tractor trailers provided by the recycling facility, where they will be stored until a full truck load is achieved. Then the tractor trailers will be picked up by the recycling companies and empty trailers will replace them. This is similar to the current system in place at most Material Reclamation Facilities (MRF) (4). However, this facility can be located inside of the city limits since no sorting is conducted at the offloading site, therefore, allowing each individual city or municipality to generate their own revenue from the sale of recyclables.

When considering the development of this prototype it is imperative to understand whether or not the vehicle will provide a financial benefit when compared to the system which is the current standard. Initial analysis was conducted to determine the quality of

the mobile baling system by comparing bale properties against those from commercial and industrial balers. This would ensure that the mobile baling system would produce processed recyclables that would be acceptable to all recyclable processors. The design team also conducted a thorough study of the MSW and recycling collection process in Clemson, South Carolina, comparing the results against projected estimates for the "lean" collection process. Due to below average recycling rates in the area, a suggestion was generated which can be used by local municipalities to encourage recycling.

Is an Undersized Bale Acceptable in the Market?

After applying Design for Standardization principles on the current EAI prototype vehicle (17), a mobile baling system was created that would minimize the total number of sub-systems required on the vehicle, reducing the number of unique processing systems from four to two. Since nearly all commercial vertical balers exceed the design team's maximum dimensional constraints, a unique design solution will have to be investigated. The proposed baling system is a standalone unit that is made up of five baling compartments that are serviced by one sliding compacting head. This system is able to process a wide variety of recyclable materials such as PET, HDPE, cardboard/chipboard, paper, steel and aluminum. The major benefit with this mobile baling system is that the individual bale compartments can be configured in multiple arrangements, allowing collection providers to customize the vehicle to their specific demands. This customizability is very important because the collected volume of recyclables varies by region and local demographics. Additionally, the vehicle could be used to collect and process one or two materials such as PET and/or aluminum at a stadium event, which EAI envisions as a future market place. Since this baling system is indeed revolutionary,

tests were conducted to determine the effectiveness of the baler by focusing on bale density, size, and market value.

The study focused mainly on determining whether or not the mobile baler system would be able to produce bales that are acceptable to all customers. Since the mobile unit produces bales which are significantly smaller than standard commercial bales, $10ft^3$ versus $17ft^3$, respectively, it is vital to determine the viability of the undersized bales. In order to quantify the quality of the bales, a PET bale was created using the mobile baling system and the density and bale size was compared to standard commercial and industrial balers. As mentioned in the previous sections, the mobile baling system was able to create a bale of PET which had outer dimensions of 24 x 28 x 30 inches and a weight of 208 pounds, resulting in a density of approximately 17 pounds per cubic foot. It was later determined that the bale density could be significantly increased by eliminating the neck of the PET bottles, which have minimal deflection under load. Thus, the bale density achieved by the prototype baler should be a conservative estimate of what will be produced by its successor.

By surveying the field of commercial and industrial balers a range for bale density and size was determined. The bale density in commercial and industrial balers ranged from approximately 10 to 25 pounds per cubic foot for a bale of PET plastic. Therefore the mobile baling system produces bales with acceptable densities; with further development, it is believed that densities of 20 pound per cubic foot could be achieved. With respect to bale size, unfortunately, the range was too large, due to the wide variety of applications for balers. After producing the bale using the mobile system, a number of

recyclable processors were contacted to determine if the bales would be acceptable, the quoted values for the bales are found below in Table 3.1.

Table 3.1: Quoted PET Bale Value (March 2007)

	Cost, ¢/lb
Supplier 1	20-25
Supplier 2	12-18
PET Market Value	16

Table 3.1, pictured above, shows that both suppliers would accept the bales from the mobile system. Unfortunately, Supplier 2 determined that the smaller bales were more labor intensive than regular industrial bales; therefore the quoted a lower value for the bales. As a result, the mobile baler was redesigned, allowing for the production of larger bales which are easier to handle in an attempt to make the bales more desirable. On the other hand, Supplier 1 quoted a higher value than the projected market value (23) because the bales created by the mobile system contain PET plastic bottles which are free of caps, therefore reducing the level of contamination. By comparing the bales produced by the mobile system to those from conventional balers, it is apparent that the system creates bales which will meet or exceed the market standards, therefore yielding higher returns. After establishing that the mobile baling system is capable of producing bales which are widely acceptable, analysis was conducted to determine the benefit of the "leaned" collection process proposed by EAI.

CHAPTER 4

BALING SYSTEM OVERVIEW

As discussed in previous sections, the baling unit is the most important as well as the most distinctive feature on the prototype collection vehicle because it is the first of its kind. The baler unit is able to process multiple recyclable materials through the use of its moveable crushing head, which is a unique feature of this design and is a first in the baling market. The current prototype baler can process three different types of recyclable materials onboard the vehicle in the space that would be utilized by approximately two stationary commercial units. The design team will focus its efforts on reducing baler unit size, weight and cost, while maintaining or improving system strength and stability.

Discussion of Baling System

The current baler prototype utilizes are four distinct components, the baler frame, ram fixture, hydraulic ram, and the ram face. Each of the four components serves a unique purpose and allows for the unit to bale multiple materials in a mobile setting. Figure 4.1, shown below, illustrates the current baling system arrangement. The baler frame, ram fixture and hydraulic cylinder are shown in Figure 4.1 and are denoted by the colors blue, red, and yellow, respectively.

Figure 4.1: Current Prototype Baling Unit- Front View

An alternate view which presents the inside of the baler is introduced below in Figure 4.2, again, the ram fixture is shown in red and the ram face in green.

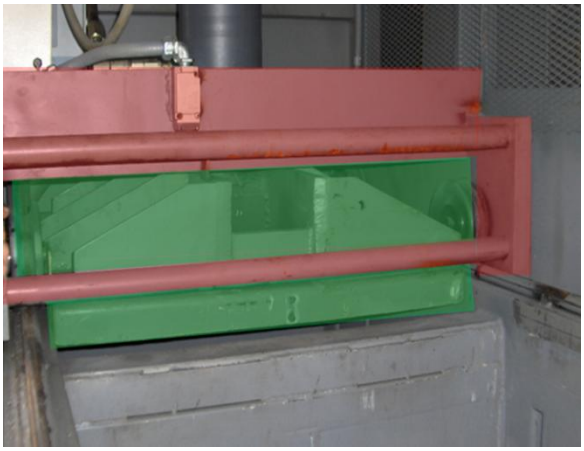

Figure 4.2: Current Prototype Baling Unit - Ram Fixture & Ram Face

In order to fully understand how the unit operates as well as the complexities of the system, each component must first be defined.

Face Plate

The ram face plate is defined as the interface component between the hydraulic ram and the recyclables. The face plate is simply a crushing surface used to spread the force exerted by the ram over a large surface area. The ram face plate seems basic in it needs, but it is extremely important in the design because it must be able to withstand large point loads from the hydraulic cylinder as well as high pressures exerted by the recyclables, while remaining light and strong.

Ram Fixture

The ram fixture is the component used to couple the vertical hydraulic ram to the baler frame. In the current prototype design, as well as the proposed design solution, the ram fixture is mounted on a fixed rail system which allows the assembly to move from bin to bin through the use of a track and roller system, as shown above in Figure 4.1. A spring loaded pin restricts the movement of the fixture by locking the unit in place when positioned properly above the desired bin. When the hydraulic cylinder is actuated, the fixture is lifted off of the track and is held firmly in place using a steel rail located on the side of the balers, the track and interface between the fixture and the rail system is pictured below in Figure 4.3.

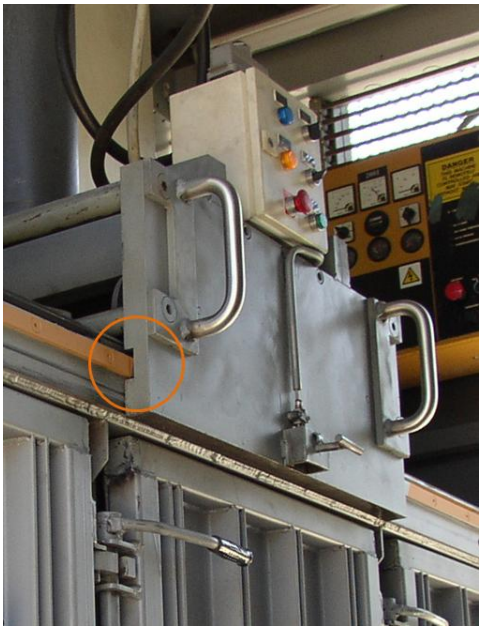

Figure 4.3: Baler Frame Rail System

The current fixture experiences approximately 60,000 lbs. of force, which is applied in the center of the fixture via a small flange on a 6 in. bore hydraulic cylinder. The force applied on the fixture is a reaction force from the ram compacting the recyclable materials, it acts in the vertical direction, and is regulated by the hydraulic line pressure. Unfortunately, as discussed in previous sections, the mobile baler must be able to produce high density bales, therefore requiring higher compaction forces. It was determined that approximately 80,000 lbs. of force is required to achieve this goal, therefore the new fixture must be designed to accommodate this elevated force constraint.

Baler Frame

The baler frame encompasses the structure located under the ram fixture with the purpose of containing the recyclables while in a loaded or unloaded scenario. Since the baler frame determines the number of individual recyclable materials that can be

processed, multiple similar wall structures will be required, thus design for standardization principles should be considered when developing a new system. For instance, the current baling system utilizes multiple structural arrangements for the inner and outer walls of the system; making the design extremely difficult to manufacture. The use of similar structures from wall to wall will not only simplify the design but it will reduce lead time as well as manufacturing cost.

The current frame uses smooth inner walls to separate the bins and to ease the removal of a complete bale. Unfortunately, due to a lack of information recorded by the manufacturer, the structure hidden beneath the walls is unknown. The baler door and rear wall are constructed using vertically aligned c-channel, see Figure 4.4 below. The purpose of this arrangement is to facilitate strapping once a full bale is achieved.

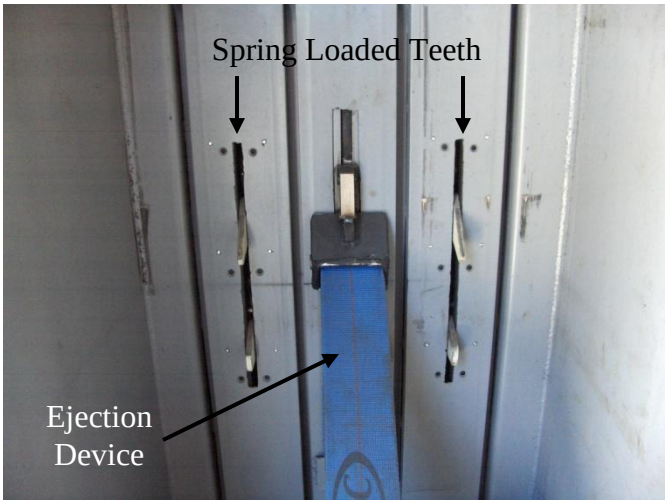

Figure 4.4: Current Baler Rear Wall Configuration

Similarly, identical channels are located in the floor so that the strapping wire can easily pass under the bale while loaded. In order to keep baled recyclables, primarily plastics, from rebounding after loading, spring actuated teeth have been added to the

current prototype to control the recyclables after compaction, as seen in Figure 4.4. The figure shown above also illustrates the ejection device which assists with the removal of a full bale. It is powered by a vertically mounted pneumatic cylinder, which is hidden behind the rear wall of the baler and is actuated by the operator. Although the ejection device seems beneficial to the removal of the bale, it unfortunately comes coupled with an extensive list of critical problems.

Pros and Cons of Current Baling System

The mobile baling system developed by EAI is very unique and utilizes many desirable features, but it also contains a number of critical design flaws. Until these flaws are investigated and fixed or removed, the system will not be practical for large scale production. The number and severity of the design flaws were not apparent to the design team until testing began on the current prototype vehicle. The hands on experience gave the design team the proper cues to facilitate the development of a new baling system with fewer design errors. From this research it was obvious that there were a number of areas that needed to be investigated and improved: the baler door hinges, spring loaded teeth mechanisms, ease of bale removal, baler weight, baler cost, & strapping technique/mechanism.

The first major area for improvement in the baler system is the hinge and lock utilized to hold the door in place. Due to the high pressures experience by the baler walls, which will be discussed in following sections, it is apparent that a significant locking mechanism must be utilized in this application. The locking mechanism which is used in the current prototype is a vertical cam lock, as seen below in Figure 4.5.

Figure 4.5: Current Baling System Locking Mechanism

When locked, the handle lies flat against the door's surface, as seen above, in order to eliminate operator error, when in the unlocked position the handle protrudes into the aisle way limiting operator movement. The locking system uses three sleeves in order to minimize deflection of the door when loaded. The sleeves double as the pivot point for the adjacent door, therefore when one door is open, the neighboring door must remain closed. Although this will reduce user error, the hinge design also limits the range of motion of the door, approximately 90 degrees. On the surface, the range of motion of the door does not seem very significant, but when coupled with other systems it causes major problems. For instance, when removing a densified bale, the limited door range causes the spring loaded teeth, located on the inside of the door, to dig into the bale, making it nearly impossible to remove it in an efficient manner. If the hinges would accommodate a larger range of motion, approximately 125 degrees, the bale would easily clear the teeth

and the removal process would be simpler, therefore this must be considered in the redesign.

The spring loaded teeth, which are designed to keep the recyclables from springing back after compaction, not only cause clearance problems in the door but also restrict the vertical movement of the bale when unloading. As discussed before, the current baling system uses a pneumatic cylinder to aide in the ejection of the bale. Unfortunately, due to the location of the teeth relative to the ejection device, shown in Figure 4.4 above, the bale is only able to move directly forward, rendering the device useless, since it attempts to rotate the bale forward around its leading edge. Similarly, after testing, the ejection device no longer functioned, most likely due to an overload scenario which was not expected; therefore the system should be improved or eliminated in future designs.

In order to utilize the sprung teeth mechanism, which is vital to the design, the new unit should be designed to ease the removal of a densified bale, allowing the bale to move forward on one plane only. The problem with the current system lies in the shape of the bale. The large amount friction force caused by material barreling coupled with movement constraints caused by the retaining teeth create an over constrained scenario, thus making the removal process extremely difficult. The effect of this large frictional force can be reduced by adding a small draft angle to the inside walls of the system, allowing the bale to be easily removed by hand or by forklift. Experiments conducted on the baling system only utilized PET plastic which is most prone to barreling under load, therefore all future balers should be designed to easily handle and off-load PET.

Weight and cost considerations were not made when developing the prototype baling unit. As discussed previously, standardization techniques were not observed when developing the structure for the prototype making the baler extremely difficult and costly to reproduce from a manufacturing standpoint. The designers were more concerned with minimizing baler deflection by overdesigning the system, therefore resulting in a product that weighs approximately 7,500 lbs and can only process three individual types of recyclables. The design team should consider both baler weight and cost when redesigning the system, all attempts should be made to optimize the system for strength while maintaining or improving the stability of the unit.

Finally, the design team determined that a new strapping technique or mechanism must be developed in order to simplify the current process. Since the current prototype vehicle utilizes a baling system that runs perpendicular to the frame rails, only one side of the baler is accessible to the operator. Due to this configuration, strapping the bale is an extremely difficult process. Figure 4.6 shows the current technique used when strapping a densified bale.

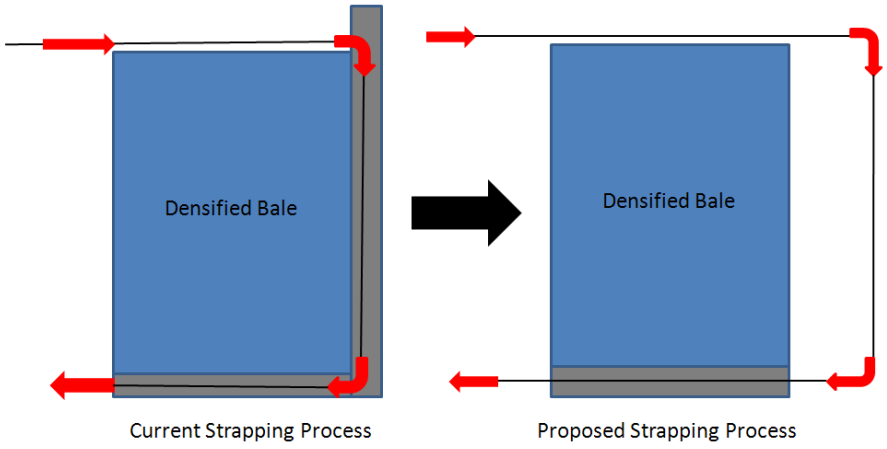

Figure 4.6: Densified Bale Strapping Processes

The process begins by compacting the bale completely, then the operator feeds a piece of heavy gauge wire, used specifically for this application, between the top of the bale and the ram face. The strapping wire is fed across the top of the bale until it impacts the rear wall of the baler. Filleted channels, shown in Figure 4.4, force the wire to deform and travel down the rear of the bale. Theoretically, once the wire reaches the bottom of the bale it would be forced into another channel which would return the wire back to the operator from beneath. Unfortunately, due to the material choice for the strapping wire, once bending occurs on the rear wall the material remains deformed, causing the wire to jump out of the channels and into the baled recyclables, therefore the wire cannot reach the bottom of the bale. To remedy this problem, the wire strapping can be inserted into the channels before loading the recyclables for processing, but this causes a hazard to the operator due to the loose ends of the wire which would remain in the aisle. Thus, a new strapping system should be developed to improve the process. The design team

determined by altering the configuration of the vehicle, the operator could have access to both the front and the back of the bale, easing the strapping and bale removal process.

Suggested Vehicle Layout

Due to unexpected complications with the strapping and the removal of baled recyclables in the current prototype, the design team decided to investigate alternative vehicle layouts which would ease both processes. Figure 4.7 shows the current arrangement of the recyclable and MSW processing systems.

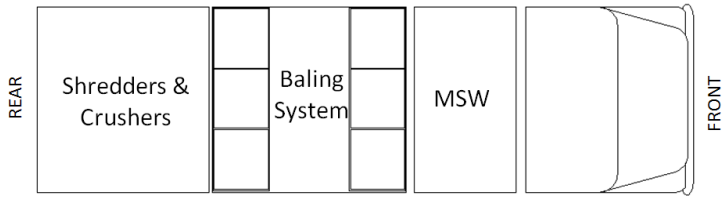

Figure 4.7: Current Prototype Vehicle Layout

The baling system is composed of two balers which can process three individual materials each. The balers face a center aisle which supplies sufficient space to open the baler doors and unload processed materials. However, the design is extremely awkward since all of the off loading work must be accomplished by hand. Also, since the rear wall of the baler shares a wall with the MSW processing unit or the shredders/crushers, access is extremely limited making strapping the densified bale almost impossible to accomplish. By rotating the balers 90 degrees, as shown in Figure 4.8, so that access doors open to the outside of the vehicle, off loading would be much more efficient since the work could be accomplished by a forklift.

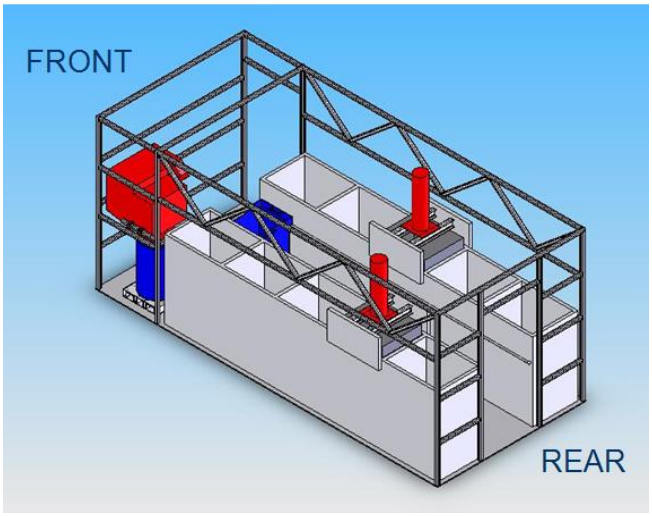

Figure 4.8: Conceptual Design of Suggested Recycling Area

As discussed previously, this arrangement would also significantly improve the strapping process. By adding access behind the baler, the strapping wire could be passed over the top of the bale to a worker on the other side, see Figure 4.6. Then the wire would then be passed back underneath the bale to the original operator, making the process much simpler since the wire will not have to be passed through a complex channel system. Although it will require another crew member to strap the bale, it will save a significant amount of time since in all previous field tests it took the design team approximately two hours to completely strap a single bale.

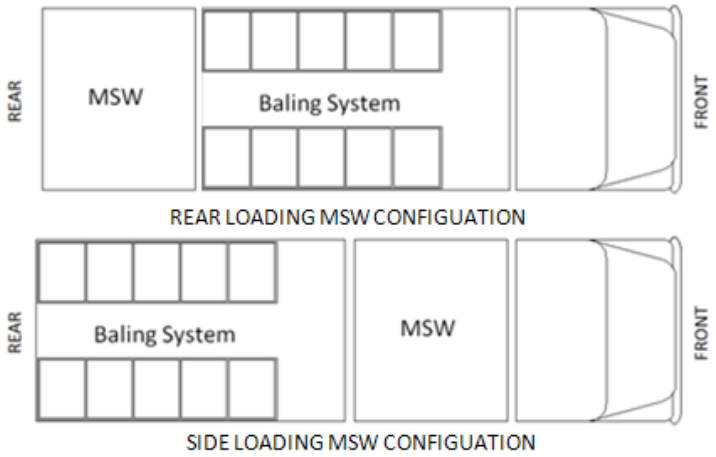

Figure 4.9: Suggested Vehicle Layouts

Figure 4.9 shows the two unique configurations that are possible when considering an outward facing baler system. The first layout utilizes a conventional rear loading/rear off loading MSW compactor with centrally located balers. The alternative uses a more compact side loading/side off-loading MSW compactor and balers located at the rear of the vehicle. The first design solution utilizes proven technology through the use of a standard MSW compactor. Unfortunately, the rear loading/rear offloading compactors have a significant amount of "dead" space as well as a much larger footprint than side loading units with the same capacity and would therefore require a longer vehicle, which would negatively affect vehicle maneuverability. Similarly, the side loading/side off-loading compactor would be unique in its design and would be accompanied with a large amount of development time. However, the second scenario allows for the implementation of a MSW compactor that could process the refuse in a closed container, which would fully realize the "lean" curbside collection process as

proposed by EAI. Since either layout is feasible in this application, a basic vehicle dynamics study was conducted to determine the preferred configuration.

Weight Distribution Analysis

Given that both vehicle configurations will significantly improve the efficiency of the baling process, a vehicle dynamics study was performed in order to establish whether a superior design exists when considering vehicle stability. Since many characteristics of a vehicle can affect the performance, only the weight distribution and center of gravity will be analyzed. Assuming that all characteristics are held constant from vehicle to vehicle, if the overall dimensions are similar, the weight distribution can help determine the performance of the vehicle.

The design team's analysis considered both unloaded and loaded scenarios, in order to observe any shift in performance that could occur throughout the course of a normal day. Information regarding MSW and recyclable weights were determined using the information gathered in EAI's "blue box" test. Similarly, subsystem weights correspond to values in the current EAI prototype and are likely to change slightly in the new vehicle design. However, if the configuration of the vehicle layout remains similar, the results will still reflect the vehicle performance with a slight margin of error. Since this test was developed to prove whether or not one configuration is superior, this error can be disregarded.

Two unique programs were developed using MATLAB to simulate both vehicle configurations (24; 25) and can be found in Appendix A. The location of all point loads associated the vehicle subsystems are hard coded into the individual program, but the weight of each subsystem can be input by the user. Therefore, if these values change

significantly, the program can be rerun with the new weights and the stability of the system will be displayed. The free body diagrams as well as the synthesis of the system equations can be found in Appendix A. Using simple static equations the weight distribution and center of gravity can be pinpointed, thus yielding preliminary information on the vehicle's stability. For instance, a vehicle with a weight distribution towards the rear will tend to over-steer in high speed cornering scenarios. Similarly, if a vehicle's center of gravity is elevated off of the ground the vehicle will be more susceptible to body roll than a vehicle with the same characteristics with a lower center of gravity.

Table 4.1 shows the results of both vehicle configurations, the weight distribution is represented from the front to the rear.

Table 4.1: Weight Distribution of Suggested Vehicle Layouts, (Front/Rear)

	Unloaded	Loaded
Rear Loading Trash Compactor	48.4/51.6	40.25/59.75
Side Loading Trash Compactor	42/58	42.3/57.7

It is obvious, since the weight distribution in all scenarios is located toward the rear, that the vehicles will tend to over-steer in cornering situations. In this case it is important to notice the weight distribution transition from unloaded to loaded, which will occur over the course of normal collection day. The rear loading scenario undergoes a transition from neutral steering to high over-steer when loaded. This is a result of the large amount of MSW collected per day when compared to the weight of the collected recyclables. The side loading compactor layout does not respond to steering transitions when loaded and therefore is the more suitable layout. Once the design team completes the new

subsystems, the updated values should be input and the response should be noted. In the future, vehicle characteristics, such as cornering stiffness and damping, should be determined so that a more conclusive vehicle dynamics study can be developed.

CHAPTER 5

REDESIGN OF RAM FACE PLATE

The focus of this redesign is on the ram face plate which is used as an interface between the hydraulic ram and the recyclables. Due to weight restrictions and a lack of engineering knowledge utilized while designing the current system, a new face plate will be designed and optimized. The goal of the redesign was to create a new face plate that would be able to handle 100,000 lbs. of downward force, while being as light as possible and easy to manufacture. The redesigned face plate is loosely based on current designs used in commercial balers. CosmosWorks 2005[2] was used along with the solid modeling package in order to perform finite element analysis on the suggested designs.

Current Face Plate

A picture of the current EAI prototype ram face plate is shown in Figure 5.1. The prototype face plate is fully welded to the hydraulic cylinder to ensure minimal movement of the plate during operation. As discussed above, the ram face plate serves as an interface between the recyclables and the ram in order to achieve an even distribution of force. The current fixture was designed to reduce deflection without the consideration of weight or cost constraints.

[2] http://www.solidworks.com/pages/products/cosmos/cosmosworks.html

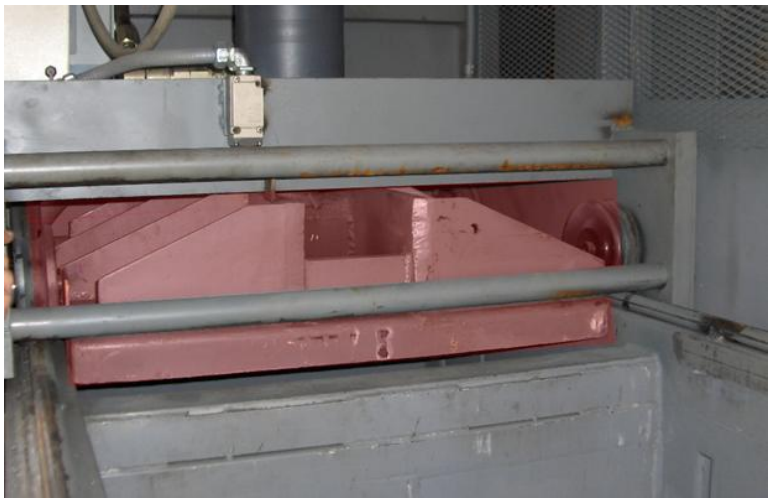

Figure 5.1: Current Ram Face Plate (Pictured in Red)

Currently, approximately 60,000 lbs. of force is applied to the face plate from the 6in. bore hydraulic cylinder which is attached to the ram fixture and is regulated by the hydraulic line pressure of the cylinder. However, due to the decision to bale high density plastics, it was determined that approximately 80,000 lbs. of pushing force would be required. Because of the new force requirement, a force of 100,000 lbs. was used for analysis in order to build in a small initial factor of safety of 1.25.

Problems with Current Face Plate

As mentioned above the ram face plate was designed without the use of engineering knowledge, resulting in clumsy design. First, in an attempt to minimize movement of the system during operation, the face plate was fully welded to the vertical hydraulic ram. Although this design does achieve minimal movement, it does not allow for efficient replacement of the face plate or the ram in case of an emergency. Since the baling system experiences a large number of cycles during its service life, a modular design should be developed, in which either the ram or the face plate can be replaced

independently of one another. Thus, a threaded interface should be considered when redesigning the components. Additionally, the face plate is extremely heavy, weighing approximately 650 pounds. Since the face plate was fully welded to the ram, designers added a significant amount of bulk to the system to ensure that the component would not fail.

Analysis of Current Model

A solid model of the current ram face plate on EAIs prototype truck was developed using SolidWorks 2007, see Figure 5.2 below.

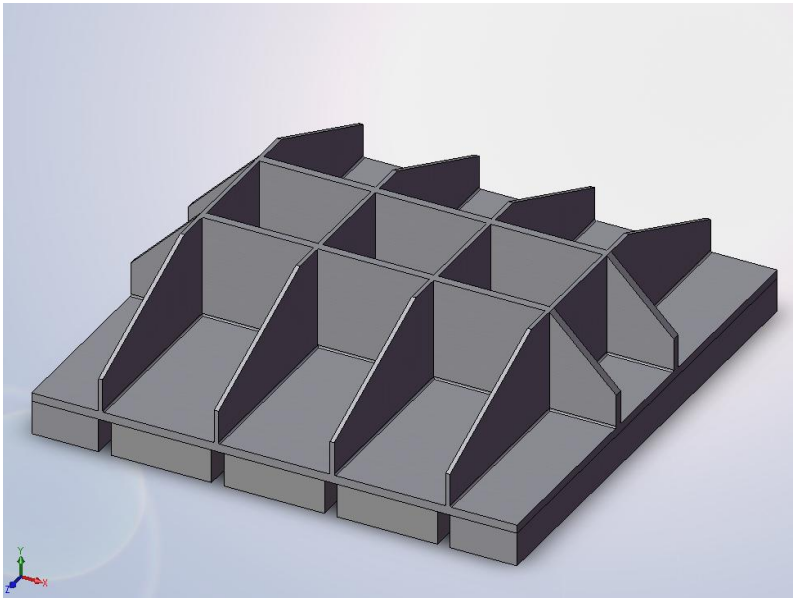

Figure 5.2: Model of Current Ram Face Plate

The virtual model served as the benchmark for the redesign as well as the basis for analyzing stress, strain and deflection of the current prototype while under static load. The 100,000 pound compacting force was applied on the bottom surface of the face plate in the form of an equivalent pressure. Also, a small sleeve, located in the center of the

face plate, was restrained using zero normal displacement in the vertical direction, shown in Figure 5.2. This restraint accurately simulates the coupling between the face plate and the hydraulic ram. The loading and restraints of the face plate are shown in Figure 5.2; the pressure is represented by vertical red arrows and the location of the restraint set is denoted by a red box (the actual restraint set cannot be seen in Figure 5.2).

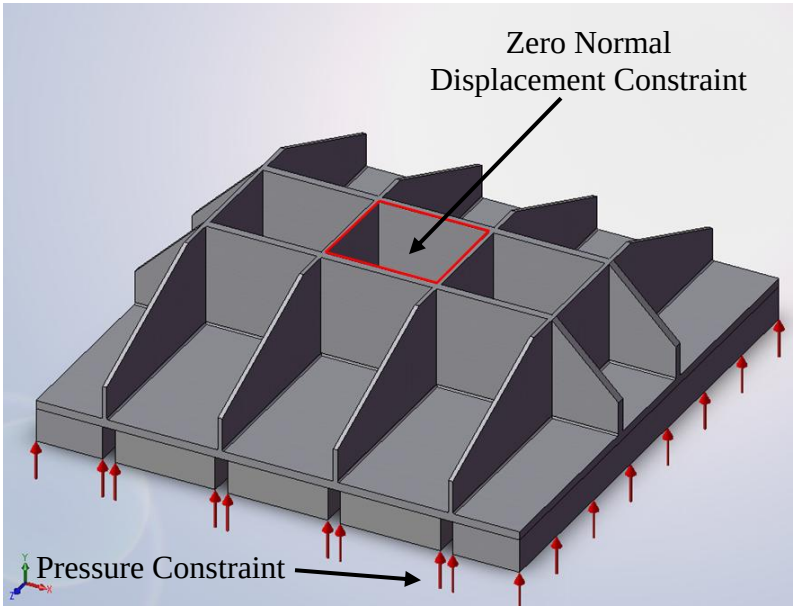

Figure 5.3: Constraint Set for Current Ram Face Plate

After creating the virtual model and applying accurate load/constraint scenarios, a solid mesh was created so that finite element analysis (FEA) could be conducted. Due to the overall size of the model, an extremely large number of elements, nearly 250,000, were necessary to converge on accurate results. Unlike the redesign of the ram fixture, which will be presented in following sections, an unlimited time constraint as well as access to high powered computers allowed analysis of a full model with an extremely fine mesh.

In order to carry out the finite element study, materials had to be defined for the system. The manufacturer was contacted to determine the material(s) used in the construction of the face plate. The bottom surface of the face plate, which contacts the recyclables, is made from 2 inch thick pieces of AISI 1020 steel bar stock, either four or six inches wide. They are stitch welded to a ¾ inch piece of AISI 1020 plate to minimize heat distortion while maintaining a high level of strength. The frame structure, which is located on the top of the face plate, is made of multiple pieces of ¼ inch thick AISI 1020 plate and is fully welded on all contact surfaces. The properties of AISI 1020 steel, as specified by COSMOSWorks, can be found in Appendix B. Once the materials were properly specified, the model was meshed and the finite element study was conducted. Figure 5.4 shown below, displays the state of stress of the face plate with a 100,000 pound force applied from the recyclables.

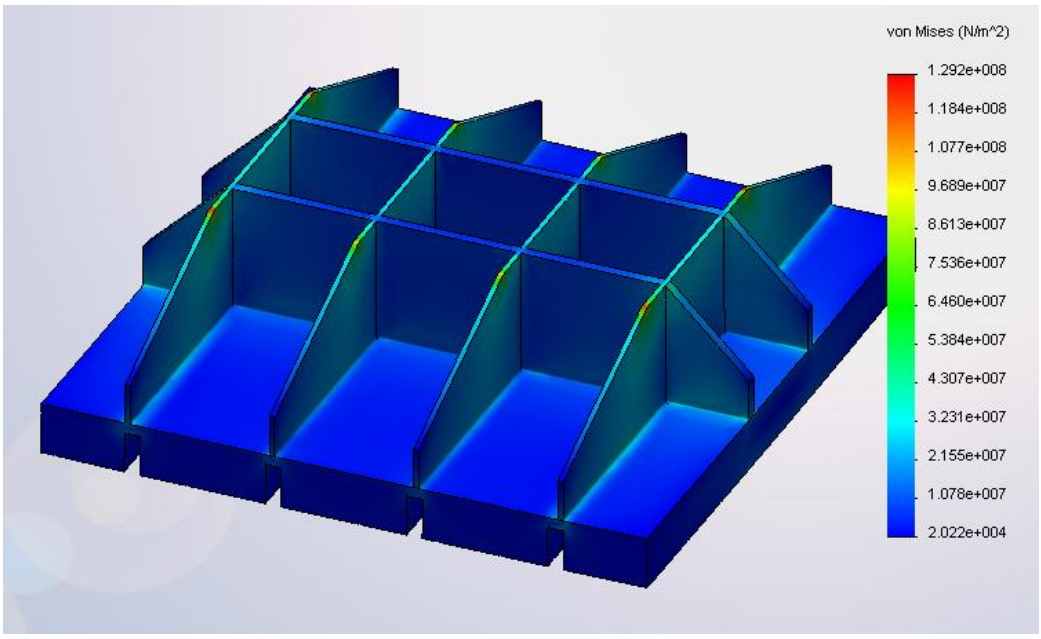

Figure 5.4: Stress Plot for Current Ram Face Plate

As demonstrated in Figure 5.4, there is minimal stress in the current face plate prototype, with the highest concentration occurring at the beveled corners of the frame structure. Due to the small amount of stress on the face plate, a factor of safety plot was created to determine the robustness of the current design, seen in Figure 5.5.

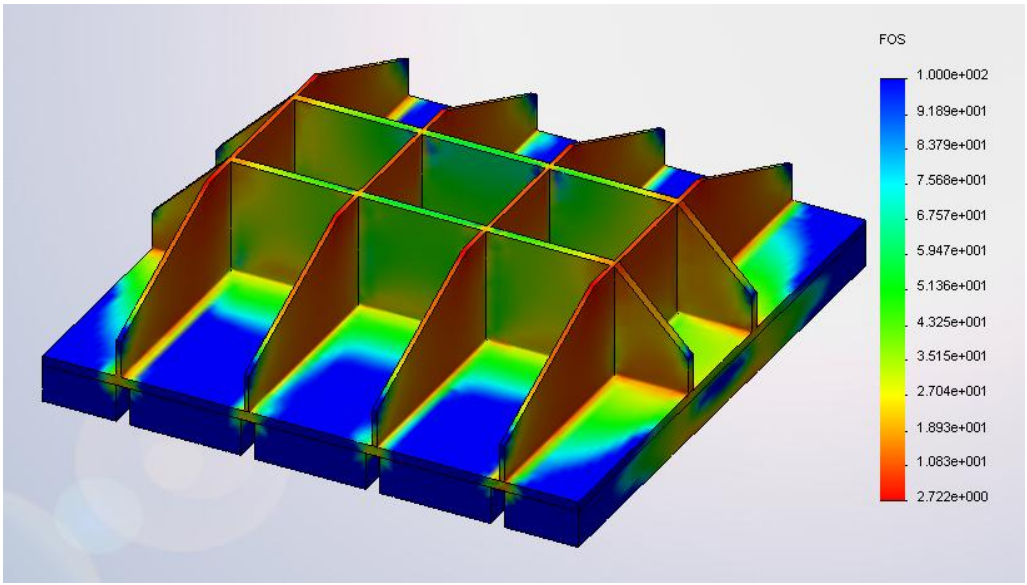

Figure 5.5: Factor of Safety Plot for Current Ram Face Plate

Figure 5.5 shows that the current face plate is significantly over designed, with a minimum factor of safety of 2.72. It is important to note that this face plate was loaded using a force of 100,000 pounds, which already contains a factor of safety of 1.25 since only 80,000 pounds will actually ever be seen by the face plate in real life applications. Therefore, it is obvious that the face plate is overdesigned and could benefit from redesign or optimization of the system.

Analysis of Suggested Face Plate Model

The finite element analysis conducted on the current face plate prototype illustrated that that system is extremely robust, with a minimum factor of safety of 2.72.

The design team determined that a new face plate needed to be designed and attempted to minimize weight and cost while maximizing strength. Figure 5.6, pictured below, shows the proposed design solution.

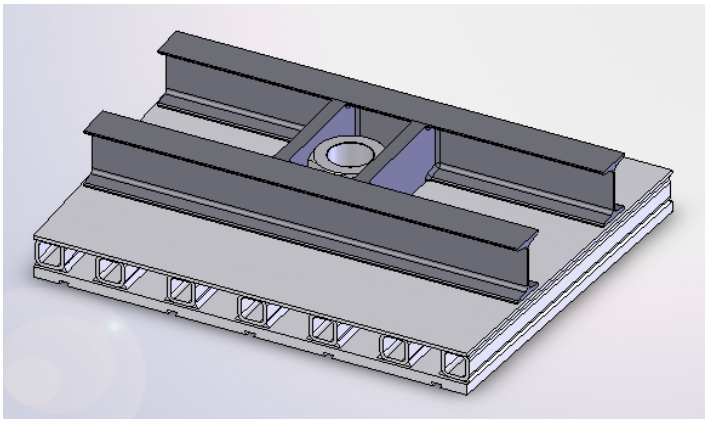

Figure 5.6: Proposed Ram Face Design

The ram face consists of two, 4 inch ANSI spec I-beams, 2 x 2 x 0.25 inch square tubing and two pieces of plate steel (¼ inch and ¾ inch thick). The structural members and plate section are made of 1020 steel, allowing the assembly to weigh in at approximately 362 lbs. A "floating" upper plate was utilized in this design in an attempt to minimize stress induced by bending. The upper plate is considered to be "floating" because it is only welded on the outermost edge allowing the plate to translate freely across the top of the square tubing, therefore reducing stress induced hot spots. I-beams and square tubing were selected based on fundamental engineering knowledge. Both are highly resistive to bending per unit volume (26) which is advantageous to the objective of system optimization. Furthermore, standard I-beams and square tubing can be purchased from numerous suppliers, therefore reducing the cost of the purchasing.

Finite element analysis (FEA) was carried out on the assembly to test the structural stability of the system while in a loaded scenario. Again, in order to properly

represent the system response, accurate constraints must be placed on the system. Similar to the previous FEA study the 100,000 pound force generated by the hydraulic ram was represented as an equivalent pressure on the bottom surface of the face plate. The plate was constrained from moving in the vertical direction through the addition of a zero vertical displacement constraint placed on the attachment nut, as seen in Figure 5.10. The upper and inside faces of the nut were limited to movement only on the horizontal plane, representing the presence of the hydraulic ram. Figure 5.7 illustrates the constraint set for the redesigned face plate; the pressure exerted by the recyclables is denoted by red arrows while the zero vertical displacement constraint is indicated with green arrows.

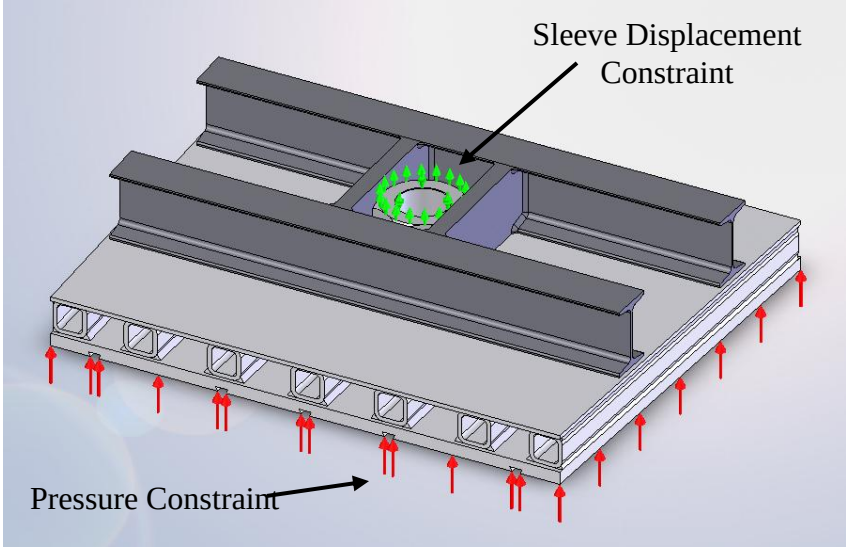

Figure 5.7: Constraint Set for Proposed Face Plate

Once the load scenario was accurately represented the FEA study able to be conducted. Again, due to an unlimited time constraint as well as access to a high speed computer, a full model with an extremely fine mesh was utilized for the study. Figure 5.8, pictured on the following page, shows the stress state of the face plate under load.

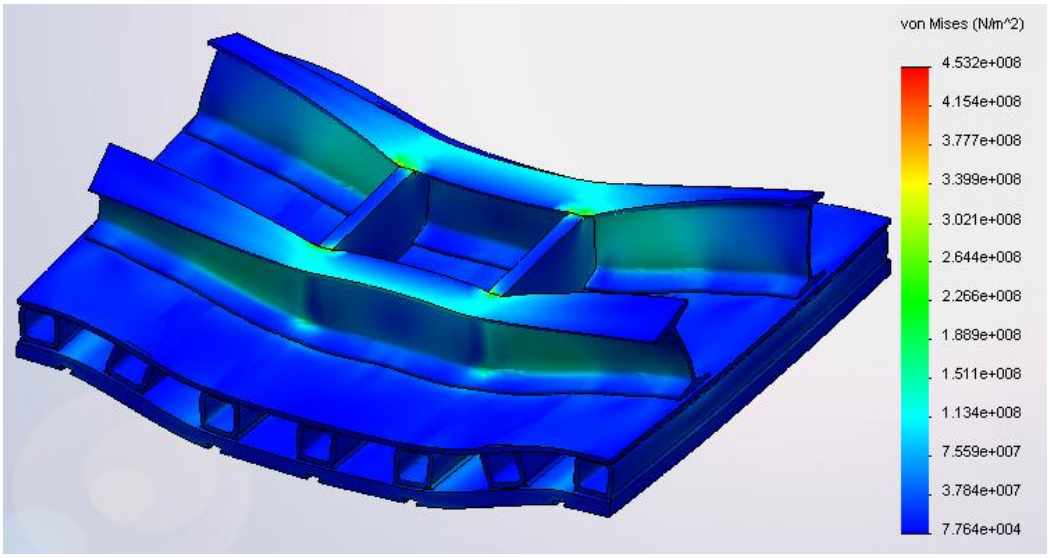

Figure 5.8: Proposed Design Stress Plot (Deformation scale of ~165)

Figure 5.8 above shows the elimination of stress across the upper plate through the use of the "floating" design. Similarly, a deflection plot was created in order to demonstrate the deflection of the face plate under a loaded scenario. Figure 5.9 illustrates the deflection of the face plate while compacting. It is important to note that although the deflection looks rather significant, a deflection scale of approximately 165 was utilized to emphasize the movement of the component; the actual maximum deflection of the face plate is 0.021 inches and occurs at the extreme corners of the plate because they have the least amount of support.

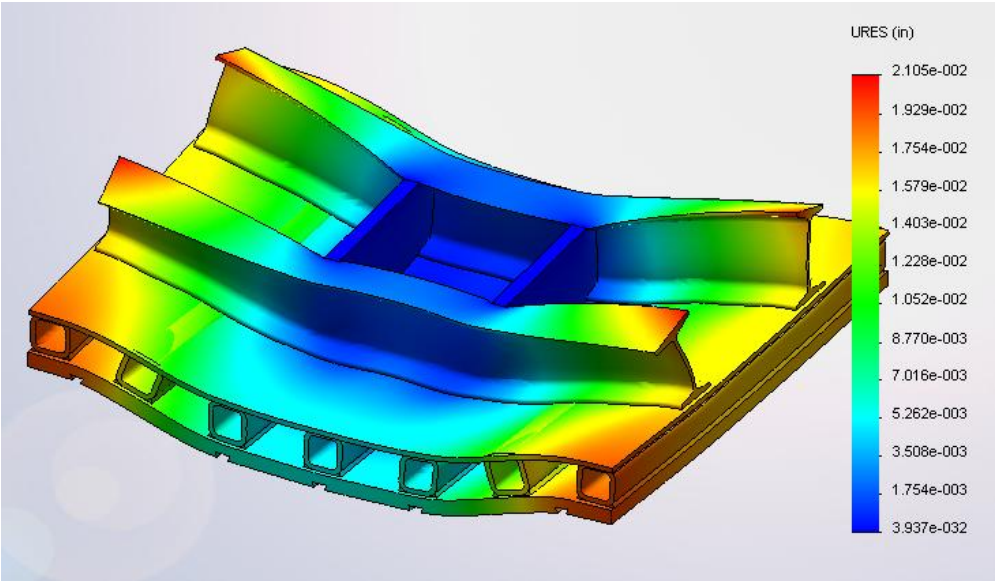

Figure 5.9: Proposed Design Displacement Plot (Deformation scale of ~165)

Referring to Figure 5.8, four critical "hot spots" were identified and are located at the interfaces between the center cross members and the I-beams. In order to investigate the affect of the "hot spots" on the design, a factor of safety plot was generated, see Figure 5.10 below.

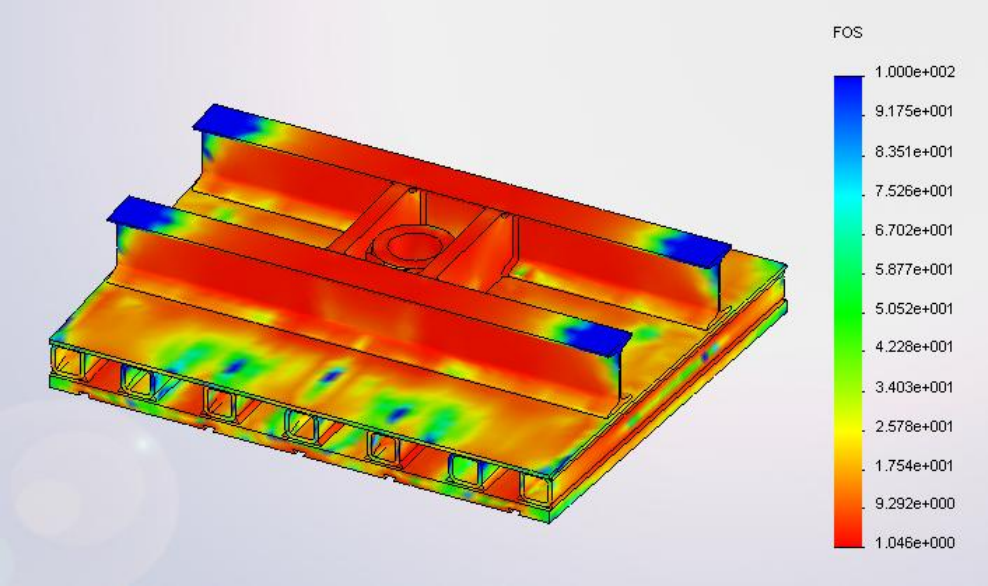

Figure 5.10: Proposed Design Factor of Safety Plot

As shown above in Figure 5.10 the estimated factor of safety of the face plate is approximately 1.05. Since a factor of safety has already been built into the magnitude of the force seen by the plate, it is safe to assume that the design will not fail while under real life loading conditions. However, the "hot spots" should be investigated to determine if they actually occur or if they are just an anomaly associated with FEA.

Through the operation of a virtual sensor, the user is able to examine the data regarding stress, strain, deflection, and factor of safety near a point of interest, which are the hot spots in this case. Multiple sensors were established on the virtual model in and around the "hot spots" in question. The stress concentrations were focused mainly near the location of welds and sharp edges, which is a common place to find irregularities in computer based FEA. The sensors showed that the factor of safety quickly elevated to around 2.5 only a millimeter away from the "hot spot". This indicates that the "hot

spots” were simply anomalies associated with FEA packages and that the redesigned face plate will not fail under normal loading conditions.

CHAPTER 6

REDESIGN OF THE RAM FIXTURE

This chapter discusses the redesign of the baler subsystem of the Environmental America Inc. (EAI) combined trash and recycling collection truck. The redesign focuses on the support structure which is used to hold the recycling compacting ram. The current fixture is mounted on a rail system which allows the whole hydraulic assembly to translate laterally from bin to bin, eliminating the need for multiple rams. The CAD package used to model the current system and design the suggested system was SolidWorks 2005[3]. The redesigned fixture is based largely on the current design by EAI, but the goal of the redesign was to allow the new fixture to support an 8 inch bore hydraulic cylinder that can generate approximately 100,000 lbs. of downward force. The current ram used by EAI is a 6 inch bore diameter and can only generate approximately 60,000 lbs. of pushing force. CosmosWorks 2005 was used along with the solid modeling package in order to perform finite element analysis and optimization on the current and suggested designs. The fixture will be optimized for volume which will therefore reduce the weight of the overall system.

In meetings with EAI, it was stated that minimal engineering had been conducted on the design of the fixture on their current prototype truck and recent observations and experiments indicated that the system could be significantly improved. Using the reverse engineering techniques discussed in (27; 28), the original assembly will be decomposed and a new design will emerge from the information that was gathered from the current prototype.

[3] http://www.solidworks.com/

Current Design

A picture as well as a solid model of the current EAI prototype system is shown in Figure 6.1. The prototype design is mounted on a fixed rail system that allows the ram assembly to translate laterally across the bins by utilizing a track and roller system. When the hydraulic cylinder is actuated and force is applied to the material in the bin, the fixture is lifted off of the track rollers and is held in place using a steel rail on the side of the bins. This configuration allows the assembly to move freely between the bins while the cylinder is at the top of its stroke and locks the assembly in place when the cylinder is actuated.

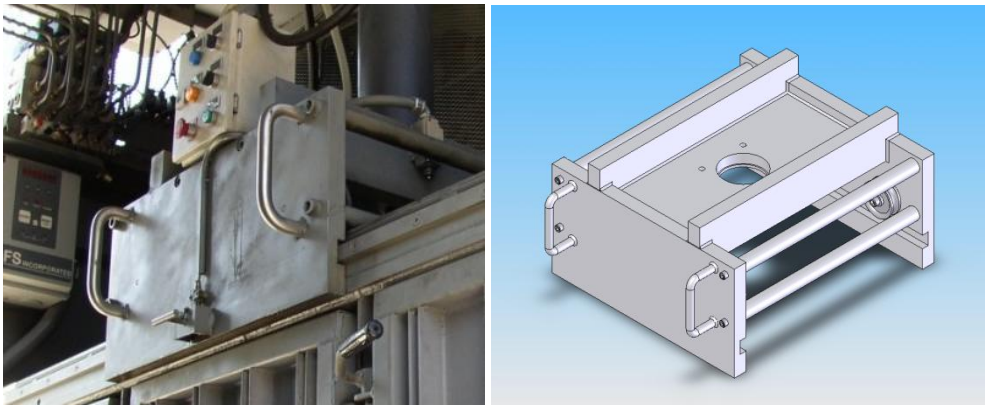

Figure 6.1: EAI Prototype Fixture and Fixture Model

Due to the decision to bale high density plastics, it was determined that approximately 80,000 lbs. of pushing force would be required. This force can either be achieved by increasing the line pressure of the 6 in. diameter bore hydraulic cylinder, or utilizing an 8 in. diameter cylinder at a lower pressure. By using the larger 8 in. diameter cylinder at lower line pressures, the service life of the cylinder should be significantly improved, reducing maintenance cost. As a result of the new force requirement, a force

of 100,000 lbs. was used for analysis in order to build in a small initial factor of safety of 1.25.

Problems with Current Fixture

The first major problem with the current fixture is that it is very heavy, weighing approximately 1,024 pounds, thus making it difficult for operators to translate the fixture across the bins even with the use of low friction track rollers. The redesigned fixture will first be optimized for material, reducing the overall weight of the system, while maintaining or improving structural integrity, using the techniques discussed by Ashby (29). Also, the design will be optimized for volume, which will also reduce the system's net weight.

Another issue with the current fixture design is that large displacements are seen in the system while under full load. The deflection in the system has already created issues in the current prototype; multiple welds have failed under load. The fixture was redesigned previously because the supporting cross members failed under the 60,000 lb. load. It is assumed that the large vertical deflection of the center of the support beams caused the welds, which are holding the fixture together, to break, rendering the system useless until redesigned. Larger cross members and a thicker bottom support plate were added, but deflection in the system is still noticeable by the naked eye while loaded. Since the forces on the system are being increased by the addition of a larger cylinder, the fixture will need to be redesigned to minimize deflection.

Analysis of Current Model

A solid model of the current system on the EAI prototype truck was created using SolidWorks 2005 and is illustrated below in Figure 6.2.

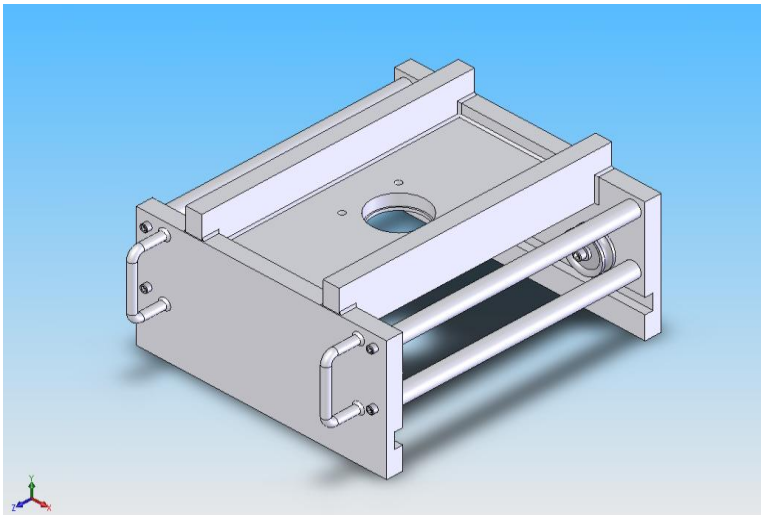

Figure 6.2: Solid Model of Current Fixture

This model served as the basis for analyzing the stress, strain, and deflection in the fixture under static loading. The 100,000 lb. compacting force is applied normal to the hydraulic cylinder mounting flange and is approximated as a uniformly distributed force. This is an accurate approximation due to the relatively small surface area of the flange. Furthermore, the bottom face of the rail notch is restrained with zero normal displacement because under standard loading it anchors the fixture to the bin and cannot move on the Y or Z axis, as shown in Figure 6.2 above. The loading and restraints of the fixture are shown in Figure 6.3; the pushing force is pictured in magenta and the zero displacement restraints in red.

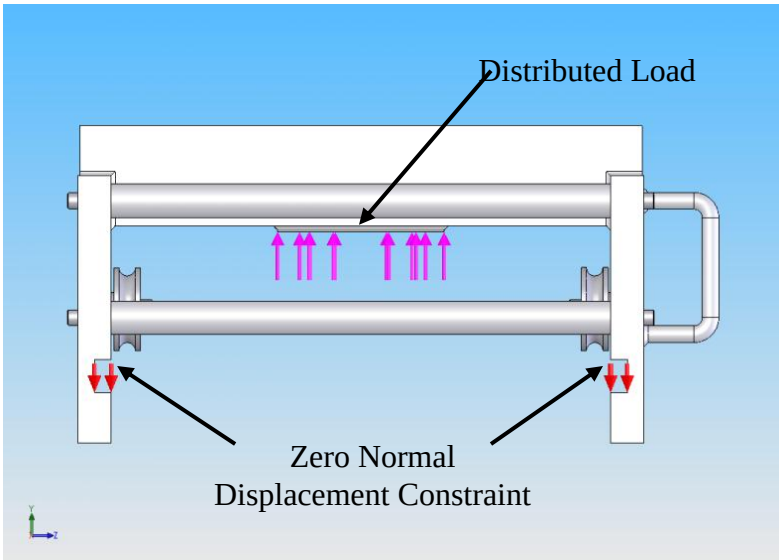

Figure 6.3: Solid Model Load Scenario

After creating the model and applying the loads and restraints, a solid mesh had to be created for the model in order to perform a finite element analysis. Due to the size of the model, an extremely large number of elements and computational power would be required to achieve accurate results. Fortunately, the model is symmetric about two axes and this symmetry allowed a quarter of the model to be used for analysis as shown in Figure 6.4 on the following page.

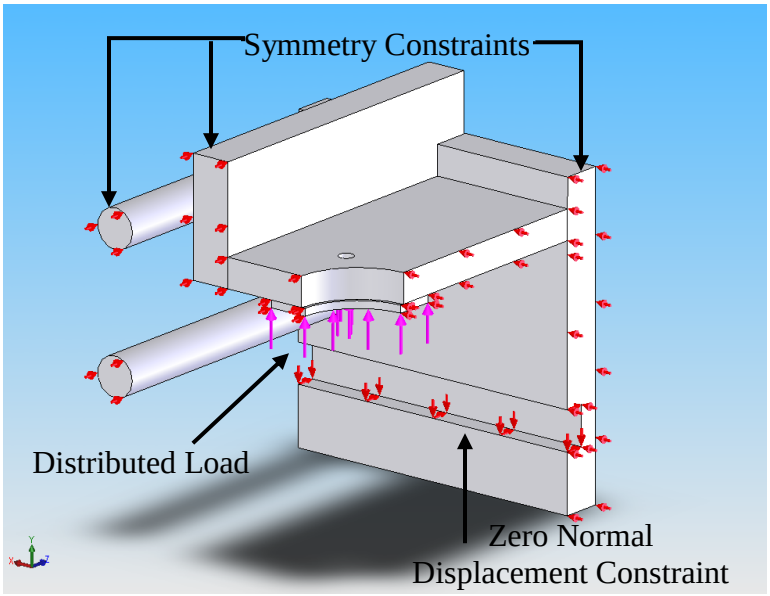

Figure 6.4: Quarter Model Constraint Set

It was absolutely paramount that the model was properly restrained with zero normal displacement/symmetry constraints on the surfaces of the model at the lines of symmetry in order to accurately model the system's behavior. Also, the force was reduced accordingly to 25,000 lbs. since a quarter model was being used.

A static stress analysis was conducted on the quarter model, which consisted of removing components that are irrelevant to finite element analysis. The components that were removed were the handles and rail idler rollers along with all unnecessary fasteners and welds. Material type was specified for the remaining components from the CosmosWorks library. Plate metal components were specified as plain carbon steel, fasteners as Grade A2 Tool Steel and weld beads as tungsten. The properties of the selected materials, as specified by CosmosWorks, can be found in Appendix B.

The next step was creating a solid mesh over the quarter model. CosmosWorks 2005 was used to create this mesh and fine mesh constraints were applied to the tapped

holes, thru holes, and filleted surfaces of the model to help ensure an accurate resolution around areas of high stress concentrations. With the mesh created, a static stress analysis was conducted, which calculated and illustrated the stress, strain, displacement and factor of safety in the model. Next, a finer mesh was created across the model and a new analysis was run in an effort to verify the results. This process was repeated for multiple mesh resolutions, as seen in Figure 6.5.

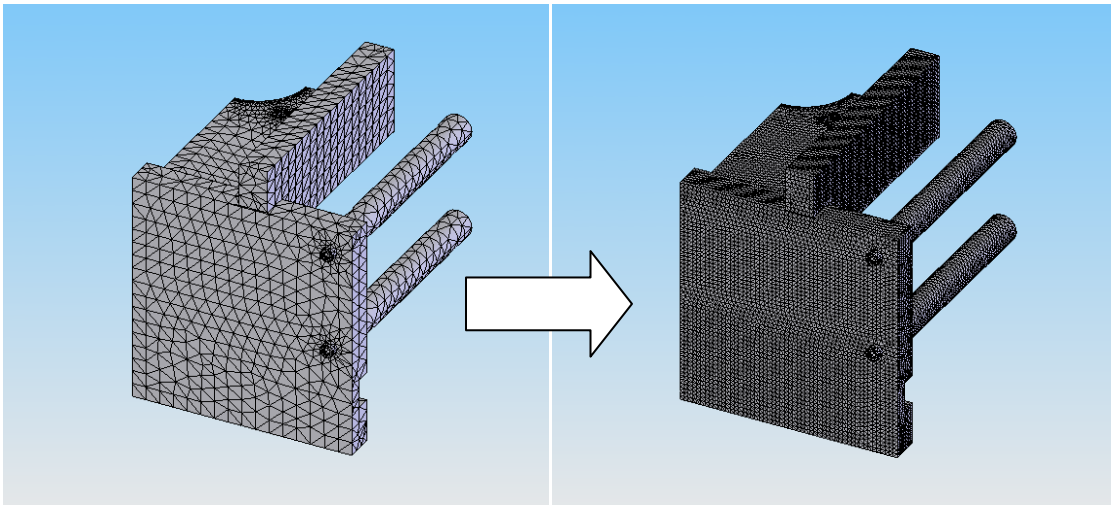

Figure 6.5: Mesh Progression (Studies 1 & 4)

Each time the model was meshed, the stress state was found for each study in an attempt to reach convergence of results. The results of the studies are shown in Table 6.1 below:

Table 6.1: Static Stress Results

Study	No. of Elements	No. of Nodes	Von Mises Stress, Pa	Deflection, mm	Factor of Safety
1	25580	41520	3.53E+08	0.8	0.62
2	34912	55587	3.30E+08	0.8	0.67
3	67209	103896	3.16E+08	0.8	0.7
4	230614	340092	3.52E+08	0.8	0.63

Due to fact that satisfactory convergence was not observed after three mesh cycles, a very fine mesh was applied. This mesh showed a large stress concentration around the surface of the flange bolt thru hole, which had previously gone unnoticed. Regardless, the results indicate that the fixture failed under the 100,000 lb. load as it had a minimum factor of safety of only 0.63, see Figure 6.6.

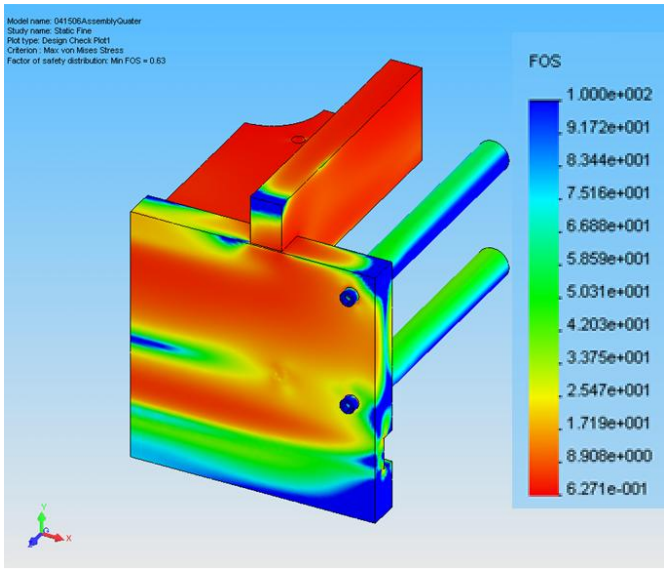

Figure 6.6: Factor of Safety Plot for Current Fixture

The current fixture design failed, therefore it was necessary to redesign the model. The factor of safety plot along with the stress plot, shown in Figure 6.7, indicate areas where the current model is under-designed and changes should be made.

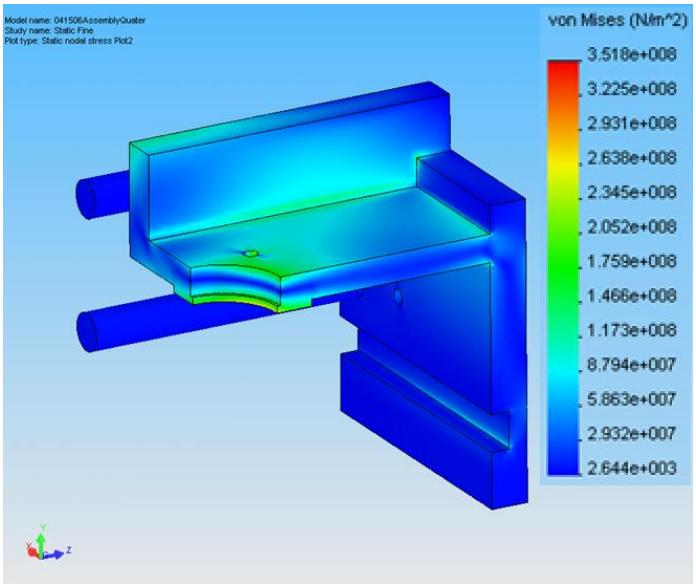

Figure 6.7: Stress Plot for Current Fixture

According to Figure 6.7, the highest area of stress is located near the bolt hole in the hydraulic mounting flange. From the information gathered, the components that need to be redesigned are the horizontal hydraulic mounting plate and the primary support beams.

Analysis of Suggested Model

Using the problem definition techniques suggested by Pahl & Beitz (12), it was determined that the center support structure needed to be redesigned. The support beams were redesigned using I-beams based on fundamental engineering knowledge. I-beams are very resistive to bending with the advantage of high strength and low volume (30; 26), which is beneficial to the objective of this optimization. Furthermore, standard I-beams can be purchased from numerous suppliers. When looking at the original design, it was apparent that the horizontal plate which mounts to the hydraulic flange was not

optimal; therefore vertical plates were used in the redesign due to their greater resistance to bending in this application.

The same symmetry, restraints and loading applied to the original model were applied to the redesigned model. The resulting quarter model used for the finite element analysis is shown below in Figure 6.8.

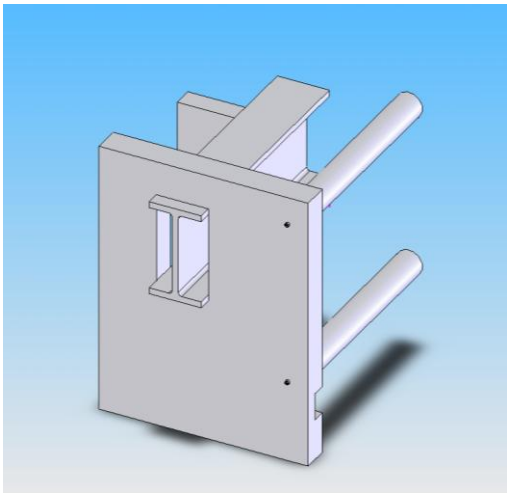

Figure 6.8: Quarter Model of Redesigned Fixture

After doing an initial static stress analysis on the model, it was observed that the front plate of the fixture would yield before the I-beam. The particular I-beam in this design is from McMaster Carr and the material was specified as ASTM 572 Grade 60 steel (31). By optimizing the material of the front plate, using the material selection techniques from (29), switching from plain carbon steel to AISI 1045 medium carbon steel, the overall minimum factor of safety of the system was increased from 0.86 to 2.1 and the I-beam became the component most likely to yield first. Due to minimal stress in the cross rods, the size of the fasteners was reduced from ¾-24 to ¼-20 in order to accommodate for future design optimization.

Multiple meshes with varying levels of resolution were created for the model until convergence was achieved. A static stress analysis was run for each mesh and the results are shown in Table 6.2.

Table 6.2: Static Stress Analysis Results for Redesigned Fixture

Study	No. of Elements	No. of Nodes	Von Mises Stress, Pa	Deflection, mm	Factor of Safety
1	158763	246428	2.53E+08	0.5	2.1
2	171686	264791	2.58E+08	0.5	2.1
3	180288	278630	2.58E+08	0.5	2.1

With convergence reached, the model was further analyzed. The minimum factor of safety for this design was 2.1, indicating that the design could successfully support the 100,000 lb. load. The factor of safety plot is shown in Figure 6.9.

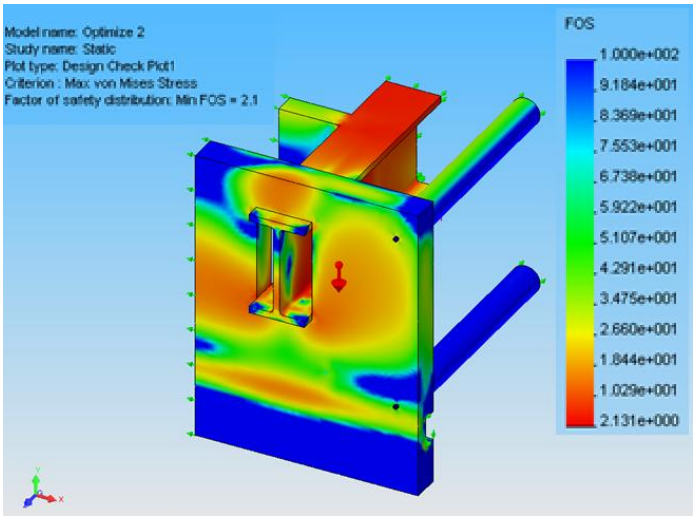

Figure 6.9: Factor of Safety Plot for Redesigned Fixture

The plot shows that the minimum factor of safety is located in the I-beam, meaning that the I-beam will likely fail first which is desired in this application. This is beneficial from a maintenance standpoint because the I-beam is a standard commercial

part that can be easily purchased and replaced with minimal effort. If the front plate were to yield first, the cost of material alone would be far more than that of the I-beam. A large amount of labor would be required on the front plate as well. The bolt hole would have to be precisely drilled and the channel groove would have to be cut, adding addition cost to the already expensive component. The stress analysis plot, shown in Figure 6.10, supported the likelihood of the I-beam failing first as it has the highest stress of the system.

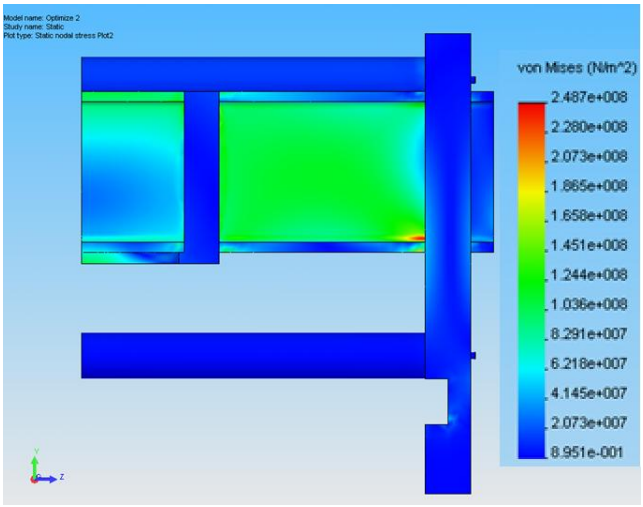

Figure 6.10: Stress Plot for Redesigned Fixture

The stress plot shows a stress concentration in the I-beam near the weld attachment to the front plate. This indicates that the attachment method could be revised in order to reduce the stress concentration. A short fatigue analysis was conducted to ensure that the I-beam would not be affected over time due to the high stress in the lower I-beam. The results showed that the I-beam would be able to tolerate infinite cycles without damage because the stress was far below the endurance limit of the material.

Redesign of Attachment Method

From the stress plot pictured above, it was determined that a new attachment method should be investigated in order to eliminate the large stress concentration in the lower portion of the I-beam. The stress concentration is the result of the weld which is holding the I-beam in place. When the normal force is applied to the system, the center of the I-beam begins to deflect vertically. Since both the top and the bottom of the I-beam are welded to the front plate, the I-beam is being stressed at the bottom due to the moments generated by the welds. By eliminating the welds altogether and replacing them with a pin, which does not transmit moments, the stress in the I-beam should be eliminated. Figure 6.11 shows the new system quarter model with I-beam pin connections.

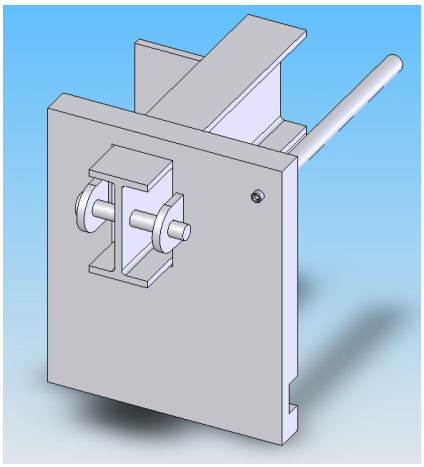

Figure 6.11: Pinned I-Beam Design

One benefit to this design over the welded fixation technique is that the pinned I-beam can be replaced much more easily than the I-beam that is welded in place. By

eliminating welded components, the down time of the pinned fixture would be minimal when compared to the previous design.

During the creation of the new attachment method, a few design changes had to be made in order to make room for freely moving components. First, brackets had to be welded to the face of the front plate in order to properly hold the pins in place. In order to accommodate for the vertical displacement of the I-beam, a small draft angle was cut where the I-beam enters the front plate. The draft angle allows the I-beam to deflect up to ten degrees before there is interference with the front plate. Figure 6.12 below, shows the deflection of the pinned design under loading.

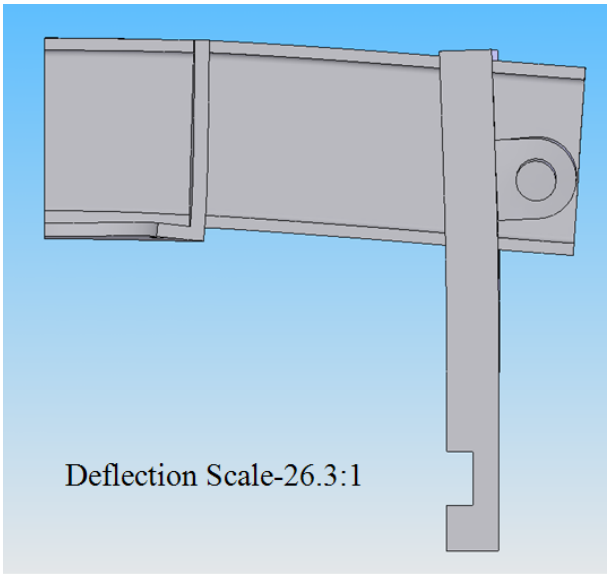

Figure 6.12: Pinned I-Beam Design Deflection Under Load

The revised pin attachment design achieved the deflection profile that we had intended, but there was a large amount of displacement in the one inch steel pin holding

the I-beam in place. The stress plot pictured on the following page in Figure 6.13 shows the stress in the system.

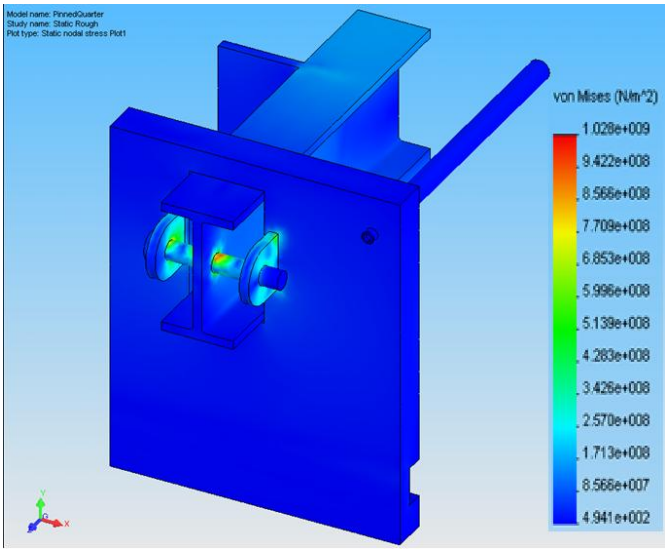

Figure 6.13: Pinned I-Beam Stress Plot

It is obvious that the maximum stress in the system is located in the pin where it passes through the I-beam. Multiple material types were tested to determine if there is a more suitable material for this application. Gray cast iron was the most appropriate because it had the highest yield and failure strengths. The Von Mises stress in the iron pin is approximately 10.29×10^8 Pa, suggesting that the pin will fail under this loading scenario. In order to verify this failure, the factor of safety plot was evaluated, see Figure 6.14.

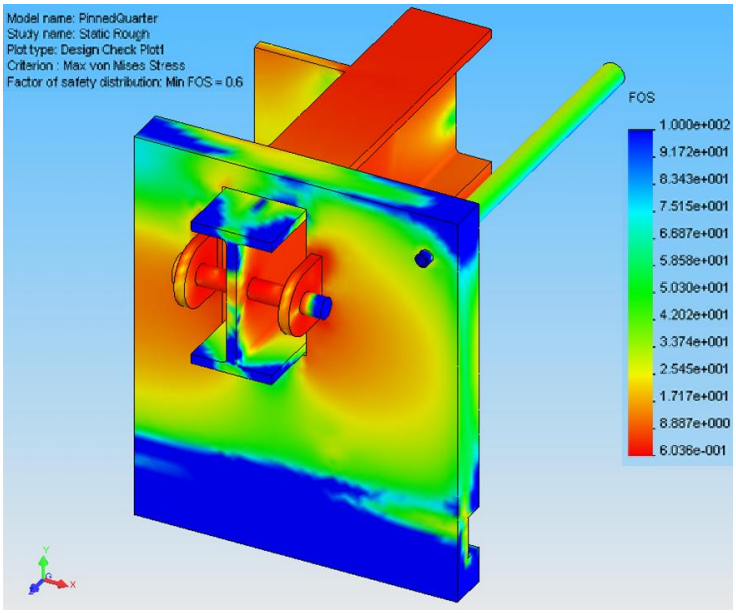

Figure 6.14: Pinned I-Beam Factor of Safety Plot

The minimum factor of safety as seen in the figure above is 0.6 and is located in the holding pin. Furthermore, the addition of the pin has created a stress concentration in the I-beam which will make the beam yield under the specified loading. Although the pinned I-beam fixture is easier to maintain and repair, it does not properly support the loads which it was intended for. Based on the results of the static stress analysis above, the original redesigned fixture was indeed optimal for this application.

Optimization of Suggested Design

CosmosWorks 2005 was used to optimize the suggested model. First, the objective of the optimization was defined, minimize volume. Next, upper and lower bounds were specified for the component dimensions which the functionality of the fixture allowed to be changed. These dimensions, or design variables, are illustrated in Table 6.3 and Figure 6.15.

Table 6.3: Optimization Design Variables

Design Variable	Initial Value, in.	Lower Bound, in.	Upper Bound, in.
Frontplate Thickness	2	1.25	3
Frontplate Tongue Height	3	1	4.5
Vertical Distance to I-beam	2.25	1	4
Crossrod Diameter	2	0.5	3
Support Thickness	1.5	0.5	2.5

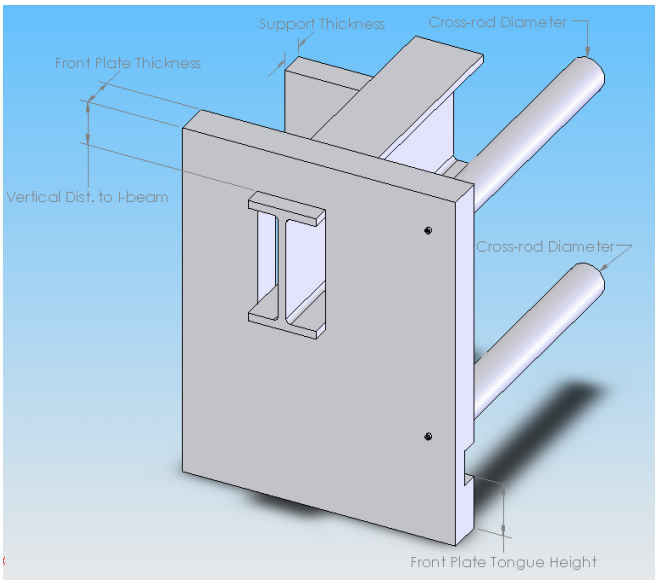

Figure 6.15: Definition of Design Variables

The dimensions of the I-beam were not parameterized as EAI would like to purchase these as standard parts from a supplier. Therefore, standard I-beam dimensions and material were utilized. The I-beam is from McMaster Carr and is made from ASTM 572 Grade 60 steel with dimensions of 7 x 3.375 x 0.4 inches (31). Also, it has been mathematically proven that I-beams have the optimal shape in terms of strength to weight ratio (30). Therefore, there is no need to try to optimize the dimensions of a given I-beam since the shape is already the best possible solution.

With the design variables defined, the optimization constraints had to be established before the study could be conducted. Based on the results of the static stress analysis, the constraints shown in Table 6.4 were created.

Table 6.4: Optimization Constraints

Type	Component	Units	Upper Bound
Nodal Stress	Von Mises Stress	Pa	2.60E+08
Displacment	Displacement (Y-dir)	mm	1

After identifying the optimization objective, design variables, and constraints, the study was carried out and convergence was achieved after 6 iterations. The final results are illustrated in Table 6.5 and Figure 6.16.

Table 6.5: Optimization Results

Variable	Initial Value	Optimum Value
Volume	.0134 m^3	.0111 m^3
Front Plate Thickness	2 in.	1.95 in.
Front Plate Tongue Height	3 in.	1.69 in.
Vertical Dist. to I-beam	2.25 in.	1.27 in.
Cross-rod Diameter	2 in.	1.125 in.
Support Thickness	1.5 in.	0.84 in.

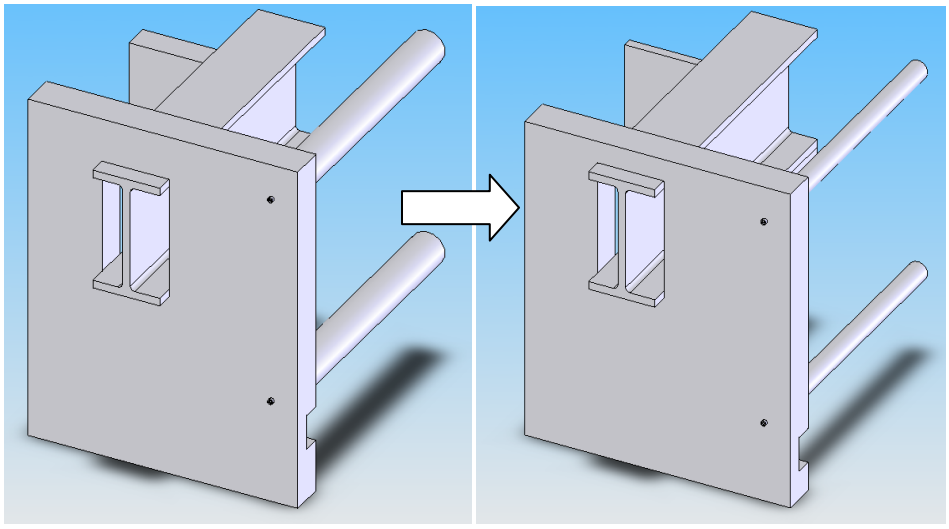

Figure 6.16: Optimized Design

The factor of safety plot generated, Figure 6.17, indicated that the overall minimum for the system is two. This is the due to the fact that the location of the minimum factor of safety is in the I-beam, thus changing these parameters had little effect on the overall minimum factor of safety.

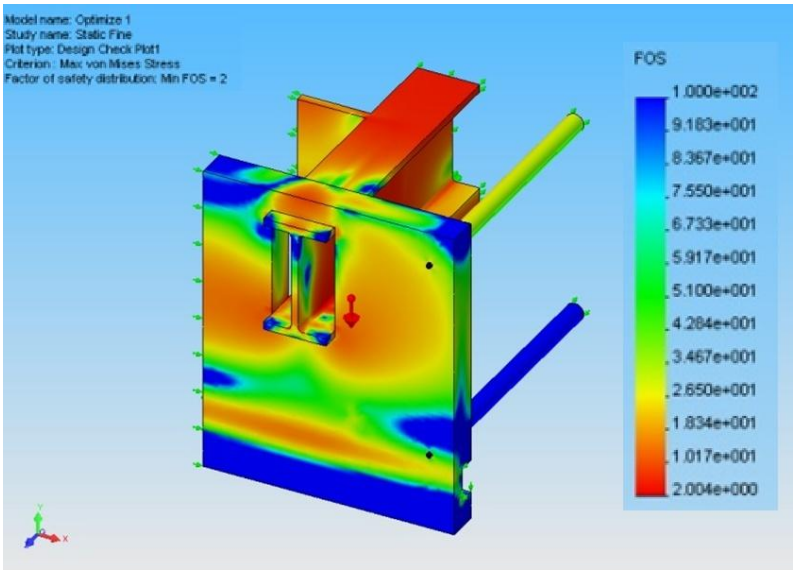

Figure 6.17: Optimized Design Factor of Safety Plot

The stress plot confirmed that the highest stresses were indeed in the I-beam. However, the factor of safety throughout the lower cross-rod was roughly equal to 100. This suggests that the rod may not be necessary. However the optimization parameter of the cross-rod diameter had to reflect the existence of the specified fastener, CosmosWorks therefore was unable to completely remove this component. Also, both cross-rods in the design changed simultaneously because they were brought into the assembly as dependent components, thus the factor of safety in the upper rod dictated the diameter of the lower rod.

Based on the construction of the model and the large factor of safety in the lower cross-rod, a static stress analysis was conducted with the rod removed. It was observed that the removal of the rod had zero effect on the minimum factor of safety or the maximum stress in the optimized fixture as shown in Figure 6.18.

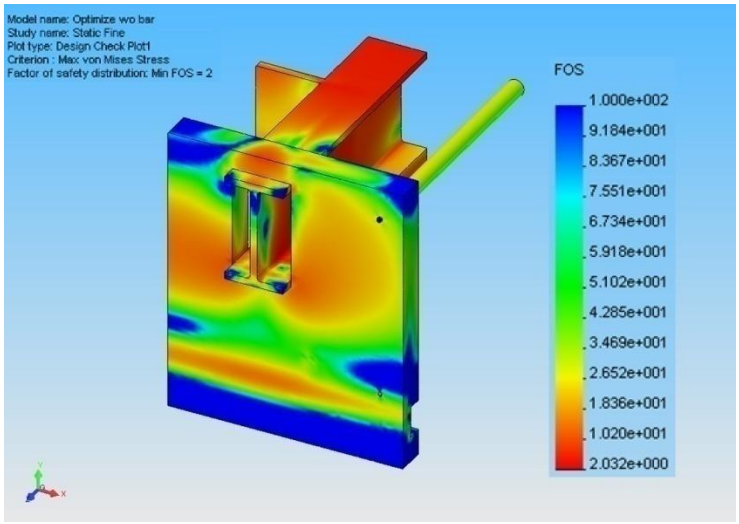

Figure 6.18: Optimized Design Factor of Safety without Lower Cross Rod

This proves that the lower cross-rod should have been eliminated in the optimization of the design, but was not because of the construction of the model. Therefore, the final suggested model is shown below in Figure 6.19.

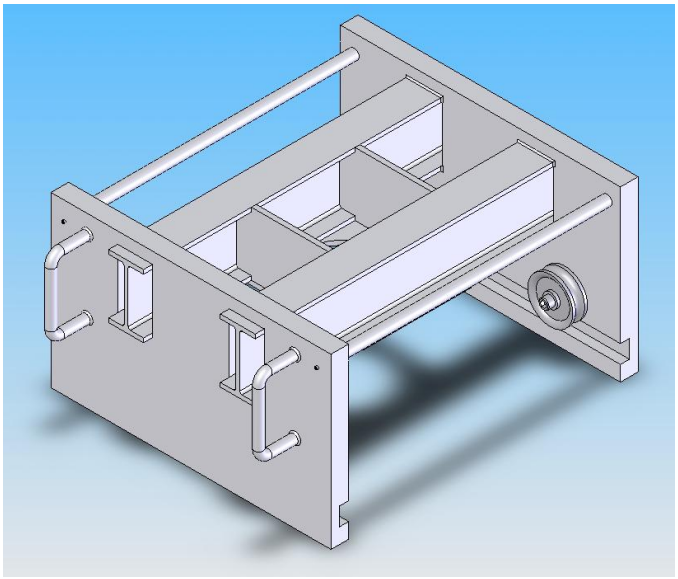

Figure 6.19: Final Optimized Fixture Design

The objective of the optimization was to minimize the volume of the fixture therefore reducing the overall weight. The initial weight of the system was calculated as 1,024 lbs. Redesigning and optimizing the fixture reduced the overall weight by roughly 40%, bringing the final weight to only 616 lbs. The factor of safety plot, seen in Figure 18, illustrates that it may be possible to further reduce the weight of the fixture by optimizing the front plate for shape. This is a potential area for further work.

Design Cost

After completing the static stress analysis and optimization on the suggested design, a cost analysis was carried out in order to determine the price of the entire assembly. The material costs that are shown in Table 6.6 reflect the values of a given material as stated by McMaster Carr (31), in Atlanta, GA.

Table 6.6: Cost of Suggested Fixture

Component	Material	No. Required	Cost per Unit	Total
Fasteners	A2 Tool Steel	8	-	$5.00
Cross-Rods	Plain Carbon Steel	2	$23.45	$46.90
Front Plate	AISI 1045 Steel	2	$700.00	$1,400.00
I-Beams	ASTM 572 Grade 60 Steel	2	$250.00	$500.00
Support	Plain Carbon Steel	1	$42.00	$42.00
Bracket	Plain Carbon Steel	1	$42.00	$42.00
Rollers	Type 304 Stainless Steel	4	$72.00	$288.00
Labor	---	4	$70.00	$280.00
Total Cost				$2,603.90

The total cost for all purchased products as well are the manufacturing cost for one fixture is approximately $2,600, including all necessary fasteners, materials and labor hours. Since two fixtures will be required for each vehicle the total cost for installing the suggested fixture design into an EAI vehicle is $5,208. Further investigation should be

done to determine the cost of the hydraulic cylinder as well as the control system and all necessary hoses and fittings for the hydraulic system.

Conclusion

The suggested fixture design, seen in Figure 6.19, represents that optimal design solution for the problem at hand. The proposed design meets or exceeds all existing specifications that are seen in the current EAI prototype fixture. The suggested I-beam design reduces the weight of the fixture by over 40%, taking the original weight of 1,024 lbs. down to 616 lbs. This drastic reduction in weight should allow the fixture to translate with ease from bin to bin unlike the current prototype. Also, with the addition of strong and light I-beam cross members, the factor of safety in the fixture is slightly larger than two, which does not account for the additional built in factor of safety when 100,000 lbs. of force was used instead of the required 80,000 lbs. Additionally, further research should be conducted to determine the performance of the fixture while using a weld fit, laser cut opening for the I-beam. Fundamentally, this should eliminate or minimize the stress concentrations, while only minimally affecting manufacturing cost. Furthermore, the selection of stiffer materials, such as AISI 1045 Steel and ASTM 572 Grade 60 Steel, has minimized the deflection in the system, which allows the fixture to have an infinite service life. The cost of implementing the suggested system per vehicle is just slightly over $5,200. This is a very conservative estimate because all of the costs were quoted on a single purchase basis. Since the proposed fixture will be mass produced using bulk materials, the cost per unit should drop significantly. Due to the unit cost, high strength, and long life, the suggested fixture is indeed an optimal solution for this application.

CHAPTER 7

REDESIGN OF BALING FRAME

This chapter presents the redesign of the baler frame of the EAI combined refuse and recycling collection vehicle. The baler frame is defined as the structure which is located below the ram fixture with the purpose of containing the recyclable materials while in a loaded or unloaded scenario. The current baler frame is able to process multiple individual materials in its three collection bins. The baler frame also contains the track and rail system to support the ram fixture as well as to allow it to translate freely from bin to bin. The redesign will be conducted using SolidWorks 2007 as the primary CAD software coupled with CosmosWorks 2007 for finite element analysis. Also, ANSYS[4] was utilized as redundancy software to ensure accurate results in FEA.

Due to a lack of information regarding the structure hidden below the surface of the current frame, benchmarking with respect to the current prototype will not be possible. However, the goal of the redesign was to develop a frame system that could withstand 100,000 lbs. on its rail system as well as support force and pressure exerted by the recyclables on the structure while loaded. A test will be developed to determine the pressure experienced on the baler walls when loaded since this information is not currently available. Due to the complexity of the visible frame structure as well as through formal correspondence with EAI, it was apparent that minimal engineering development was utilized when designing the current baler frame. Therefore, the design team should develop a new baler frame while attempting to reduce weight while maintaining or improving system strength.

---

[4] http://www.ansys.com/

Current Baler Frame

An image of the current EAI prototype baler frame is shown below in Figure 7.1. The frame is able to hold three individual recyclable materials in its separated bins. A rail and track system located on the top cross member of the frame allows the ram fixture to translate freely over the multiple bins. Currently, a 6 inch bore hydraulic cylinder services the system and is able to apply approximately 60,000 lbs of force, which is regulated by the hydraulic line pressure.

Figure 7.1: Current EAI Baler Frame

From the current design, it is obvious that there are a number of unique sub-systems incorporated in the baler frame: the baler structure, the rear wall, baler door, baler floor, and internal baler walls. Each sub-system is exposed to different loads when the hydraulic cylinder is actuated. For instance, the baler walls, which include the door, internal walls, and rear wall, are subjected to a small pressure caused by the barreling of the recyclables when loaded, while the baler floor experiences the full amount of the

force applied. It is important that the magnitude of these forces and pressures are known so that an accurate computer model of the system can be developed and analyzed.

As discussed in earlier sections, the current system uses multiple structural arrangements in the internal baler walls. When developing a new system, designers should consider Design for Standardization and Design for Manufacturing principles in order to reduce lead time and manufacturing costs (17; 32). The prototype system utilizes a single piece of plate steel on the internal wall to separate the bins and to ease the removal of a densified bale. The structure underneath the plate steel as well as the thickness of the steel is unknown.

The rear baler wall is constructed using vertically aligned lengths of c-channel of constant width. This not only minimizes deflection of the rear wall when loaded, but allows for the creation of channels in which strapping material may be passed through, see Figure 7.2 below.

Figure 7.2: Baler Rear Wall Configuration

The c-channel is fully welded onto a piece of sheet steel of unknown thickness in order to allow the strapping material to bend around the back of the bale once complete. However, due to the poor material choice for the strapping wire, permanent deformation occurs causing the wire to break out of the designed channels, therefore making strapping nearly impossible to achieve. The baler floor is created using a piece of plate steel of unknown thickness and was intended to minimize deflection without considering weight. Lengths of angle iron are stitch welded to the floor to form channels which match those found on the rear wall and allow the strapping wire to pass underneath the densified bale.

Problems with Current Baler Frame

The current frame presents a number of problems which must be considered in the redesign of the system. As mentioned in previous sections, there are a few elements in the system which must be utilized, but unfortunately are flawed in their current application. Using information gathered during experiments on the baling system, the design team determined that the process of removing the bale must be simplified. The process can be streamlined through the implementation of a few changes in the vehicle layout and the baler frame design.

Simple changes in vehicle layout will significantly improve the strapping and removal of a densified bale. As discussed previously, the current baling system has no rear access, making strapping and removal difficult since the process must be accomplished entirely by hand. Figure 7.3 demonstrates the current layout of the vehicle as well as the proposed vehicle configuration.

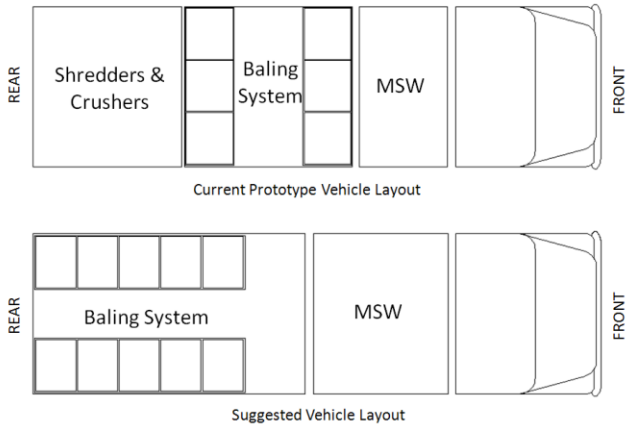

Figure 7.3: Vehicle Configuration Change

By utilizing a baling system that runs parallel to the frame rails, access to the baler is available both from the inside and outside of the vehicle, making the strapping process much easier to accomplish. Also, the baler doors open outwards so that the bale can be removed via forklift instead of manually.

Finally, the design team realized through multiple experiments, that the densified bale is extremely difficult to remove due to the frictional force between the bale and the baler. The tests were conducted only using PET plastic, which is commonly associated with barreling under load. In order to minimize the effort required to remove the bale, a small draft angle should be added to the interior walls of the baler. Through the implementation of a draft angle, the distance required to disengage the bale from the baling unit is significantly reduced. The combination of these minor design and layout changes should make the mobile baling process much more efficient and marketable.

Experimental for Determining Wall Pressure

Before a realistic baler model can be created, system constraints and loads must be properly assigned in order to yield accurate results. Minimal traceable research has been conducted to determine the physical and material properties of recycled goods while loaded. A test was created that will reveal the pressure that is generated on the walls of baler due to material barreling while loaded. The gathered information will be used to create an accurate finite element model of the baler, which will allow for the optimization of the system.

Procedure

In order to guarantee accurate results from the array of displacement gauges, a fixture was created to serve as a solid mounting surface for the gauges. The fixture was made of 2 inch square steel tubing to minimize deflection, and utilized two adjacent vertical supports on the vehicle's superstructure. Since the balers were developed without the use of a high level of engineering knowledge, the frame and wall design change structurally from baler to baler. The access point and fixturing location was chosen due to the simplicity of the baler wall design, as seen below in Figure 7.4.

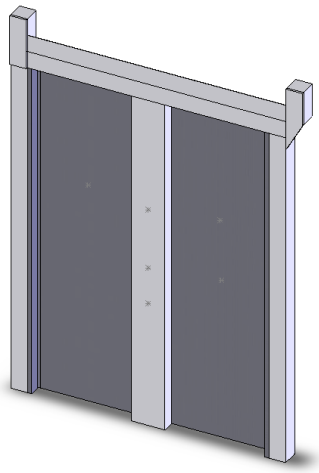

Figure 7.4: Model of Baler Wall

Three digital displacement cells and three dial calipers were utilized in this experiment. Although the digital displacement cells are accurate to ±0.0001 inches, the dial calipers were employed as a redundancy system and would also provide a few additional data points. The fixture allowed for adjustment on the X-Z plane, as described in Figure 7.4 above. After determining the desired arrangement for the digital gauges, steel rods were attached to the baler wall; they were required to offset the position of the gauges without compromising the results. The dial calipers were mounted directly onto the fixture using a high powered magnetic base. Figure 7.5, pictured below, illustrates the arrangement of the testing apparatus for this experiment.

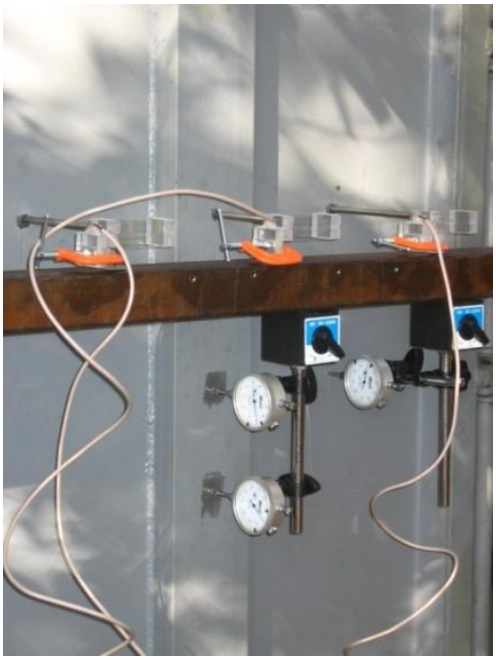

Figure 7.5: Testing Apparatus

The physical arrangement of the displacement gauges is displayed below in Figure 7.6, this information will be used to assign sensor locations on the virtual model.

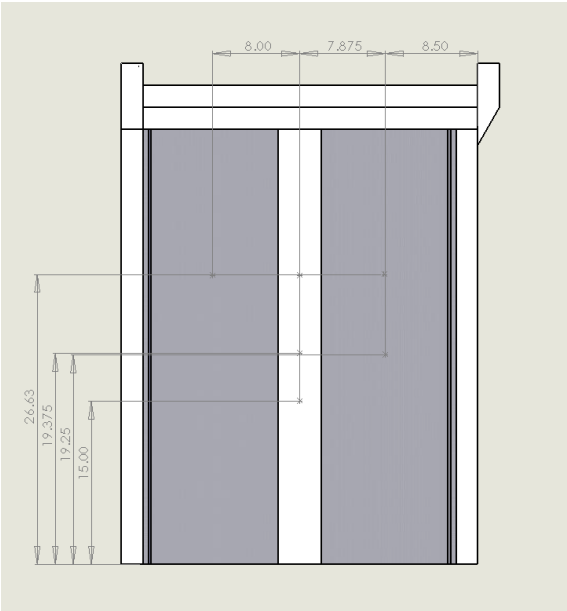

Figure 7.6: Displacement Gauge Locations

After positioning all of the displacement gauges and zeroing them, the baler was loaded and compacted multiple times. PET plastic was loaded into the baler using large storage containers. Due to the fact that the experiment is only testing wall pressures, total PET volume is irrelevant. The baler is loaded and compacted continuously until the bale becomes solid and "spring back" is minimized. This stage occurs when the cylinder stroke is reduced and the loaded volume decreases. A few more cycles should be completed to ensure that a densified bale is achieved. After attaining a densified bale, the bale height was recorded; this will correspond to the vertical dimension of the pressure field on the baler wall during FEA testing. Similarly, the final value was recorded from all of the displacement gauges; a voltmeter was utilized to measure the resistance through the digital gauge. A conversion factor of $\frac{30\text{k}\Omega}{9\text{mm}}$ was used to transform the resistance into a displacement.

After the completion of the physical testing, a virtual model of the wall section was created, as seen in Figure 7.4. The unknown dimensions and materials were determined by contacting the original manufacturer of the baling system. "Sensors" were placed on the virtual model in the same arrangement that was used during testing. FEA analysis was carried out using multiple pressures on the wall; a step size of 5 psi was utilized to achieve the results in the most efficient manner.

Results

Figure 7.7, shown below, demonstrates the deflection of the baler wall when subjected to a 30 psi pressure field, which simulates the force applied due to the barreling of PET when compacted.

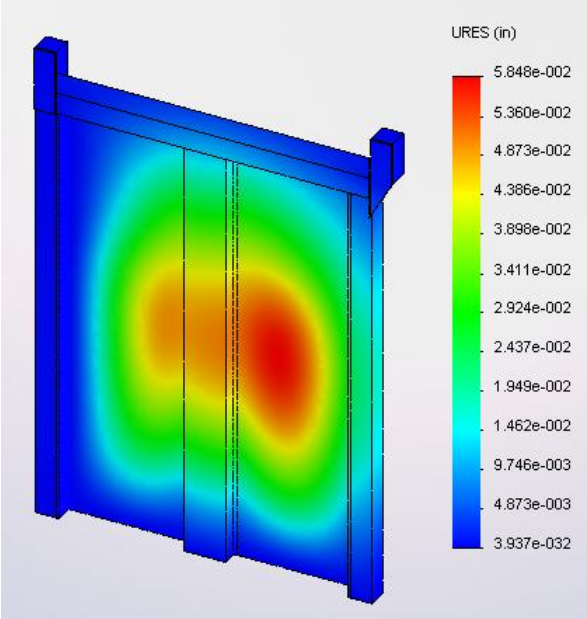

Figure 7.7: Deflection of Baler Wall (30psi)

Table 7.1 contains the displacement results from both the physical and simulated experiments. Only the results from the 30 psi FEA study were shown due to the

similarity to the actual displacements. All other tests yielded results with large amounts of error.

Table 7.1: Displacement Results

	Measured Displacement, in	FEA Displacement at 30 psi, in
Digital Gauge 1	0.01843	0.01887
Digital Gauge 2	0.0346	0.04007
Digital Gauge 3	0.09236	0.08448
Dial Caliper 1	0.05	0.0427
Dial Caliper 2	0.043	0.03681
Dial Caliper 3	0.1161	0.0563

Discussion

After running a number of studies on the virtual model, it was determined that the pressure exerted on the baler wall by PET plastic is approximately 30 psi. Table 7.1, shown above, displays the results of the FEA study, conducted at 30psi, compared to the actual results from the experiment. The results of similar studies yielded large amounts of error when compared to the test results. The table also shows that there is significant error associated with dial caliper 3. This error is possibly the result of human error, device error, or incorrect material selection in the virtual model. Due to the large number of displacement gauges, dial caliper 3 may have been missed when zeroing the gauges, resulting in a large amount of error once the testing was completed. Also, the gauge itself may be faulty, but this is not likely due to the high amount of accuracy and precision associated with the device. Finally, the most likely option is that the incorrect material was specified for the plate steel wall in the virtual model. This data was gathered from the manufacturer of the baling system, who unfortunately had no information documenting the materials used. By using the incorrect material, the displacement results

for digital gauges 1 & 3 as well as dial caliper 3 would be affected negatively. Since the results from the digital gauges were highly accurate, it can be assumed that the material properties used were correct. Therefore, human error is most likely the culprit. However, since the results for the rest of the gauges were highly accurate, it can be concluded that the pressure exerted on the baler wall is approximately 30 psi. A small factor of safety should be considered when implementing this information.

Conclusion

The results of multiple studies show that the pressure exerted on the baler wall due to barreling of PET plastic under load is approximately 30 psi. This value, with a built in factor of safety, should be used in future studies because PET plastic is the most prone to barreling, therefore it exerts the most force on the outer walls. All other materials act like columns while loaded, therefore the baler experiences the most force on the floor, which is equivalent to the force exerted by the ram. An accurate model of the system can be represented by exerting a force, which is equivalent to the ram force on the floor and a pressure of 30 psi on the vertical walls of the baler.

Redesign of Baler Structure

Unfortunately, due to computer processing limitations at the time of the redesign, the baler system will have to be designed and analyzed on the sub-system level. Assuming that all constraints and loads on the tested models are accurate, the unit as a whole will yield results which are equal to or better than expected. The first component of the baler that required a major redesign was the sub structure, which can be seen in Figure 7.8.

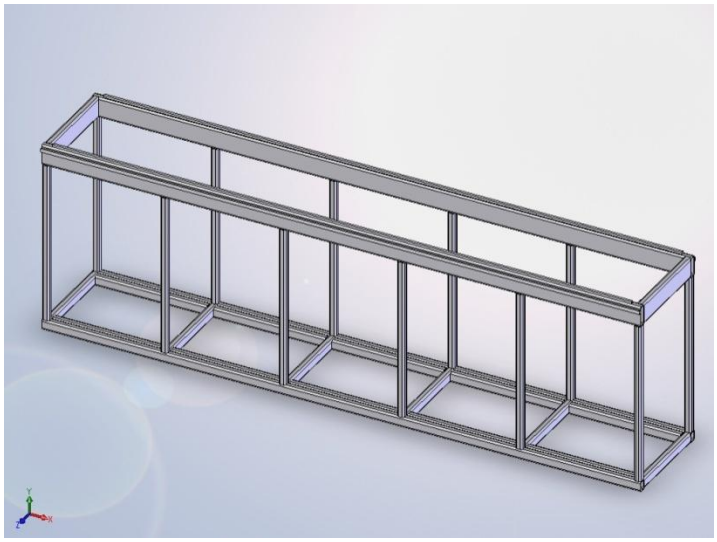

Figure 7.8: Suggested Baler Sub-Frame

The current prototype lacks any form of uniformity throughout the design, therefore Design for Standardization and Design for Manufacturing principles must be considered when developing a new solution (17). Also since there is no accurate information regarding the current design, benchmarking will not be possible, thus, the design team should design a frame which is both light and strong.

Unlike previous redesigns, due to dimensional constraints as well as the desire to maximize baler capacity, optimization was not conducted in the baler. Standard size structural members were utilized in an attempt to minimize material cost through standardization, the more common the component the less it will cost. The entire baling unit is made with 2 inch plain carbon steel tubing of various heights. Since there are only three different sizes of tubing required to manufacture the frame, 2”x2”, 2”x3”, and 2”x6”, the material will be able to be purchased in large quantities, thus reducing purchasing cost.

In order to gain accurate results from CosmosWorks and ANSYS, a realistic set of loads and system constraints must be developed. Using the information regarding the desired hydraulic ram force of 100,000 lbs, a worst case loading scenario can be created. The force from the hydraulic cylinder is applied by the fixture onto the track and rail system of the baler frame. This force can be approximated by applying a 50,000 lb distributed force over a region of the rails which have an equivalent length as the contact surface between the fixture and the rail, which is roughly 30 inches. The force was placed over the middle bin because of its limited structural support, demonstrating a worst case loading scenario. Furthermore, the baler frame was constrained from vertical movement by pinning the four lower corners, since the baler will not be welded or fixed to the floor, this approximation should be sufficient. Since the baler sub-frame is symmetric in multiple planes, a simplified model was utilized to minimize computation time while maintaining accurate results. Figure 7.9 illustrates the active constrains and forces on the solid model, the symmetry constraints are shown in green and the distributed force load in purple. It is important to note that there is an equivalent distributed load on the opposite side of the model, resulting in 100,000 lbs of vertical force.

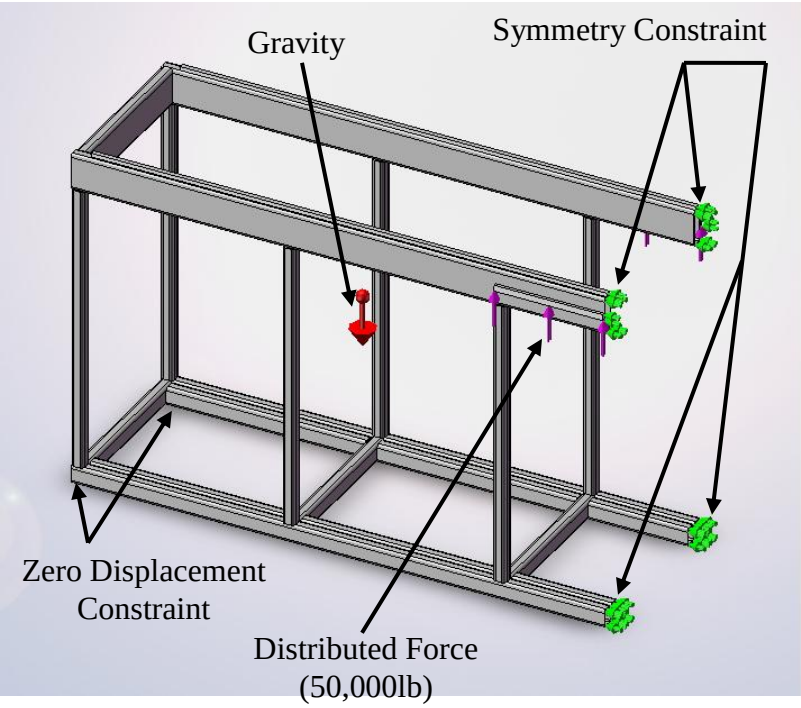

Figure 7.9: Load Scenario for Baler Sub-Frame Analysis

Moreover, gravity was enabled in this study to ensure accurate deflection of the baler sub-frame. If the study was conducted without this additional consideration, the mass of the frame would not be included in the calculations, therefore resulting in larger vertical deflections of the frame. Since the size of the model is significantly larger than the previous components, a large number of elements and computational power would be required to perform the analysis. Fortunately, the model is symmetric about multiple planes and a half model would increase the number of elements for the system, while requiring the same amount of computational strength.

Once a fine mesh was created for the baler sub-frame, a finite element study was conducted using CosmosWorks 2007. Figure 7.10, shown below, shows the stress plot for the baler sub-frame under the current loading conditions.

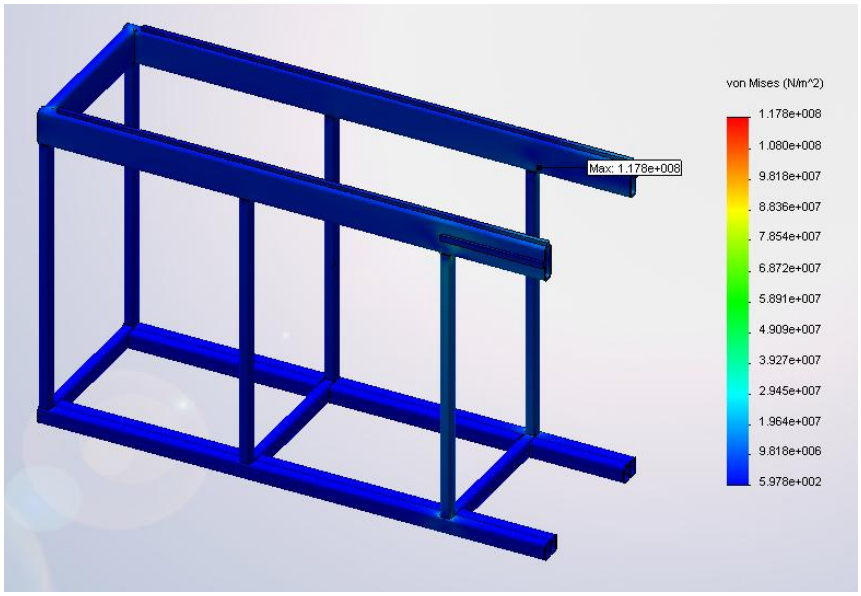

Figure 7.10: Stress Plot for Suggested Baler Sub-Frame

As illustrated in the figure above, the system has relatively low stress throughout with a minor "hot spot" located in the weld at the nearest vertical support. Since a "hot spot" has been identified it is important to understand the severity of the problem, therefore a factor of safety plot was generated, which will easily display the relative safety of the system based off of the selected materials. The results of the factor of safety plot can be seen in Figure 7.11.

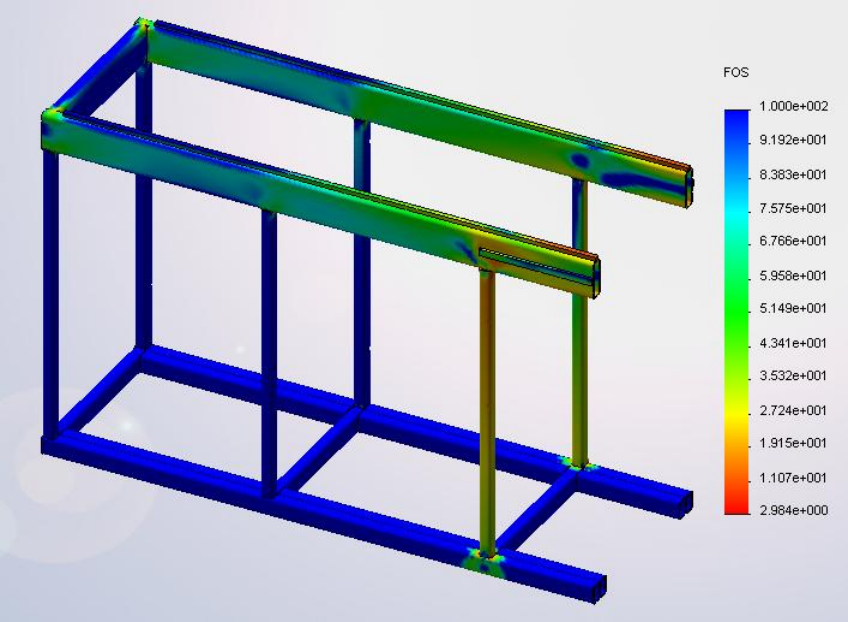

Figure 7.11: Factor of Safety Plot for Suggest Baler Sub-Frame

From Figure 7.11, it is simple to recognize that the minimum factor of safety in the system is approximately three; therefore the system will not fail under these conditions. Since this test was a demonstration of the worst case loading scenario applied to the baler sub-frame, the system should not fail under any circumstances. Also, due to limited number of cycles experienced by the frame during the life of the vehicle, the system should be able to be used in multiple generations of vehicles. Given that the proposed baler is a self contained mobile system, the entire unit should be able to be transferred from platform to platform with relative ease.

Redesign of Baler Walls

Once the design of the baler sub-frame was finalized, the interior walls, which separate the individual bins, had to be developed and tested. A number of initial designs were considered. First, the team realized the current baler frame utilized vertical c-

channel to support the rear wall and considered implementing the same system for the interior walls, as seen in Figure 7.12.

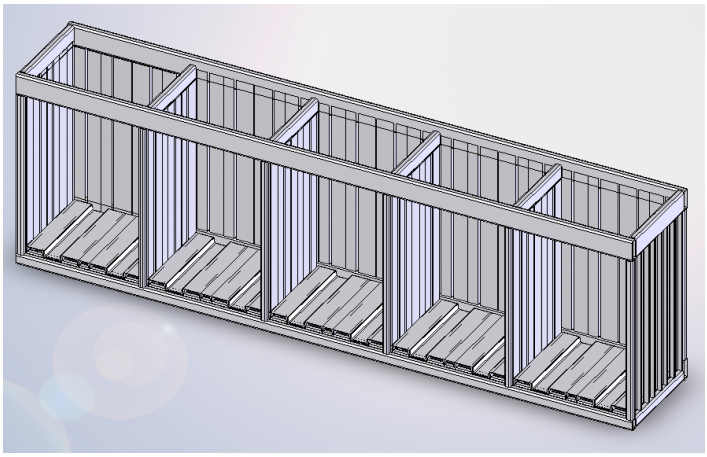

Figure 7.12: C-Channel Interior Wall Design

Unfortunately, this configuration comes with very critical problems. First, since the interior wall would require approximately eight individual pieces of c-channel per side, a special fixture would be necessary in order to manufacture the system. Similarly, due to the large number of pieces required, the draft angle would be difficult to implement. Finally, the design team also determined that the deflection of the c-channel would vary from piece to piece while loaded, thus restricting the movement of the bale when off-loading. Initial testing of the c-channel design demonstrated that a new solution had to be developed.

The design considered a number of lightweight designs for the interior walls. The two best solutions are shown below in Figure 7.13, it is important to note that these images are quarter models.

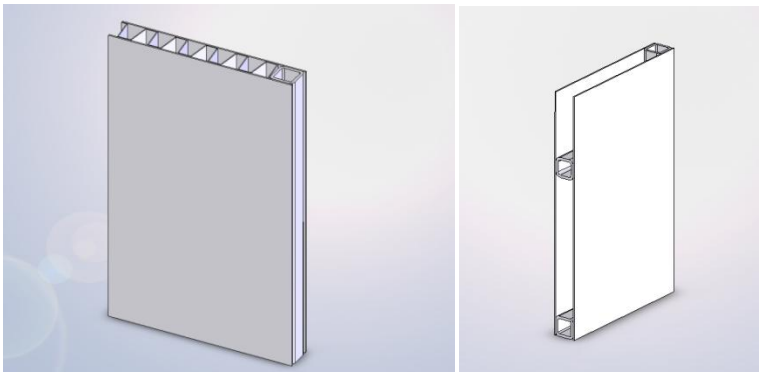

Figure 7.13: Quarter Models of Proposed Lightweight Interior Walls

The first suggested design used high strength corrugated steel or plastic to support the plate steel walls, while the second used a simple frame structure. Initial tests were conducted to determine the strength of these designs when compared to one another. A worst case loading scenario was applied to both models where 35 psi of pressure is applied to one side of the wall. The results showed that the most effective design was the corrugated steel model, but unfortunately due to the existing complexity of the shape, it cannot be implemented in a drafted wall configuration. This also is the case with the design utilizing standard structural members as a frame. Since structural members with varying cross-sectional dimensions are extremely expensive to purchase, the design is not feasible in this application. Therefore, an additional inner wall design was created which would allow for a small draft angle.

The design team determined that the most effective way of implementing a drafted wall was by using plate steel inserts that are cut to the desired shape. Figure 7.14, pictured below, illustrates the final model of the drafted inner wall design.

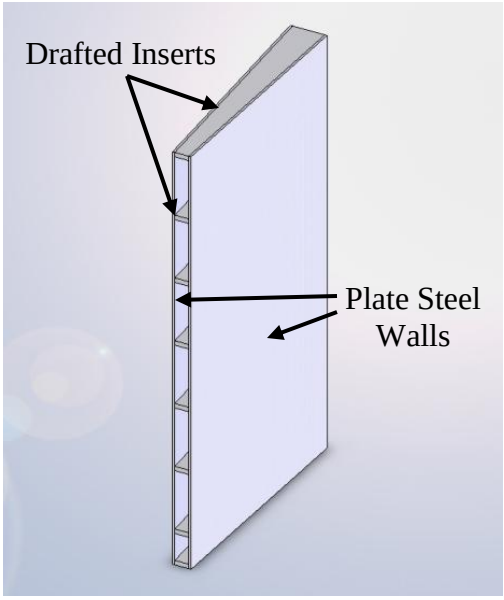

Figure 7.14: Drafted Interior Wall Design

The drafted inserts are made of half inch thick pieces of plane carbon steel plate and are fully welded to the baler sub-frame. Each wall utilizes eight draft inserts on an eight inch offset from the top to bottom. The wall surface is made from plain carbon steel plate and is only welded around the perimeter of the plate so that sliding can occur at the interface between the draft inserts and the wall material. The team investigated a number of various thicknesses for the plate wall in order to minimize weight; 1/8 inch, ¼ inch, and 3/8 inch plate were tested. In order to minimize system cost, expensive alloy steels were avoided and plain carbon steel was chosen due to its low cost to strength ratio. FEA studies were used to determine which thickness is the most appropriate for this application.

After the model was generated, an accurate constraint set was developed for the system and is shown below in Figure 7.15.

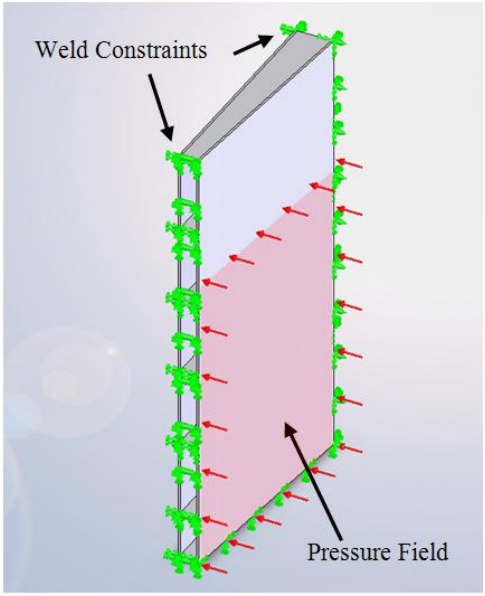

Figure 7.15: Constraint Set for Interior Baler Walls (Load Scenario 1)

Zero displacement constraints were placed on all edges where welds occur and are pictured above in green. As a result of limited testing, a wall pressure of 50 psi was utilized in finite element analysis to ensure that the wall will not fail under load, resulting in a built in factor of safety of 1.66. The design team believed that this was necessary due to the limited information regarding the activity of recyclable materials under load. The pressure field applied on the system represents the area of the wall which is affected by barreling of the bale while loaded and is shown above in red.

Unfortunately, CosmosWorks utilizes a default contact interface constraint, which is automatically set to bonded, meaning that the elements of two contacting surfaces will act as one. In order to properly model the interaction of all contacting faces, the surface-to-surface "no penetration" constraint was added. As a result, any contacting faces will be analyzed as independent entities and the components will not be able to deform through one another. A surface-to-surface "no penetration" constraint is a non-linear

approach to solve the system of equations and requires a large amount of processing capacity, but is necessary in this situation in order to model the interaction in the interior wall properly.

Initial results of the FEA study showed that the 1/8 inch thick plate steel wall would fail under load with a factor of safety of only 0.67. On the other hand, the ¼ inch and 3/8 inch design were capable of handling the pressure, but the thicker wall choice was far too heavy for the application, weighing approximately 500 pounds, therefore the ¼ inch design would be analyzed further. A stress plot, Figure 7.16, was developed for the ¼ inch wall model to determine the behavior of the wall when loaded.

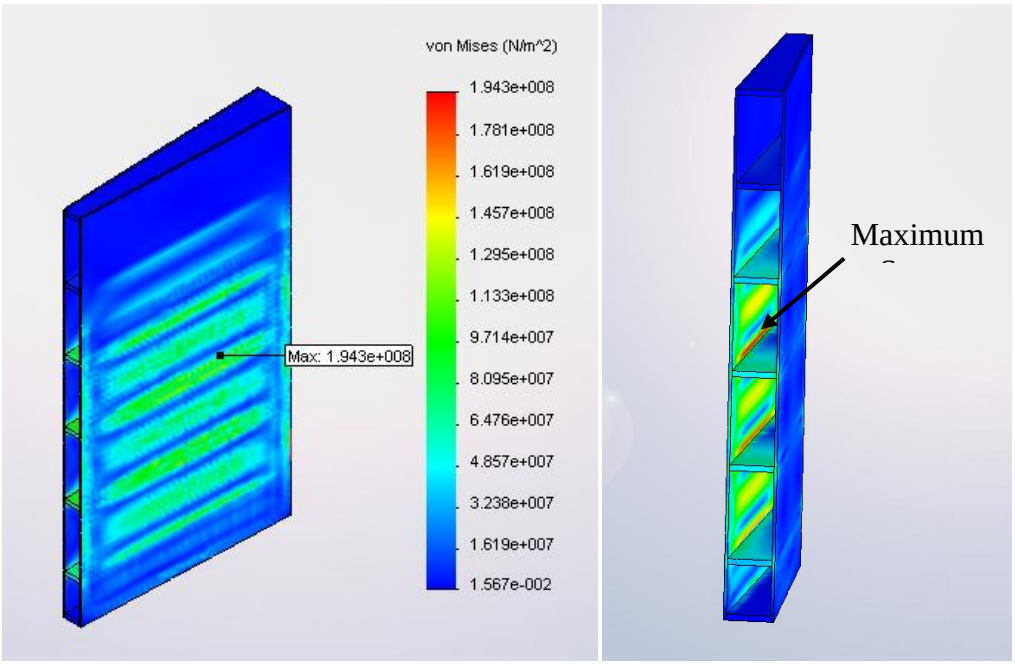

Figure 7.16: Stress Plot for Interior Baler Walls (Load Scenario 1)

Figure 7.16 illustrates that there is one major stress concentration in the system, which occurs in the plate wall and is denoted in the figure by an arrow. The magnitude of the stress, approximately 194 MPa, is relatively close to the yield stress of plain carbon steel,

thus a factor of safety plot, Figure 7.17, was created to determine if the wall will fail under load.

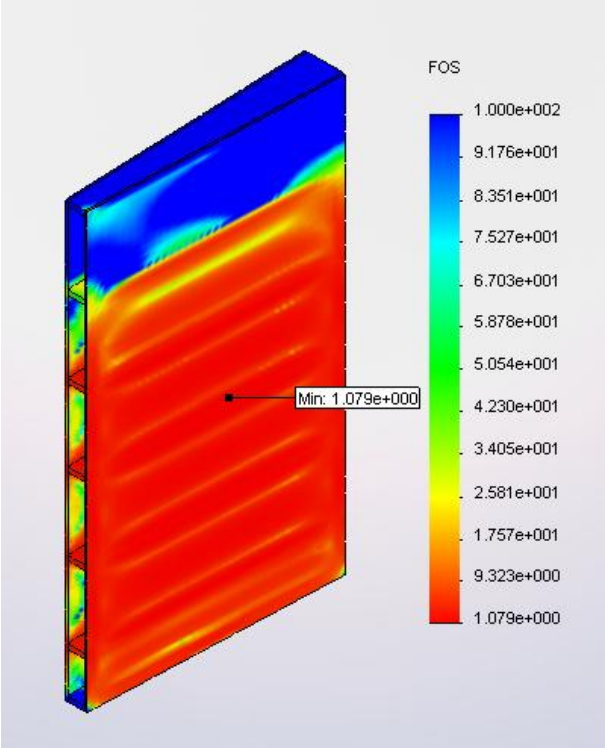

Figure 7.17: Factor of Safety Plot for Interior Baler Walls (Load Scenario 1)

Figure 7.17 clearly demonstrates that the minimum factor of safety in the interior wall model is approximately 1.08, therefore the wall will remain stable and will not fail while loaded. Since the load set which was applied on the system already contained a built in factor of safety of 1.66, it is highly unlikely that the wall will fail under any circumstances. However, slight changes can be made to the materials or in the design which would significantly improve the stability of the system. For instance, the components could be made of alloy steel instead of plain carbon steel which would make the system stronger, but would increase the purchasing cost significantly. Similarly, a

smaller offset could be used for the draft inserts, but this design change would require more material, therefore increasing system weight and cost. Since the factor of safety of the system remains in the threshold for being "safe", the proposed design solution should be implemented.

A finite element study was also conducted to determine the behavior of the wall when loaded from both sides. The constraint set utilized for the first study was held constant, while an additional pressure field was added to the opposite side of the interior baler wall.

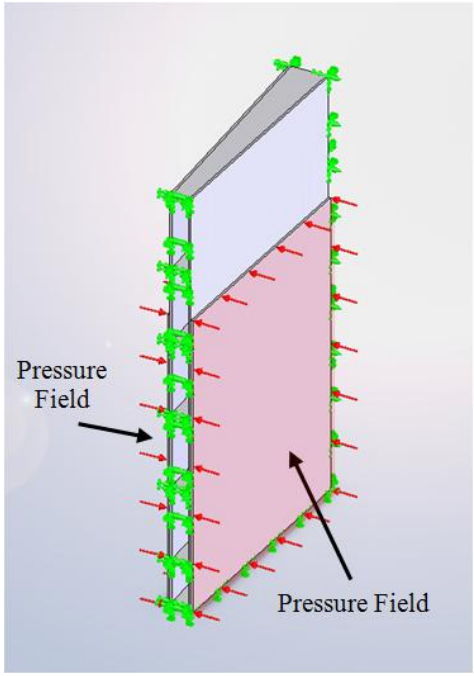

Figure 7.18: Constraint Set for Interior Baler Walls (Load Scenario 2)

Again, no penetration was allowed in this study between components, therefore the FEA analysis demanded more computational power and required approximately 24 hours on a 3.8 GHz machine. A factor of safety plot was generated, Figure 7.19, to determine if the interior wall will fail under this load scenario.

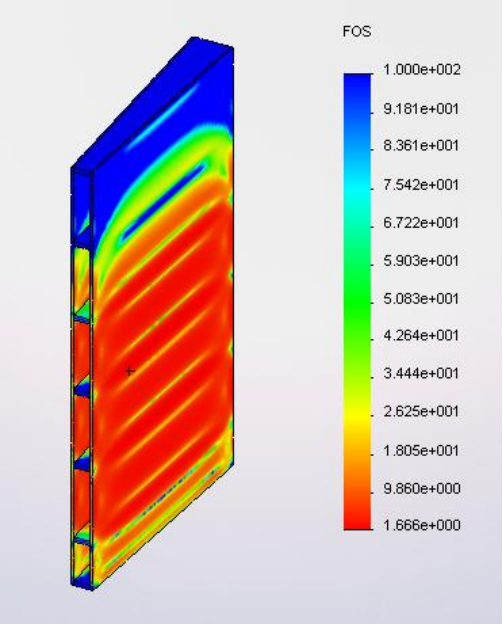

Figure 7.19: Factor of Safety Plot for Interior Baler Walls (Load Scenario 2)

As expected, Figure 7.19 illustrates that the factor of safety of the system has increased to 1.66 due to the additional pressure added to the opposite wall. Therefore, the assumption that the worst case loading scenario for the baler wall occurs when only one side experiences pressure, was indeed accurate. Thus, any additional FEA studies should only focus on the first load scenario, which will significantly reduce the amount of superfluous analysis. As seen in the previous study, the minimum factor of safety in the system occurs in the plate steel wall. As a result, the factor of safety could be easily improved by selecting an alternative material or by thickening the plate, but since the design is always in the threshold of being "safe", the material and thickness should remain unchanged.

Unfortunately, due to tight dimensional constraints for the baling system, the outermost baler walls must have a slightly different design and therefore should be subjected to finite element analysis. The major difference in the design is the draft

inserts, which were drastically changed in size and shape. Since the draft inserts must only support a single drafted wall, they were designed such that they will lie flush with the baler sub-structure.

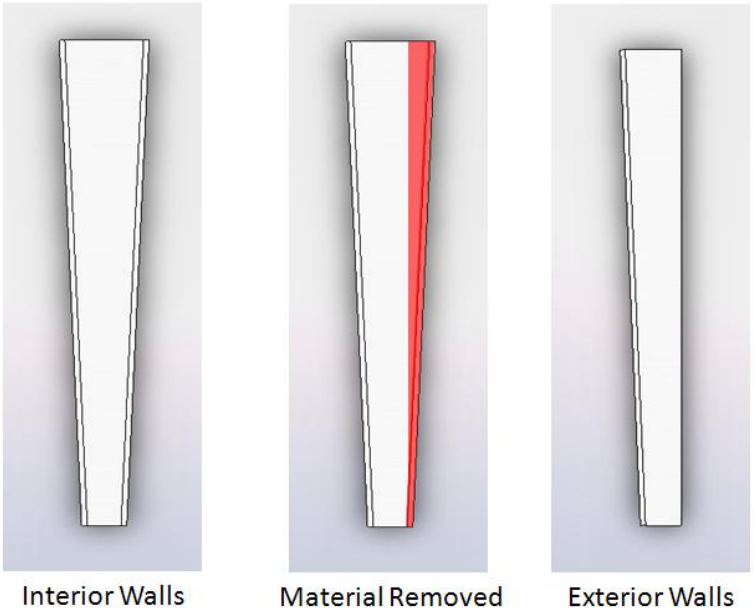

Figure 7.20: Difference in Design of Interior & Exterior Baler Walls

Because of the reduction in size as well as the change in shape, the design team was concerned about the performance of the wall while loaded. By conducting an FEA study, the design team would be able to identify any design flaws and adjust accordingly so that the design will be safe under all conditions.

The model for the outer walls of the baler is very similar to the design for the interior walls. The draft inserts are placed at an eight inch offset from top to bottom and are fully welded to the baler sub-structure at all contact points. The wall is made of ¼ inch plate steel and is welded around the perimeter to the baler sub-frame. The material for the draft insert was changed to AISI 1020 steel to accommodate higher stress, while

maintaining machinablility and weldability (31) and the plate steel wall will remain as plain carbon steel. Since the design lacks the structural support added by the adjacent plate steel wall, the design team was unsure about the strength of the system under load. The system is restrained using zero displacement constraints on all welded edges. A 50 psi pressure field is added to the system, modeling the force applied to the baler wall while compacted. The no penetration contact set was applied to ensure accurate results. A stress plot, Figure 7.21, was generated to identify any stress concentrations located in the system.

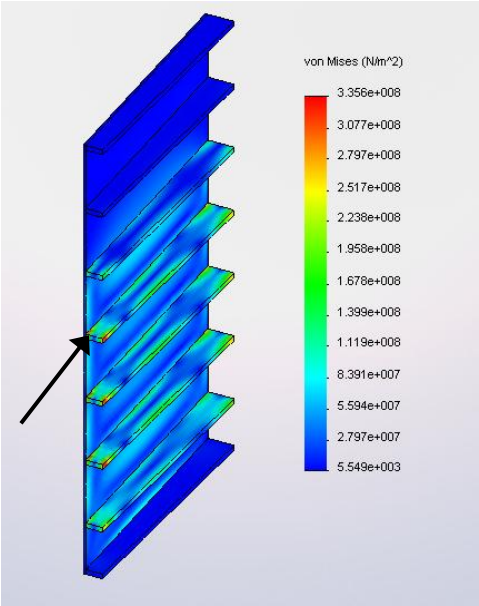

Figure 7.21: Stress Plot for Outer Baler Walls

Figure 7.21 indicates that there are six major stress concentrations in the system, which occur on the narrowest side of the draft insert. The maximum stress in the system is approximately 336 MPa and is identified in Figure 7.21 using an arrow. Since the maximum stress in the system is relatively close to the yield stress of the alloy steel being

used, a factor of safety plot, Figure 7.22, was developed to determine if the design will fail under the current conditions.

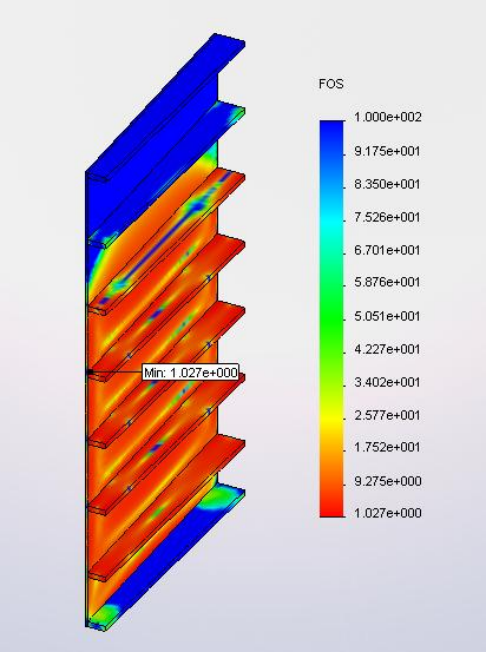

Figure 7.22: Factor of Safety Plot for Outer Baler Walls

Figure 7.22 demonstrates that the outer baler walls will not fail under this specific loading scenario. As expected, due to high stress concentrations in the design, the factor of safety is particularly low, approximately 1.03, however, it is important to note that the load scenario already considered a factor of safety of 1.66. Therefore, the outer baler walls will not fail under normal loading conditions. However, if the system were to fail under abnormal loading conditions, the draft inserts would be able to be easily replaced due to the accessibility of the components. Since the designs for the interior and exterior baler walls have been optimized and will function under normal conditions without failing, a new configuration had to be established for the baler floor.

Redesign of Baler Floor

Due to a lack of information regarding the sub-structure of the current baling system, the design team determined that it would be beneficial to redesign the baler floor in an attempt to minimize manufacturing cost and system weight. The current baling system utilizes a one inch thick piece of plain carbon steel plate as the baler floor. Although the prototype system is able to support the load applied by the hydraulic ram, it is unknown whether the increase in hydraulic force will cause the system to fail. Therefore, the design team developed a new baler floor which would minimize system weight and manufacturing cost through the implementation of only standard structural members.

The entire baler floor was redesigned using multiple lengths of c-channel based on fundamental engineering knowledge. C-channel is very resistive to bending with the definite advantage of high strength and low volume (33; 26), which is extremely beneficial when the goal is to reduce the weight of the system. Also, standard c-channel can be purchased from numerous suppliers, which allows for a reduction in purchasing cost.

Figure 7.23, shown below, illustrates the proposed baler floor design. The floor is made of seven individual pieces of c-channel, either three or five inches in width. The floor rests on the baler sub-structure and is tack welded in place. The baler floor must be designed to support a normal force which is equal to that applied by the hydraulic cylinder plus the weight of the recyclables.

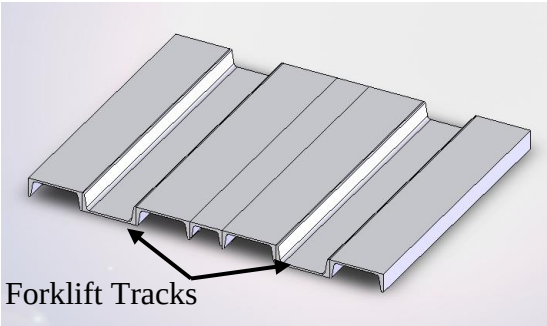

Figure 7.23: Suggested Baler Floor Design

From multiple experiments conducted on the current prototype vehicle, it was established that the bale must be removed using a system which did not rely on manual power. By changing the vehicle layout, it is possible to allow forklift access to the densified bales, which will significantly reduce the amount of time and effort required to offload the bale. However, extreme precision would be required to pick the strapped bale off of a flat surface without causing some damage. Thus, it was established that the redesigned baler floor must accommodate for error proof forklift accessibility. This can be achieved through the implementation of c-channel because it can be configured as a flat floor surface, but it also permits for the creation of recesses, which can be used as forklift tracks, as shown above in Figure 7.23.

An FEA analysis was conducted on the baler floor to determine the strength of the system while loaded. The floor is manufactured using 26 inch lengths of standard c-channel, either three or five inches in width, and are made from ASTM A36 grade steel, which is common in this application. As discussed previously, the floor must be able to support both the weight of the baled material as well as the force applied by the hydraulic

ram. However, since the weight of the recyclables is minute when compared to the 100,000 lb force exerted by the ram, it can be neglected in the FEA study.

As in all previous FEA studies, the creation of a realistic set of loads and restraints is absolutely paramount when accurate results are desired. The 100,000 lb force applied by the hydraulic cylinder was modeled using an equivalent pressure field, approximately 100 psi across the floor, shown in Figure 7.24. Since the baler floor simply rests in place due to the design of the baler sub-frame, it was important that the default global contact set was changed to the "no penetration" setting. This allows the c-channel to move independently and realistically when loaded, but requires a vast amount of computational power to complete the calculations, approximately 36 hours on a 3.8GHz machine. A tubular plane carbon steel frame was restrained underneath the assembly to simulate the support structure which the floor rests on.

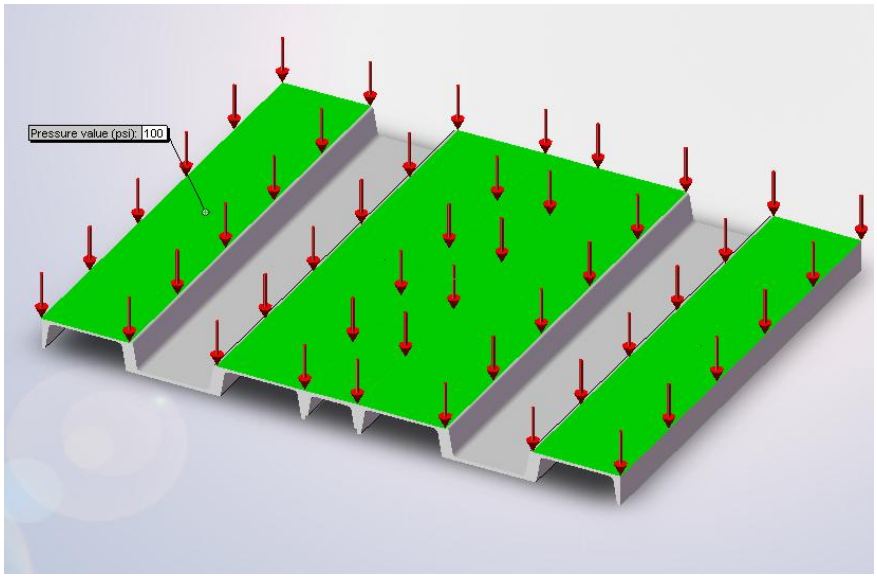

Figure 7.24: Constraint Set for Baler Floor

A number FEA studies were created, with increasing numbers of elements, to ensure accuracy of the results. Low resolution tests revealed a number of large hot spots in the c-channel located on the contact surface with the frame. It was unclear whether these hot spots were anomalies due to the geometry of the system or if they were "real" stress concentrations. Mesh controls were added to the areas in question, yielding more localized elements and therefore producing system results with a higher resolution. This would allow the use of probes to determine if the stress concentrations are legitimate. Similarly, the cross-sectional geometry of the c-channel was altered to reflect a more realistic model. It was believed that the hot spots were due to limitations in the FEA package with respect to edge-to-edge contact between the c-channel and the frame. By modifying the cross-sectional geometry of the c-channel, as shown in Figure 7.25, the influence of this error could be investigated.

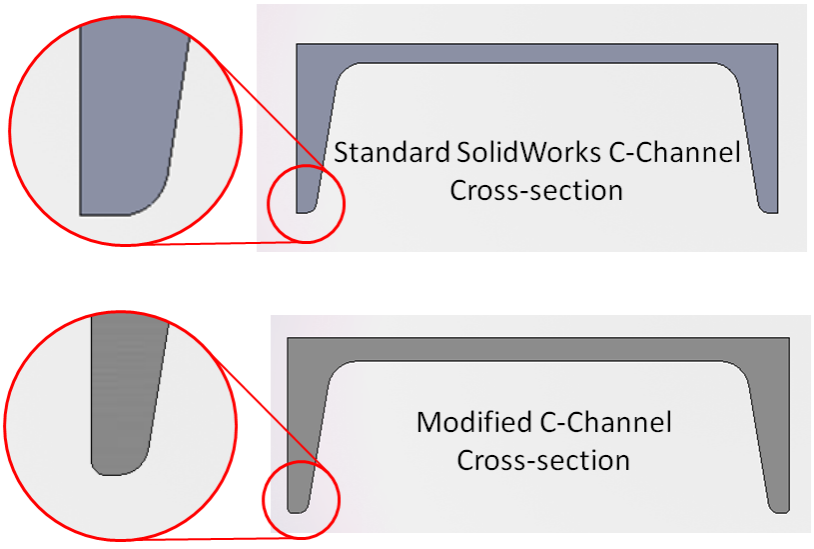

Figure 7.25: Geometrical Modification to C-Channel Cross-section

Fillets, measuring 0.01 inch in diameter, were added to the sharp corners of the c-channel in an attempt to reduce the effect of geometry on the results. Stress plots, Figure 7.26 & Figure 7.27, were generated for the system and contained approximately 150,000 elements.

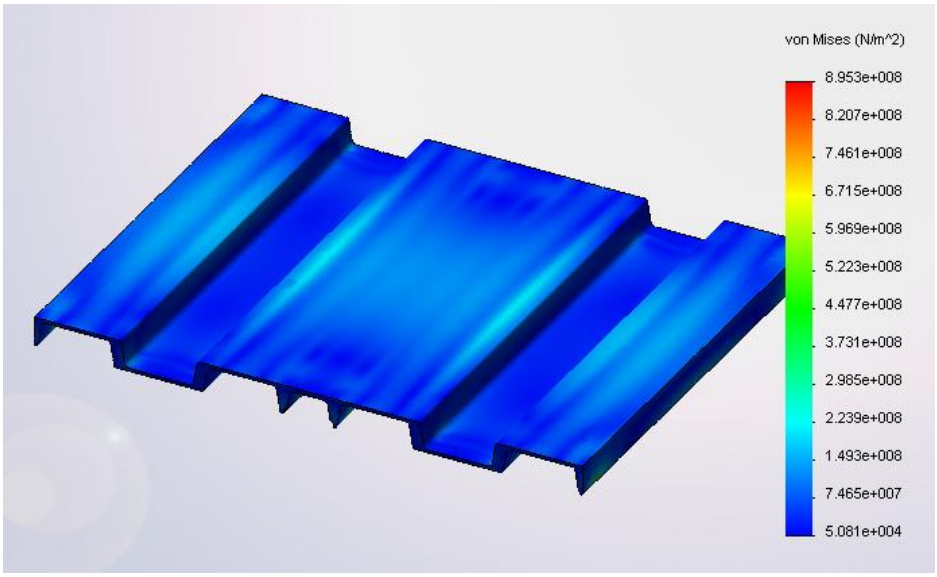

Figure 7.26: Stress Plot for Proposed Baler Floor: Isometric View

Figure 7.26 illustrates that the state of stress in the structural members is relatively low on the upper surface of the baler floor. It appears that the floor will be relatively safe when loaded. However, upon further inspection, the hot spots found in previous models still remained, but the magnitude of the stress had been reduced significantly. Figure 7.27, shown below, presents the location of the stress concentrations.

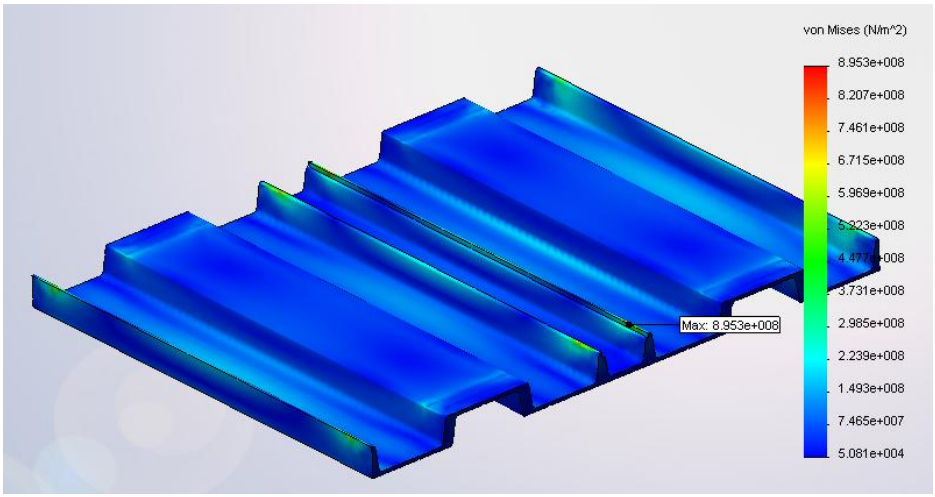

Figure 7.27: Stress Plot for Proposed Baler Floor: Alternative View

The maximum stress found in the system is approximately 900 MPa, which is significantly higher than permitted by ASTM A36 grade steel, therefore resulting in failure of the system. A factor of safety plot, Figure 7.28, was generated to show the effect of the hot spots on the system performance and behavior.

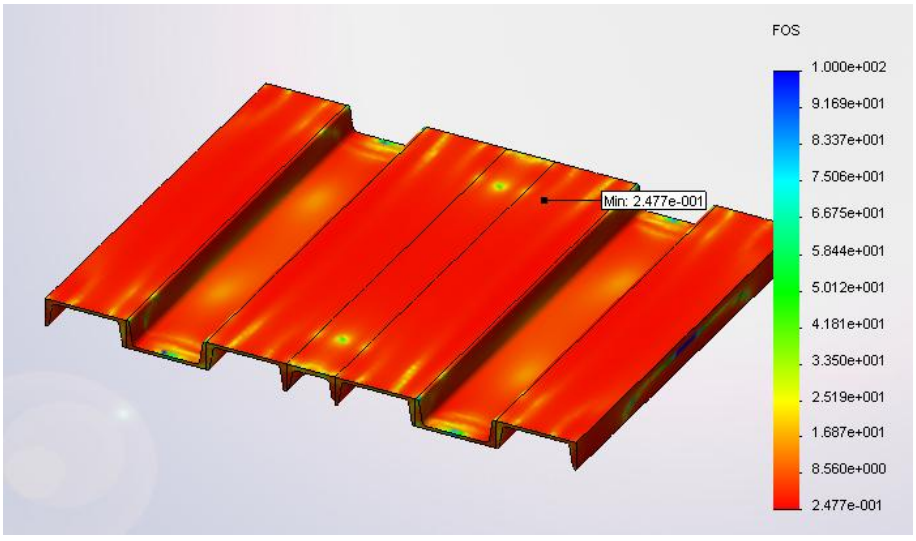

Figure 7.28: Factor of Safety Plot for Baler Floor

Figure 7.28 demonstrates that the minimum factor of safety in the baler floor is 0.24 and occurs at the four centralized hot spots. Although the FEA study says that the system will indeed fail under load, the model was probed near the location of the hot spots to determine if the results are accurate or if it is possibly an anomaly associated with FEA packages. The results from nearby elements show that the factor of safety quickly climbs from 0.24 to 1.15 only a millimeter away, which is a characteristic of a geometric anomaly. If the results from the hot spots are removed from the system, the minimum factor of safety of the structural member is approximately 1.15, meaning that the system will not fail. Again it is important to note that the force applied on the system already considered a built in factor of safety of 1.25.

Since the materials required to fabricate the baler floor are relatively cheap, physical testing should be conducted to confirm the results. If the floor does indeed fail in physical testing, alternative materials should be investigated. Similarly, c-channel with increasing web thickness is available and should also be tested, however, this would add to the weight and cost of the system. Since the stress concentration appears to be a geometric error associated with many FEA packages, the system should not fail under load, but physical testing should be conducted before large scale baler fabrication occurs.

Redesign of Baler Rear Wall

Currently, the rear baler wall is constructed using vertically aligned lengths of c-channel of uniform width which are stitch welded to a steel plate of unknown thickness. The current design not only minimizes the deflection of the wall through the use of strong and light structural members, but it also accommodates for the creation of recesses which will aide in the strapping process. However, the design team determined that the rear

baler wall must be redesigned in order make the baling and strapping process more efficient.

The proposed solution for the rear baler wall borrows many design cues from its predecessor; however the redesign allows access to the rear wall which aides in the strapping process. Figure 7.29, shown below, illustrates the c-channel configuration of the rear wall.

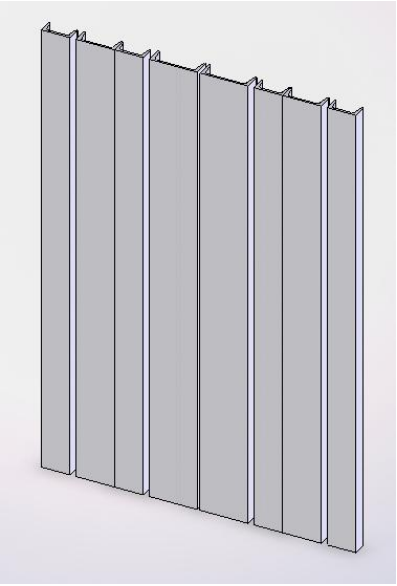

Figure 7.29: Suggested Rear Baler Wall

The wall is made of 47 inch length of c-channel of varying widths, three, four, and five inch, and is made of structural ASTM A36 grade steel. The c-channel is fully welded around all contact surfaces with the baler frame. It is important to note that the individual pieces of c-channel are allowed to move independently of one another when loaded.

Once the virtual model of the rear wall was generated, a finite element analysis was conducted to in an attempt to understand the behavior and strength of the system under load. A force and constraint set was generated which properly simulates the load

scenario when compacting, seen below in Figure 7.30. A simple tubular steel frame was utilized to simulate the baler substructure and to properly constrain the system. Zero displacement constraints were placed around the outside of the frame.

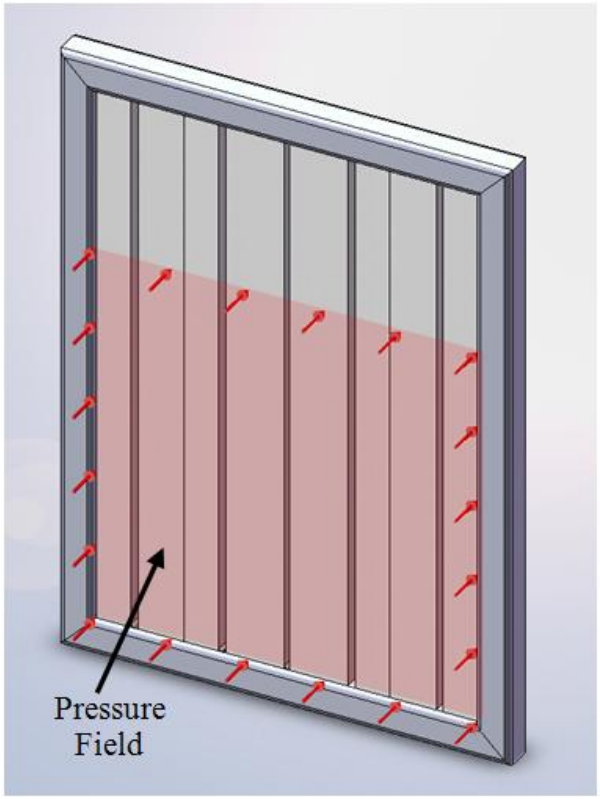

Figure 7.30: Constraint Set for Baler Rear Wall

The force exerted on the wall, due to barreling while loaded, was again modeled using an appropriately sized pressure field at 50 psi. Since the c-channel is allowed to move independently, a non-linear approach was taken by applying the "no penetration" contact set. The c-channel was restrained using zero displacement constraint along all welded edges. Once an accurate force and constraint set was developed, a coarse mesh was generated in an attempt to minimize computational effort. However, by limiting the number of elements in the system, the resolution of the results is poor, but a general

understanding of system behavior can be achieved. Figure 7.31demonstrates the resulting stress state for the system.

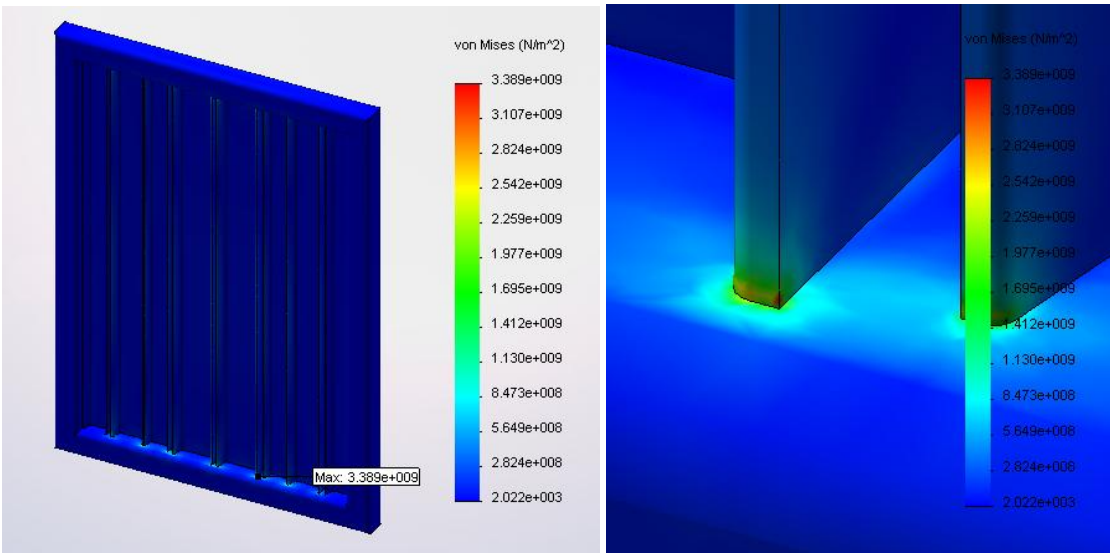

Figure 7.31: Stress Plot for Rear Baler Wall (Coarse Mesh)

The stress plot reveals that the system is relatively stable throughout, but again, there are a number of stress concentrations located at the contact interface between the c-channel and the frame. On the surface, it appears like the system will fail immediately when loaded, but geometric limitations involved in FEA may be responsible. The major piece of evidence for this claim is the location of the hot spot. These stress anomalies regularly appear on sharp edges or at the interface between multiple components. Since the stress concentration is located both on a sharp edge and at a joint, further investigation should be conducted.

A new model was generated which attempted to minimize or eliminate the possibility of stress anomalies. Due to the symmetry of the rear wall, the new model utilized virtual welds on half of the supports at the contact interface between the c-

channel and the baler sub-structure. By applying welds only on half of the contact surfaces, the results can be compared within the same test.

Figure 7.32: Welded Rear Wall Model

Also, a finer mesh was utilized throughout the model in order to provide more accurate results. Moreover, a mesh control was applied to the weld to provide a high level of resolution around the areas in question, resulting in a mesh with approximately 190,000 elements. Figure 7.33 illustrates the increased number of elements around the location of the high stress concentrations.

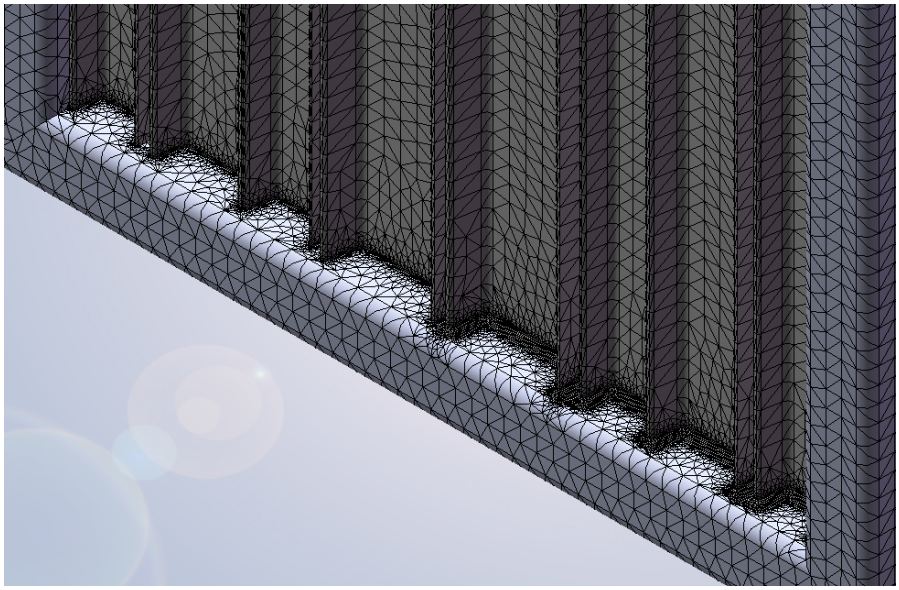

Figure 7.33: Mesh Controls Applied to Contact Interfaces

Although, the new model would produce more accurate results at a higher resolution, the computational effort required to solve the system was increased significantly, approximately 120 hours to complete the study. The stress plot generated for the new model, Figure 7.34, shows that the magnitude of the stress has been significantly reduced at the hot spots, from 340 MPa to 240 MPa.

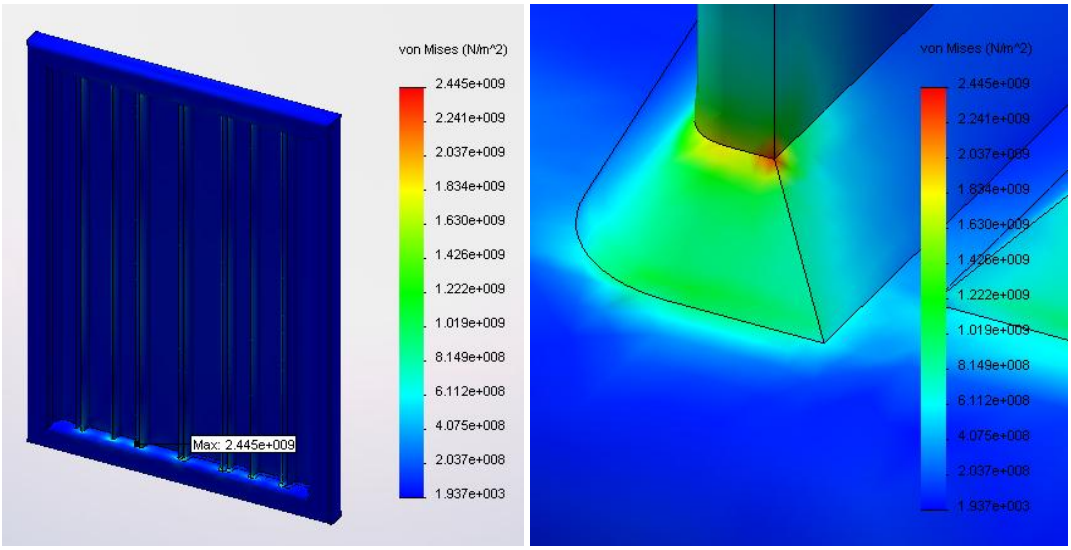

Figure 7.34: Stress Plot for Rear Baler Wall (Fine Mesh with Welds Enabled)

The stress plot, Figure 7.34, also shows that the welds have significantly reduced the effect of the hot spots on the model. Again, due to geometric limitations of the solver, it appears as if stress concentrations have developed at the interface between the weld and the c-channel, as shown above in Figure 7.34. In order to see the effect of the hot spots on the design, a factor of safety plot, Figure 7.35, was developed.

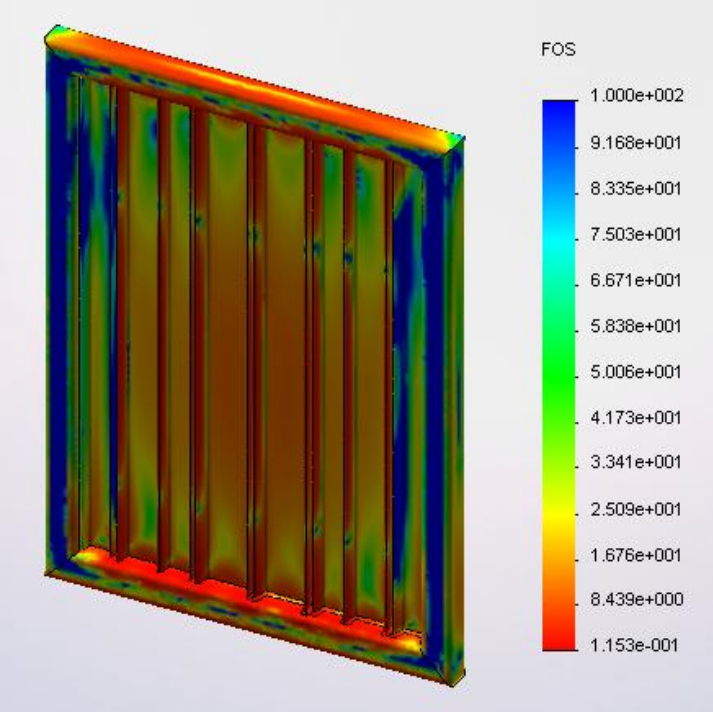

Figure 7.35: Factor of Safety Plot for Rear Baler Wall (Fine Mesh with Welds Enabled)

Figure 7.35 demonstrates that the factor of safety in the system is extremely low at the location of the stress concentrations, approximately 0.115 and 0.25 for the unwelded and welded interfaces, respectively. Again, a probe was utilized to investigate the factor of safety near the stress concentrations to help determine the validity of the results. The results from neighboring elements on both the unwelded and welded sides of the design show that the factor of safety rapidly increases. On the unwelded side the factor of safety changes from 0.115 to 1.02 only 1 millimeter away from the hot spot. Similarly, on the welded side, the factor of safety climbs from 0.25 to 1.6 only 0.5 millimeters away from the epicenter of the stress concentration. As discussed previously, the rapid change in stress around a sharp corner or joint is a common characteristic of a

geometric anomaly. Therefore, if the outlying results are discarded, the system appears to remain in the threshold of being safe while loaded. Again it is important to note that the force applied on the system already considered a built in factor of safety of 1.66.

Due to the possibility of error in the stress calculations, physical prototyping and testing should be conducted to determine if the system will fail under normal loading conditions. Since all of the required components are standard in the market, the tests should be relatively inexpensive to conduct and will yield valuable information. If the wall configuration fails during physical prototyping, alternative materials and weights of c-channel should be examined.

CHAPTER 8

CONCLUSIONS

Through the application of lean manufacturing principles to the current curbside collection process for MSW and recyclables, an abundance of wasteful steps were exposed. By eliminating or reducing the number of non-value added processes, the efficiency of the process as a whole was be significantly improved (8; 2). EAI has proposed a "lean" combined collection process through the implementation of a specialized vehicle which can collect and process both MSW and recyclables (14). Figure 8.1, shown below, illustrates the "lean" collection process as proposed by EAI.

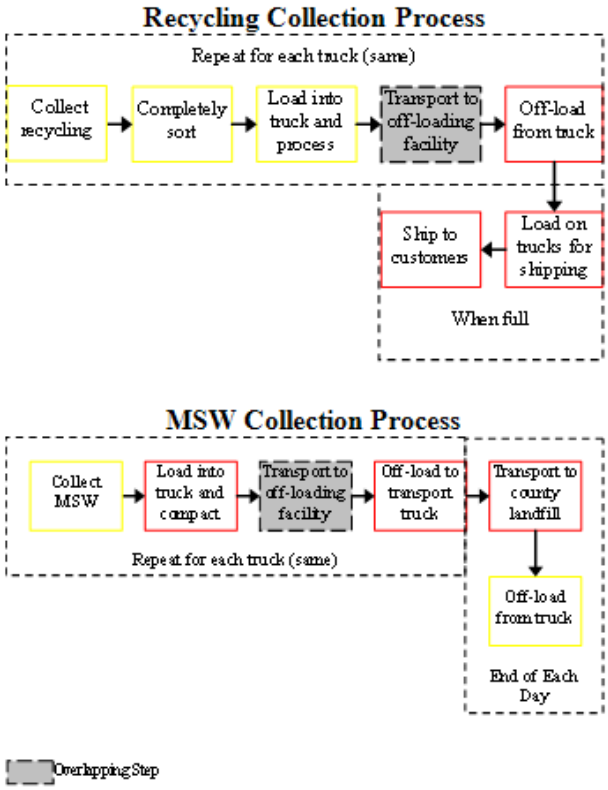

Figure 8.1: Proposed MSW & Recycling Collection Process (5)

The suggested curbside collection process eliminates nearly fifty percent of all non-value added steps by processing all of the collected recyclables onboard the vehicle. This vehicle, coupled with localized, low-impact material offloading facilities has the potential to revolutionize the curbside collection process. The proposed system will not only significantly increase process efficiency, but will also allow the owner to generate revenue through the direct sales of the processed recyclables.

Initial research, conducted by Troy (15), has uncovered that the city of Clemson could swing their annual budget deficit to a possible $31,000 budget surplus through the full scale implementation of the combined MSW and recyclable collection vehicle. Table 8.1 shows the current operating cost for trash collection in Clemson along with the revised operating cost after implementing the combined collection vehicle and associated collection process.

Table 8.1: Recommended Sanitation Dept. Revenues & Expenses (Fiscal Year 2005-2006) (16)

Total Operating Revenues	$135,350.00
Total Operating Expenses	$181,577.00
Operating Income	($46,227.00)
Projected Recycling Revenue	$77,720.46
Revised Operating Income	$31,493.46

The revenue that can be directly generated through the sale of the processed recycling is approximately $78,000 annually. Although the recyclables do generate a large amount of income for the city, it is important to note that Table 8.1 does not consider the budget savings from the “leaned” collection process. Thus, further research should be conducted to determine the effect of the combined collection vehicle on the

city's overall operating expense. The design team believes that the combined collection vehicle will have a considerable influence on the city's annual operating cost, therefore the budget surplus shown in the table above reflects a conservative estimate of the financial benefit of the system.

The application of lean manufacturing principles not only allowed the design team and EAI to justify the creation of a new combined collection vehicle, but it also created a framework to help generate new system constraints and criteria. The proposed combined collection process shown above in Figure 8.1, illustrates operations or steps which must be achieved with the proposed vehicle, resulting in a number of system constraints. Using the "lean" process tree combined with existing customer constraints and criteria, the design team generated two unique design solutions, in which either the collection vehicle or a transfer truck travels to the landfill at the end of the day to discard the processed MSW. With the current local governmental policies in place, the truck design which offloads MSW at the landfill can be implemented immediately. Although this solution does not fully realize the potential of the "lean" collection process, it is an improvement when compared to the current standard. While this may not be the ultimate solution to eliminating "waste" from the curbside collection process, it is certainly a viable solution and a step in the right direction.

The design team was able to develop a prototype vehicle which satisfied all constraints and criteria through the use of SolidWorks, a commercially available CAD/CAE package. The software provided a simple platform for the manipulation and optimization of design solutions; however of the user must be aware of its inherent limitations. The case study illustrated that the absolute benefit of using CAE software

over conventional methods was that the design team was able to generate solid models that maintained the functionality of physical prototypes without having to spend the time or money associated with a physical model. By conducting experiments on the existing prototype, the design team was able to answer a number of questions which have not been previously covered by researchers or manufacturers. Without a physical prototype, it would be extremely difficult to create realistic models in a virtual atmosphere. While CAE may reduce the time required to successfully create a novel design solution, it is obvious that it will always be necessary to create a physical prototype to generate a realistic model and to validate the simulated results. Although the case study only demonstrated the redesign of the baling unit, it is important to note that the vehicle superstructure, floor, and balers were developed during the 9 month period. The only investments associated with the redesign were the cost of labor, computer systems, and software, totaling approximately $45,000. Since the redesign did not include the cost of creating a physical prototype representing the proposed system, it is extremely difficult to compare both design time and cost with the previous prototype vehicles and sub-systems.

Another benefit of CAE based systems, is that manufacturing drawings are generated with ease when compared to previous 2-D drafting software like AutoCAD[5]. Once a final design solution was identified and selected, the design team was able to create a complete set of manufacturing and assembly drawings in only a number of days. Also, the solid modeling tools allowed the design team to present complex systems to the customer in a much simpler fashion since the model contains all of the functionality of a physical prototype. The team was able to generate system animations and walkthroughs,

[5]http:// www.autodesk.com

which give the customer a simulated “real-life” experience with the product which was once impossible with 2-D applications.

Although the combination of CAE and engineering knowledge yielded a superior baling system, which is lighter, cheaper, stronger, more flexible, and easier to manufacture and maintain than the current system, a number of limitations were identified during development. Among these is the observation that CAE has become too user friendly, accurate results come at a high cost, and mathematical limitations still exist in FEA software. The interface in most CAE software was developed to be extremely user friendly, allowing anyone to create models and studies quickly, regardless of previous experience with CAD or engineering. On the surface this may not seem like a problem, but this technology can be extremely dangerous when operated by an inexperienced user. For example, a model could be developed which does not properly simulate the real life scenario, yet the system will still yield results regarding performance and safety. While the model is not accurate and could possibly fail, the system will not inform the user, which could cause significant problems in the future. An example of this presented in the case study, is that the default settings for the FEA software are set to utilize the simplest design scenario with bonded contact surfaces and a linear approach. Although this will minimize the computational effort required to solve the system of equations, the results will be inaccurate. A novice CAE user will likely overlook the error. Therefore, it is extremely important that only experienced designers utilize and rely on CAE simulated models.

As with any CAE package, highly accurate results come with a cost. In order to properly simulate the activity in a system, a non-linear approach is often required due to

interaction between components. Although this approach will yield more realistic and accurate results, a significant amount of additional computational power is required when compared to a linear study. As a result, servers or computer clusters are almost necessary in order to minimize the amount of time required to solve the large system of equations. However, with the recent boom in technology, systems with higher processing speeds are becoming available at lower prices, allowing small businesses and students to utilize CAE. The use of a non-linear approach in multiple occasions in the redesign of the baling unit demonstrated the effect that accuracy has on computation time. When comparing the time necessary to model the behavior of the ram fixture, a linear approach utilizing 250,000 elements required approximately 3 minutes to converge on results, using a 3.8GHz machine, whereas when a non-linear approach was applied on the same design, with the same number of elements, over 72 hours were required. This example shows that in order to yield highly accurate results in an efficient manner, high powered machines or cluster are required.

Finally, CAE users must be aware of the limitations of the finite element solver. As shown in the development of the baler walls and floor, certain geometrical constraints can cause inaccurate stress concentrations, which occur due to the mathematics used to solve the system of equations. In the future, both the user and the supplier should be aware of the limitations and design accordingly. An example from the case study shows that the user should accurately model welds in an attempt to limit the influence of geometrical anomalies in the finite element study. Similarly, the supplied library of structural members provided by the software company should not include cross-sections that contain sharp edges, which can cause inaccurate results.

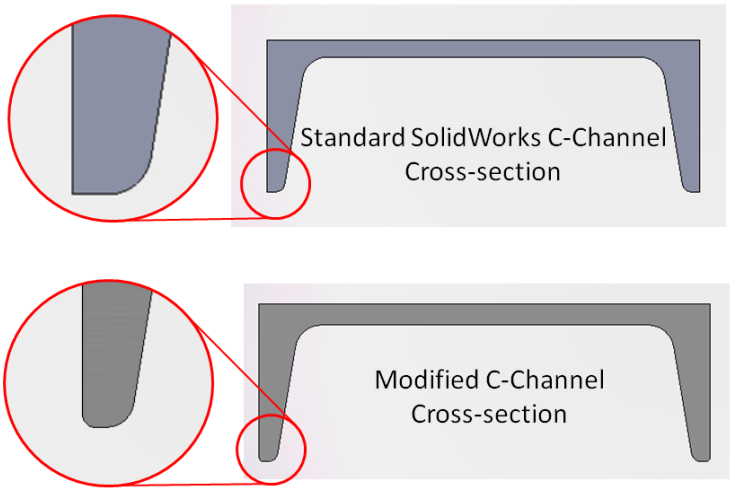

Figure 8.2: Geometrical Modification to C-Channel Cross-section

By editing the supplied cross-sections, as shown in Figure 8.2, the possibility for inaccurate stress results will be minimized. Currently, it appears that there is a disconnect between the users, developers and programmers, resulting in a mediocre software package. Through beta testing, developers are able to identify and eliminate a large number of problems, however, due to the limited scale of this testing a large number go unnoticed. By working concurrently with users in industry, the remaining issues can be easily identified and resolved, resulting in a superior next generation CAE package. Thus, a symbiotic relationship needs to exist, in real time, between the software company and the customer in order to develop a future system which reduces the opportunity for error.

Software companies should also consider developing an FEA preprocessor which will accurately predict stress anomalies based solely on geometric analysis. For example, the preprocessor could detect sharp edges and the union of multiple surface lines at a contact face, which are known to cause irregularities in FEA results. Upon

identification, the system could warn the user of the possibility of incorrect results and ask before proceeding further. In the past, designers and engineers relied on their intuition and previous design experience to filter inaccurate results, which could lead to eventual error in the future. The introduction of a geometric preprocessor would not only reduce the possibility of human error associated with FEA and CAE, but it would teach the designer how to avoid these anomalies in the future.

Through the implementation of engineering knowledge and CAE software, significant advancements were made in EAI's mobile baling system. Since limited information was available regarding the manufacturing of the current baling system, the structural design and total weight of the baler frame was unknown. However, through the use of both physical experiments and virtual testing, a superior baling system was developed, **Figure** 8.3.

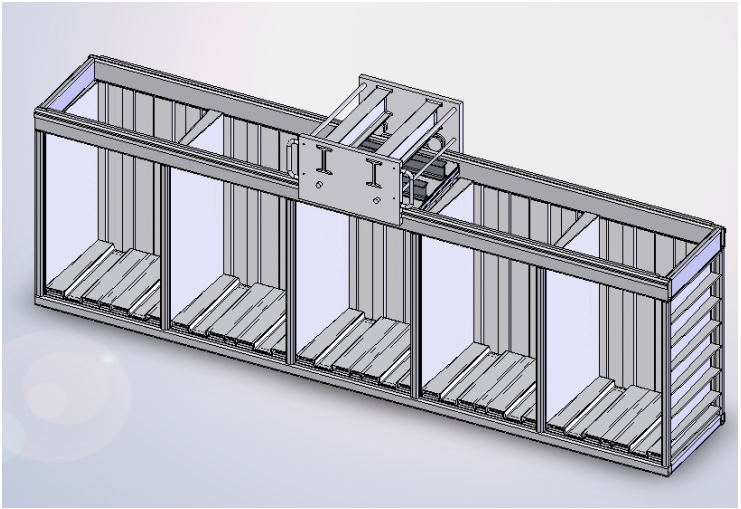

Figure 8.3: Proposed Baler System Design

Design for manufacturing and design for standardization principles were utilized in an effort to reduce manufacturing cost and time, without compromising the strength of

the system. As discussed previously, investors associated with EAI have spent more than 3 million dollars over the past decade developing prototype vehicles. Unfortunately, to date, not a single prototype vehicle has conformed to national standards regarding vehicle dimensions, weight and noise, resulting in a product which is not marketable. However, through the combination of engineering knowledge and CAE software the design team produced a unique mobile baling system that weighs approximately 5,250 lbs, which includes the weight of the ram fixture, ram face plate and the estimated weight of the baler doors. The introduction of the hydraulic cylinder to the system increases the total weight of the unit to approximately 6,000 lbs. When compared to its predecessor, the proposed baling unit can process five individual materials instead of three and can achieve higher bale densities, while weighing an estimated 1,500 pounds less.

Contributions

I would like to thank Dr. Joshua Summers, Edward Smith, Stuart Miller, and Timothy Troy for their help in the expansion of this project and the development of the final vehicle design, as well as Kristi Johnston and Emilie Ford for their contributions in the editing of this document.

Future Work

- A prototype baling system should be fabricated to the designed specifications to verify the results gathered from virtual simulations.
- Demonstrate the effectiveness of the proposed combined collection vehicle through large scale testing

    - Study the viability of CAYR and PAYT programs
    - Determine the influence of the combined collection vehicle on the city's total operating cost
- Create experiment to further understand the relationship between CAE and engineering knowledge. Studies should be conducted to determine the influence that engineering knowledge has on CAE based design with regard to the number of design iterations required to achieve a final product as well as the lead time required to satisfy all customer constraints.
- Begin development of a purely geometric preprocessor which will screen for the geometric anomalies associated with FEA

APPENDICES

Appendix A

Collection Vehicle Free Body Diagram & Equation Justification

Through the use of basic vehicle dynamics principles and statics, a number of equations can be generated which properly describe the vehicle. Since all sub-system weights, sub-system locations, and vehicle dimensions are known, the equations can be used to determine the position of the center of gravity in 3-dimensional space. This information will provide some initial insight as to the performance of the vehicle when operating.

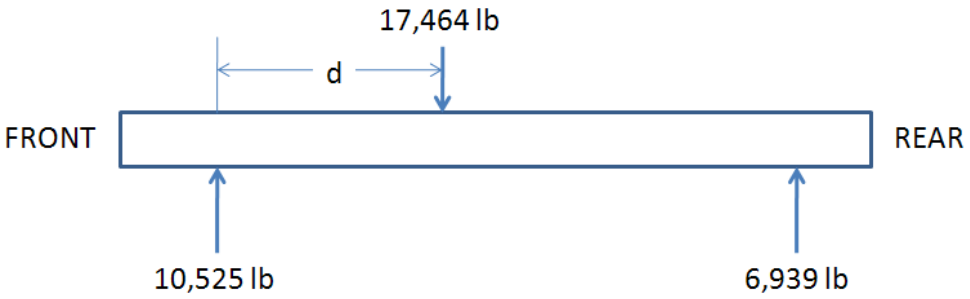

$$\Sigma M = -d \cdot 17464 + 6939(w_B) = 0$$

$$d = 99.13in$$

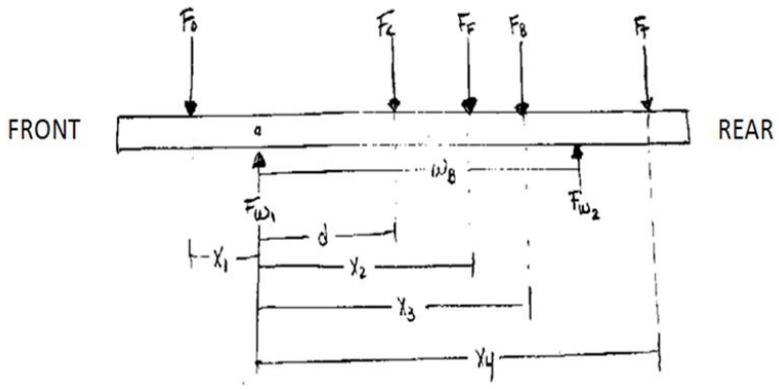

$$\Sigma M_o = F_o(x_1) - F_c(d) - F_f(x_2) - F_B(x_3) - F_T(x_4) + F_{w2}(w_b) = 0$$

$$F_{w2} = \left(\frac{1}{w_b}\right) \left(-F_o(x_1) + F_c(d) + F_f(x_2) + F_B(x_3) + F_T(x_4)\right)$$

Where,

F_o= Weight of the operator
F_c= Weight of the chassis
F_f= Weight of vehicle super structure
F_b= Weight of balers
F_t= Weight of trash compactor
d= Distance to chassis weight
x_1= Front-to-rear location of operator
x_2= Front-to-rear location of super structure center of gravity
x_3= Front-to-rear location of balers
x_4= Front-to-rear location of trash compactor
F_{w1}= Force on front axle
F_{w2}= Force on rear axle

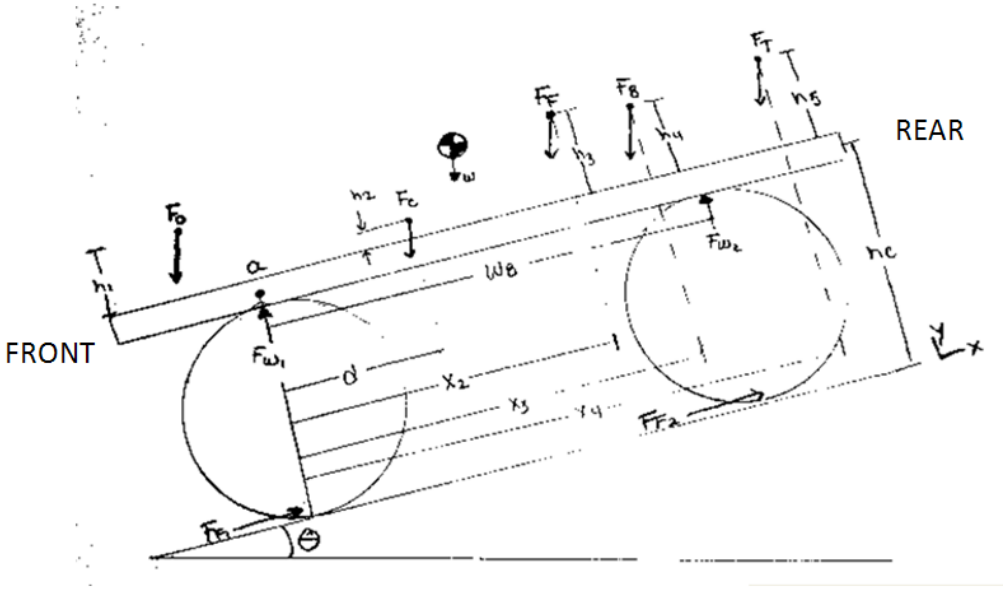

$$\Sigma F_x = F_{f1} + F_{f2} = \sin\theta_1 \left(F_o + F_c + F_f + F_B + F_t\right)$$

$$\Sigma F_y = F_{w1} + F_{w2} = \cos\theta_1 \left(F_o + F_c + F_f + F_B + F_t\right)$$

$$\Sigma M_a = \sin\theta_1 \left(F_o(h_1) + F_c(h_2) + F_f(h_3) + F_B(h_4) + F_t(h_5)\right) + F_o \cos\theta_1 \, x_1 + F_{f1}(h_c) - \cos\theta_1 \left(F_c(d) + F_f(x_2) + F_B(x_3) + F_t(x_4)\right) + F_{w2}(w_b)$$

$$F_{f1} = \sin\theta_1 \left(F_o + F_c + F_f + F_B + F_t\right) - F_{f2}$$

$$F_{w1} = \cos\theta_1 \left(F_o + F_c + F_f + F_B + F_t\right) - F_{w2}$$

Where,

F_{f1}= Frictional force on front tires
F_{f2}= Frictional force on rear tires
wb= Wheel base of truck
h_1= Height of operator cg measured from the frame rail
h_2= Height of chassis cg measured from the frame rail
h_3= Height of super structure cg measured from the frame rail
h_4= Height of baler cg measured from the frame rail
h_5= Height of trash compactor cg measured from the frame rail
h_c= Height of chassis

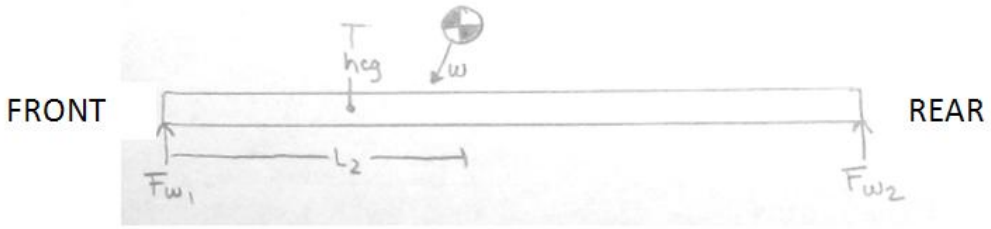

$$\Sigma M_a = F_{w2}(w_b) + \sin\theta_1\, w(h_{cg}) - \cos\theta_1\, w(L_2) + F_{f1}(h_c)$$

$$h_{cg} = \left(\frac{\cos\theta_1\, w(L_2) - F_{f1}(h_c) - F_{w2}(w_b)}{\sin\theta_1\, w}\right)$$

Where,

h_{cg}= Height of the center of gravity above the frame rails
L_2= Front-to-rear location of the center of gravity
w= vehicle weight

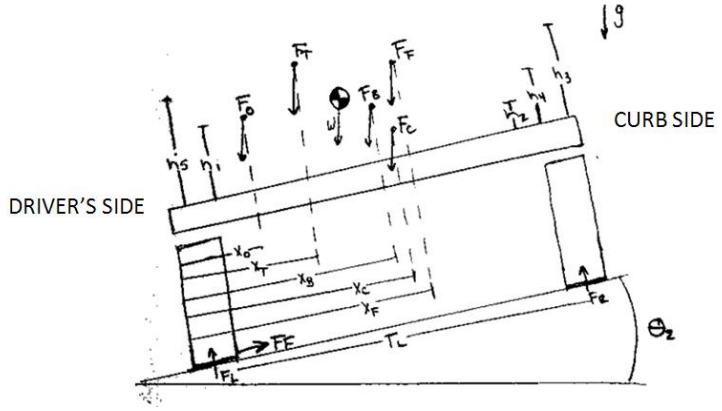

$$\Sigma F_x = F_f = \sin\theta_2 \left(F_o + F_c + F_f + F_B + F_t\right)$$

$$\Sigma F_y = F_L + F_R = \cos\theta_2 \left(F_o + F_c + F_f + F_B + F_t\right)$$

$$\Sigma \mathrm{M_a} = F_R(T_L) + \sin\theta_2 \left(F_o(h_1) + F_c(h_2) + F_f(h_3) + F_B(h_4) + F_t(h_5)\right) + F_f(h_c) - \cos\theta_2 \left(F_o(x_o) + F_c(x_c) + F_f\left(x_f\right) + F_B(x_B) + F_t(x_t)\right)$$

$$F_R = \frac{-\sin\theta_2 \left(F_o(h_1) + F_c(h_2) + F_f(h_3) + F_B(h_4) + F_t(h_5)\right)}{T_L} + \frac{\cos\theta_2 \left(F_o(x_o) + F_c(x_c) + F_f\left(x_f\right) + F_B(x_B) + F_t(x_t)\right) - F_f(h_c)}{T_L}$$

$$F_L = \cos\theta_2 \left(F_o + F_c + F_f + F_B + F_t\right) - F_R$$

Where,

F_f= Frictional force
F_r= Force on curbside tires
F_l= Force on driver's side tires
T_L= Vehicle track length
x_t= Side-to-side position of the trash compactor cg
x_o= Side-to-side position of the operator cg
x_b= Side-to-side position of the baler cg
x_f= Side-to-side position of the super structure cg
x_c= Side-to-side position of the chassis cg
L_3= Side-to-side location of the center of gravity

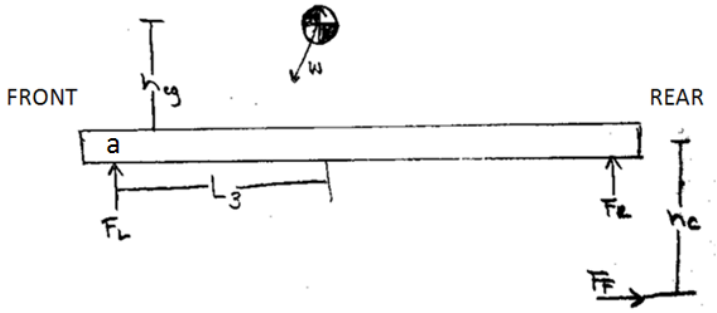

$$\Sigma M_a = F_R \cdot T_L - w \cdot L_3 \cdot \cos\theta_2 + h_{cg} \cdot w \cdot \sin\theta_2 + F_f(h_c)$$

$$L_3 = \frac{h_{cg} \cdot w \cdot \sin\theta_2 + F_f(h_c) + F_R \cdot T_L}{w \cdot \cos\theta_2}$$

When creating the equations for the alternate system, which has balers located in the rear of the vehicle, only the measured distances to the trash compactor and the baler units needed to be corrected. This code was used to determine the location of the center of gravity relative to the vehicle chassis, as well as to determine if the vehicle will understeer or oversteer in high speed applications.

A1: Vehicle Dynamics Study 1: Rear Loading & Off-loading Trash Compactor at Rear of Vehicle

Code

```
%EAI Truck Chassis Center of Gravity Calculation based on
Mack LE 613
%chassis with rear loading trash container
clear;
clc;
wb=input('Input Vehicle Wheelbase in inches   ');
f1=input('Input Chassis Weight on Front Axle in pounds  ');
f2=input('Input Chassis Weight on Rear Axle in pounds  ');
fc=f1+f2;
%Calculates the distance to the chassis center of gravity
location from the
```

```
%front axle
d=f2*wb/(fc);
ft1=input('Input the weight of the trash container when
empty   ');
ft2=input('Input the weight of the trash container when
loaded   ');
fb1=input('Input the weight of the balers when empty   ');
fb2=input('Input the weight of the balers when loaded   ');
fo=input('Input the weight of the two operators in the
front seats  ');
ff=input('Input the weight of the vehicle body  ');
disp(' ')
disp('%%%%%%%%%%%%%%%%%%%%%%%%%%%%%%%%%%%%%%%%%%%%%%%%%%%%%
%%%%%%%')
disp('%%%%%%%%%%%%  The results for the rear trash
%%%%%%%%%%%%%%')
disp('%%%%%%%%%  loading configuration are as follows
%%%%%%%%%%%')
disp('%%%%%%%%%%%%%%%%%%%%%%%%%%%%%%%%%%%%%%%%%%%%%%%%%%%%%
%%%%%%%')
disp(' ')
%All distances measured from front axle%

x1=29;        %Distance to operator weight
x2=105;       %Distance to center of body weight, assuming
frame is uniform
              %over length of covered area
x3=90;        %Distance to center of baler weight assuming
rear doorway
lt=120;       %Length of trash container
x4=wb+.5*lt; %Distance to center of trash container
assuming uniform weight
              %distribution
ftotalu=fo+fc+ff+fb1+ft1;
fw2u=(-fo*x1+fc*d+ff*x2+fb1*x3+ft1*x4)/wb; %Rear axle
weight unloaded
fw1u=ftotalu-fw2u;
du=fw2u*wb/ftotalu;
distf_unloaded=(1-du/wb)*100; %Front weight distribution
distr_unloaded=(du/wb)*100;   %Rear weight distribution
fprintf('The total unloaded vehicle weight is %6.2f
pounds', ftotalu)
disp(' ')
fprintf('The unloaded weight distrubution is %6.2f/%8.3f ',
distf_unloaded, distr_unloaded)
```

```
disp(' ')
if distf_unloaded<50;
    disp('The unloaded vehicle will tend to oversteer')
else
    disp('The unloaded vehicle will tend to understeer')
end
disp(' ')

ftotall=fo+fc+ff+fb2+ft2;
fw2l=(-fo*x1+fc*d+ff*x2+fb2*x3+ft2*x4)/wb; %Rear axle
weight loaded
fw1l=ftotall-fw2l;
dl=fw2l*wb/ftotall;
distf_loaded=(1-dl/wb)*100; %Front weight distribution
distr_loaded=(dl/wb)*100;   %Rear weight distribution
fprintf('The total loaded vehicle weight is %6.2f pounds',
ftotall)
disp(' ')
fprintf('The loaded weight distrubution is %6.2f/%8.3f ',
distf_loaded, distr_loaded)
disp(' ')
if distf_loaded<50;
    disp('The loaded vehicle will tend to oversteer')
else
    disp('The loaded vehicle will tend to understeer')
end
```

Results

```
%%%%%%%%%%%%%%%%%%%%%%%%%%%%%%%%%%%%%%%%%%%%%%%%
%%%%%%%%%%%%%  The results for the rear trash  %%%%%%%%%%%%%%%%
%%%%%%%%%%%  loading configuration are as follows  %%%%%%%%%%%%%
%%%%%%%%%%%%%%%%%%%%%%%%%%%%%%%%%%%%%%%%%%%%%%%%

The total unloaded vehicle weight is 36964.00 pounds
The unloaded weight distribution is 48.43/ 51.566
The unloaded vehicle will tend to oversteer

The total loaded vehicle weight is 46464.00 pounds
The loaded weight distribution is 40.25/ 59.747
The loaded vehicle will tend to oversteer
```

The code below was utilized to find the center of gravity of the vehicle which utilized a side loading trash compactor found in the middle of the vehicle. The information regarding the location of the vehicle sub-systems has been hard coded. However, the code can be easily changed to allow users to input these values, therefore providing more flexibility in the system.

A2: Vehicle Dynamics Study 2: Side Loading Trash Compactor Located Behind Cab

Code

```
%EAI Truck Chassis Center of Gravity Calculation based on
Mack LE 613
%chassis with front located trash container
clear;
clc;
theta=10*(pi/180);
wb=250;
f1=10525;
f2=6939;
% wb=input('Input Vehicle Wheelbase in inches   ');
% f1=input('Input Chassis Weight on Front Axle in pounds
');
% f2=input('Input Chassis Weight on Rear Axle in pounds
');
fc=f1+f2;
%Calculates the distance to the chassis center of gravity
location from the
%front axle
d=f2*wb/(fc);
ft1=6000;
ft2=12000;
fb1=12000;
fb2=15500;
fo=500;
ff=1000;

% ft1=input('Input the weight of the trash container when
empty   ');
% ft2=input('Input the weight of the trash container when
loaded   ');
```

```
% fb1=input('Input the weight of the balers when empty
');
% fb2=input('Input the weight of the balers when loaded
');
% fo=input('Input the weight of the two operators   ');
% ff=input('Input the weight of the vehicle body   ');
disp(' ')
disp('%%%%%%%%%%%%%%%%%%%%%%%%%%%%%%%%%%%%%%%%%%%%%%%%%%%%%%%
%%%%%%%')
disp('%%%%%%%%%%%%  The results for the front trash
%%%%%%%%%%%%%%')
disp('%%%%%%%%%  loading configuration are as follows
%%%%%%%%%%%%')
disp('%%%%%%%%%%%%%%%%%%%%%%%%%%%%%%%%%%%%%%%%%%%%%%%%%%%%%%%
%%%%%%%')
disp(' ')
%All distances measured from front axle%

x1=29;        %Distance to operator weight
x2=226;       %Distance to center of body weight, assuming
frame is uniform
              %over length of covered area
x3=244;       %Distance to center of baler weight assuming
front doorway
x4=81;        %Distance to center of trash container
assuming uniform weight
              %distribution
ftotalu=fo+fc+ff+fb1+ft1;
fw2u=(-fo*x1+fc*d+ff*x2+fb1*x3+ft1*x4)/wb; %Rear axle
weight unloaded
fw1u=ftotalu-fw2u;
du=fw2u*wb/ftotalu;
distf_unloaded=(1-du/wb)*100; %Front weight distribution
distr_unloaded=(du/wb)*100;   %Rear weight distribution
fprintf('The total unloaded vehicle weight is %6.2f
pounds', ftotalu)
disp(' ')
fprintf('The unloaded weight distrubution is %6.2f/%8.3f ',
distf_unloaded, distr_unloaded)
disp(' ')
if distf_unloaded<50;
    disp('The unloaded vehicle will tend to oversteer')
else
    disp('The unloaded vehicle will tend to understeer')
end
```

```
disp(' ')

ftotall=fo+fc+ff+fb2+ft2;
fw2l=(-fo*x1+fc*d+ff*x2+fb2*x3+ft2*x4)/wb; %Rear axle
weight loaded
fw1l=ftotall-fw2l;
dl=fw2l*wb/ftotall;
distf_loaded=(1-dl/wb)*100; %Front weight distribution
distr_loaded=(dl/wb)*100;   %Rear weight distribution
fprintf('The total loaded vehicle weight is %6.2f pounds',
ftotall)
disp(' ')
fprintf('The loaded weight distrubution is %6.2f/%8.3f ',
distf_loaded, distr_loaded)
disp(' ')
if distf_loaded<50;
    disp('The loaded vehicle will tend to oversteer')
else
    disp('The loaded vehicle will tend to understeer')
end

%Determine the height of the Center of Gravity from the top
of the frame
%rails.  From a drivers side view.
h1=24;     %Height of operator cg
h2=1;      %Height of chassis cg
h3=72;     %Height of body cg
h4=25;     %Height of baler cg
h4l=20;    %Height of baler cg LOADED
h5=48;     %Height of MSW cg
hc=45;     %Height from ground to top of frame rails
hcl=40;    %Height from ground to top of frame rails LOADED

%Center of Gravity Height UNLOADED
F_fricu=sin(theta)*(fo+fc+ff+fb1+ft1);
Fw2u=(cos(theta)*(fc*d+ff*x2+fb1*x3+ft1*x4)-
sin(theta)*(h1*fo+h2*fc+h3*ff+h4*fb1+h5*ft1)-
fo*cos(theta)*x1-F_fricu*hc)/wb;
Fw1u=cos(theta)*(fo+fc+ff+fb1+ft1)-Fw2u;
Du=fw2u*wb/ftotalu;
h_cgu=(cos(theta)*ftotalu*Du-Fw2u*wb-
F_fricu*hc)/(sin(theta)*ftotalu);   %Center of Gravity
Height

%Center of Gravity Height LOADED
```

```
F_fricl=sin(theta)*(fo+fc+ff+fb2+ft2);
Fw2l=(cos(theta)*(fc*d+ff*x2+fb2*x3+ft2*x4)-
sin(theta)*(h1*fo+h2*fc+h3*ff+h4l*fb2+h5*ft2)-
fo*cos(theta)*x1-F_fricl*hcl)/wb;
Fw1l=cos(theta)*(fo+fc+ff+fb2+ft2)-Fw2l;
Dl=fw2l*wb/ftotall;
h_cgl=(cos(theta)*ftotall*Dl-Fw2l*wb-
F_fricl*hcl)/(sin(theta)*ftotall);   %Center of Gravity
Height

%Determine the location of the cg laterally from a rearend
view
Tl=66;          %Track Length
xo=2*Tl/3;      %Distance to operator cg
xt=2*Tl/3;      %Distance to MSW cg
xtl=Tl/3;       %Distance to MSW cg LOADED
xb=.4*Tl;       %Distance to baler cg
xbl=Tl/3;       %Distance to baler cg LOADED
xf=Tl/2;        %Distance to body cg
xc=Tl/2;        %Distance to chassis cg

%Center of Gravity Location UNLOADED
F_Fricu=sin(theta)*(fo+fb1+ft1+ff+fc);
F_rightu=(-
sin(theta)*(fo*h1+fb1*h4+ft1*h5+ff*h3+fc*h2)+cos(theta)*(fo
*xo+ft1*xt+fb1*xb+ff*xf+fc*xc)-F_Fricu*hc)/Tl;
F_leftu=cos(theta)*(fo+ft1+fb1+ff+fc)-F_rightu;
L_cgu=(F_rightu*Tl+h_cgu*sin(theta)*ftotalu+F_Fricu*hc)/(ft
otalu*cos(theta));  %Center of Gravity Location from center
of left tire

%Center of Gravity Location LOADED
F_Fricl=sin(theta)*(fo+fb2+ft2+ff+fc);
F_rightl=(-
sin(theta)*(fo*h1+fb2*h4l+ft2*h5+ff*h3+fc*h2)+cos(theta)*(f
o*xo+ft2*xtl+fb2*xbl+ff*xf+fc*xc)-F_Fricl*hcl)/Tl;
F_leftl=cos(theta)*(fo+ft2+fb2+ff+fc)-F_rightl;
L_cgl=(F_rightl*Tl+h_cgl*sin(theta)*ftotall+F_Fricl*hcl)/(f
totall*cos(theta));  %Center of Gravity Location from
center of left tire
```

Results

%%%
%%%%%%%%%%%%% The results for the front trash %%%%%%%%%%%%%%
%%%%%%%%%%% loading configuration are as follows %%%%%%%%%%%%%
%%

The total unloaded vehicle weight is 36964.00 pounds
The unloaded weight distribution is 41.99/ 58.005
The unloaded vehicle will tend to oversteer

The total loaded vehicle weight is 46464.00 pounds
The loaded weight distribution is 42.32/ 57.681
The loaded vehicle will tend to oversteer

Appendix B

Material Properties Utilized in FEA Studies

Below is a list of all of the material properties utilized for finite element analysis studies shown in the earlier sections of the document. The material and physical properties were gathered from the existing CosmosWorks material library and were confirmed by mechanical textbooks (26).

Material name: AISI 1020 Steel

Property Name	Value	Units
Elastic modulus	1.99948e+11	N/m^2
Shear modulus	7.99792e+10	N/m^2
Mass density	7899.84	kg/m^3
Tensile strength	4.50028e+008	N/m^2
Yield strength	3.44738e+008	N/m^2
Poisson's Ratio	0.29	NA

Material name: AISI 1045 Steel, cold drawn

Property Name	Value	Units
Elastic modulus	2.05e+011	N/m^2
Shear modulus	8e+010	N/m^2
Mass density	7850	kg/m^3
Tensile strength	6.25e+008	N/m^2
Yield strength	5.3e+008	N/m^2
Thermal expansion coefficient	1.15e-005	/Kelvin
Thermal conductivity	49.8	W/(m.K)
Specific heat	486	J/(kg.K)

Material name: ASTM A572 Grade 60

Property Name	Value	Units
Elastic modulus	2e+011	N/m^2
Poisson's ratio	0.26	NA
Shear modulus	7.93e+010	N/m^2
Mass density	7850	kg/m^3
Tensile strength	5.1504e+008	N/m^2
Yield strength	4.1506e+008	N/m^2

Material name: AISI Type A2 Tool Steel

Property Name	Value	Units
Elastic modulus	2.03e+011	N/m^2
Shear modulus	7.8e+010	N/m^2
Mass density	7860	kg/m^3
Thermal expansion coefficient	1.1e-005	/Kelvin
Hardening factor (0.0-1.0; 0.0=isotropic; 1.0=kinematic)	0.85	NA

Material name: Plain Carbon Steel

Property Name	Value	Units
Elastic modulus	2.1e+011	N/m^2
Poisson's ratio	0.28	NA
Shear modulus	7.9e+010	N/m^2
Mass density	7800	kg/m^3
Tensile strength	3.9983e+008	N/m^2
Yield strength	2.2059e+008	N/m^2
Thermal expansion coefficient	1.3e-005	/Kelvin
Thermal conductivity	43	W/(m.K)
Specific heat	440	J/(kg.K)

Material name: ASTM A36 Steel

Property Name	Value	Units
Elastic modulus	2.0e+11	N/m^2
Shear modulus	7.929e+10	N/m^2
Mass density	7850.0	kg/m^3
Tensile strength	4.00e+008	N/m^2
Yield strength	2.50e+008	N/m^2
Poisson’s Ratio	0.26	NA

REFERENCES

1. Yin, Robert. Application of Case Study Research. 2nd Edition. Thousand Oaks : Sage Publications, 2003. Vol. 34. ISBN 0-7619-2550-3.

2. Solution Source: Eliminate Non-Value Added Effort. IMEC. [Online] 2005. [Cited: October 3, 2007.] http://www.imec.org/imec.nsf/All/Solutions_Source_Eliminate_Nonvalue_Added_Effort?OpenDocument.

3. Carreira, B. Lean Manufacturing That Works: Powerful Tools for Dramatically Reducing Waste & Maximizing Profits. New York : American Management Association, 2004.

4. MRF Upgrades: A Tale of Three Cities. Lepotsky, George. Sept.-Oct. 2005, MSW Management Journal.

5. Applying Lean Manufacturing Principles to Revolutionize Cubrside Equipment and Collection Processes [DETC2007-35615]. Smith, E., Johnston, P.J., Summers, J. Las Vegas, NV : ASME, 2007. Proceeding from ASME DETC Design Engineering Technical Conference Conference.

6. US, EPA. Lean Manufacturing and the Environment: Research on Advanced Manufacturing Systems and the Environment and Recommendation for Leveraging Better Environmental Performance-EAP100-R-03-005. s.l. : U.S.E.P.A., October 2003.

7. Katrina, A. The Basics of Lean Manufacturing & Maintenance. The Complete Source for the Latest Industrial Product Solutions- Thomas.Net. [Online] [Cited: June 23, 2004.] http://news.thomasnet.com/IMT/archives/2004/06/the_basics_of_1.html?t=archive.

8. Ohno, T. Toyota Production System. New York : Productivity Press, 1988.

9. Wang, Gary G. Definition and Review of Virtual Prototyping. Dept. of Mechanical and Industrial Engineering University of Manitoba.

10. Integrating Virtual Reality for Virtual Prototyping. Antonino, G.S. & Zachmann, G. Atlanta, GA : s.n., 1998. Proceesing of the 1998 ASME Design Technical Conference and Computers in Engineering Conference. DETC98/CIE-5536.

11. Enabling Digital Mock Up with Virtual Reality Techniques- Vision, Concept, Demonstrator. Dai, F. & Reindl, P. Irvine, California : ASME, 1996. Proceedings of 1996 ASME Design Engineering Technical Conference & Computers in Engineering Conference.

12. Pahl, G., Beitz, W. Engineering Design: A Systematic Approach. [ed.] Ken Wallace. [trans.] Ken Wallace & Lucienne Blessing. 2nd Edition. London : Springer-Verlag, 1996. ISBN 3-540-19917-9.

13. Co., Boeing. Boeing: Commercial Airplanes- 777 - Computing and Design Processes. Boeing Co. . [Online] 2007. [Cited: 11 9, 2007.] http://www.boeing.com/commercial/777family/compute/index.html.

14. Environmental America, Inc. E.A.I. Business Plan. Greenwood, S.C., USA : s.n., November 16, 2004.

15. Troy, Timothy. Technology as an Enabler for Recycling Policy Reform. Mechanical Engineering - AID Group, Clemson University. Clemson, SC : Clemson University, 2006. Technical Report.

16. City of Clemson, Finance Department. Annual Budget Fiscal Year 2006. Clemson, SC : s.n., 2005.

17. Poli, Corrado. Design for Manufacturing. Boston : Butterworth Heinemann, 2001. IBSN-13: 978-0-7506-7341-9.

18. Mack Trucks, Inc. TerraPro Low Entry - Redifining the Way You Work. Mack Trucks. [Online] 2007. [Cited: October 3, 2007.] http://www.macktrucks.com/default.aspx?pageid=2081.

19. Scania, Ltd. Scania Low Entry Cab Launched at CIWM 2006. Scania, Ltd. [Online] 2007. [Cited: October 3, 2007.] http://www.scania.co.uk/about_scania/pressreleases/scania_low_entry_chassis_cab_launched_at_ciwm_2006.asp.

20. Department of Labor, US. Occupational Noise Exposure 1910.95. US Department of Labor, Occupational Safety & Health Administration. [Online] [Cited: 10 15, 2007.] http://www.osha.gov/pls/oshaweb/owadisp.show_document?p_table=STANDARDS&p_id=9735.

21. Recycle.net. PET Recycling Category-Plastics Recycling. Recycle.net. [Online] [Cited: February 23, 2007.] http://www.recycle.net/Plastic/PET/index.html.

22. Recycling, Canusa Hershman. 03 15, 2005.

23. USA, Polychem. 03 15, 2005.

24. Palm, W.J.III. Introduction to MATLAB for Engineers. Boston : McGraw Hill, 2001. ISBN 0-07-234983-2.

25. Close, C.M., Frederick, D.H., Newell, J.C. Modeling & Analysis of Dynamic Systems. 3rd. Hoboken, New Jersey : John Whiley & Sons, Inc., 2002. ISBN 0-471-39442-4.

26. Hibbeler, R.C. Mechanics of Materials. 5th Edition. Upper Saddle River, New Jersey : Prentice Hall, 2003. ISBN 0-13-008181-7.

27. Otto, K.N., Wood, K.L. Product Evolution: A Reverse Engineering and Redesign Methodology. London : Springer Verlag, 1998.

28. Ingle, K.A. Reverse Engineering. New York : McGraw Hill, 1994.

29. Ashby, Michael F. Materials Selection in Mechanical Design. 3rd Edition. Amsterdam : Elsevier Butterworth Heinemann, 2005. pp. 91-171. ISBN 0-7506-6168-2.

30. Norton, Robert. Machine Design: An Integrated Approach. 2nd Edition. Upper Saddle River, New Jersey : Prentice Hall, 2000. ISBN 0-13-017706-7.

31. McMaster Carr. McMaster Carr. [Online] [Cited: May 3, 2006.] http://www.macmaster.com.

32. Kalpakjian, S., Schmid, Steven R. Manufacturing Processes for Engineering Materials. 4th Edition. Upper Saddle River, New Jersey : Prentice Hall, 2003. ISBN 0-13-040871-9.

33. Norton, Robert. Design of Machinery: An Introduction to the Synthesis and Analysis of Mechanisms and Machines. 2nd Edition. Boston : McGraw Hill, 2001.

34. University, Iowa State. Lean Manufacturing. Iowa State University Facilities Planning and Management. FP&M World Class Journey. [Online] 2007. [Cited: October 3, 2007.] http://www.fpm.iastate.edu/worldclass/lean.asp.

35. Lean Manufacturing Prinicples Guide- Version 0.5. s.l. : University of Michigan, June 26,2000.

36. U.S.E.P.A. RCRA Online. RCRA Online. [Online] February 22, 2006. [Cited: May 3, 2006.] http://www.epa.gov/rcraonline.

37. A Virtual Prototyping System for Rapid Product Development. S.H. Choi, A.M.M. Chan. 5, s.l. : Elsevier Ltd, April 2004, Computer-Aided Design, Vol. 36, pp. 401-412.

38. Siodmock, Paul. Computer Aided Design by Paul Siodmok. Design Council. [Online] 2007. [Cited: 09 29, 2007.] http://www.design-council.org.uk/en/About-Design/Design-Techniques/Computer-Aided-Design-by-Paul-Siodmok/.

39. The Changong Role of Physical Testing in Vehicle Development Programmes. Wilkinson, Paul. 2007, s.l. : Elsevier, 2006, Journal of Terramechanics, Vol. 44, pp. 15-22.

40. Gupta, Satyandra K., Paredis, Christiaan J.J., Sinha, R., Wang, Cheng-Hua, and Brown, Peter F. Intelligent Assembly, Modeling, and Simulation. Carnigie Mellon University. Pittsburgh, PA 15213 : s.n. Technical Report. ICES #05-104-97.

41. McLeod, Peter. The Availability and Capabilities of 'Low-End' Virtual Modelling (Prototyping) Products to Enable Designers and Engineers to Prove Concept Early in the Design Cycle. Wolfson School of Mechanical and Manufacturing Engineering. Loughborough, Leics : PRIME Faraday Partnership, 2001. Technical Report. ISBN 1-84402-018-5.

42. AN EXAMINATION OF PROTOTYPING AND DESIGN OUTCOME. Yang, Maria C. Salt Lake City, Utah : s.n., 2004. 2004 DETC ASME Design Engineering Technical Conferences. DETC2004-57552.

43. Virtual Prototyping for Customized Product Development. Tseng, Mitchell M., Jianxin Jiao, Chuan-Jun Su. 6, s.l. : MCB UP Ltd, 1998, Integrated Manufacturing Systems, Vol. 9, pp. 334 - 343. ISSN: 0957-6061.

44. Beer, Ferdinand P., Johnston, Russell E. Vector Mechanics for Engineers: Statics. [ed.] John J., Maisel, Jack Corrigan. 6th Edition. New York : McGraw Hill Companies, Inc., 1196. ISBN 0-07-005367-7.

45. Shigley, Joseph E., Mischke, Charles R. Mechanical Engineering Design. 6th Edition. Boston : McGraw Hill, 2001. ISBN 0-07-365939-8.